Fall 2014

Waste Heat Recovery Options in a Large Gas-Turbine Combined Power Plant

Ularee Upathumchard
Purdue University

Graduate School ETD Form 9
(Revised 01/14)

PURDUE UNIVERSITY
GRADUATE SCHOOL
Thesis/Dissertation Acceptance

This is to certify that the thesis/dissertation prepared

By Ularee Upathumchard

Entitled
Waste Heat Recovery Options in a Large Gas-Turbine Combined Power Plant

For the degree of Master of Science in Mechanical Engineering

Is approved by the final examining committee:

Eckhard A. Groll

James E. Braun

Nicole L. Key

To the best of my knowledge and as understood by the student in the *Thesis/Dissertation Agreement. Publication Delay, and Certification/Disclaimer (Graduate School Form 32)*, this thesis/dissertation adheres to the provisions of Purdue University's "Policy on Integrity in Research" and the use of copyrighted material.

Eckhard A. Groll

Approved by Major Professor(s): _____

_____

Approved by: Ganesh Subbarayan 09/05/2014

Head of the Department Graduate Program Date

WASTE HEAT RECOVERY OPTIONS IN A LARGE GAS-TURBINE COMBINED POWER PLANT

A Thesis

Submitted to the Faculty

of

Purdue University

by

Ularee Upathumchard

In Partial Fulfillment of the

Requirements for the Degree

of

Master of Science in Mechanical Engineering

December 2014

Purdue University

West Lafayette, Indiana

To my family

ACKNOWLEDGEMENTS

It is a great pleasure to express my appreciation to everyone who made this thesis possible. First of all, I would like to give my sincerest thanks to Professor Eckhard A. Groll for being my advisor, providing me the opportunity to conduct this work, patiently guiding me along the way and kindly supporting my decision. I would not have accomplished this thesis without your invaluable advice. It was an honor to work with you. I also would like to thank Professor James E. Braun and Professor Nicole L. Key for serving as my thesis committees to fulfill this work.

In addition to the professors, I would like to thank Brandon J. Woodland for the literature on Organic Rankine Cycles, supplemental knowledge and useful comments As well as Ammar Bahman, I would like to thank for every of your effort to help me with EES software. My thankful thoughts also go to my editor friends who voluntarily reviewed my thesis for language accuracy and improvement; Jebaraj Vasudevan, Harshad Inamdar, and Domenique R. Lumpkin.

Moreover, I am blessed to have such a supportive family, both Thai and American. My friends from the Mechanical Engineering department, the Ray W. Herrick Laboratories and my Thai friends; your friendship, support and encouragement are truly appreciated and have made my graduate student life memorable.

My appreciation also goes to the contribution of information from my colleagues at the Electricity Generating Authority of Thailand, especially Muncharee Preechanont for the immediate response as always.

Lastly, thank you Fulbright for the prestigious opportunity to expand my vision and explore the world as a Fulbrighter.

TABLE OF CONTENTS

Page

LIST OF TABLES……..ix

LIST OF FIGURES…… xi

NOMENCLATURE…….. xv

ABSTRACT……..xix

CHAPTER 1. INTRODUCTION……..... 1

1.1 Background……1

1.2 Motivation……..2

1.3 Objective……4

1.4 Overview…….....5

CHAPTER 2. LITERATURE REVIEW……..…… 7

2.1 Waste Heat Recovery Technologies…….. 8

2.2 Absorption Chiller……..……. 17

2.2.1 Absorption and Desorption Processes…….....17

2.2.2 Working Fluids…….....18

2.2.3 Thermodynamic Principles of Absorption Refrigeration Cycle…….....20

2.2.4 Modification of Absorption Refrigeration Cycles……..24

2.3 Organic Rankine Cycle……26

2.3.1 Thermodynamic Principles of ORC…….....28

Page

2.3.2 Pinch Point Analysis……..……..... 29

2.3.3 Past and Current Research on ORC…..…….…… 31

2.3.4 Working Fluids……...…….....31

CHAPTER 3. MODELING OF THE WASTE HEAT RECOVERY SYSTEMS……. 34

3.1 Heat Loss Analysis…….……. 34

3.1.1 Power Plant Operation and Characteristic……..….....35

3.1.2 Combustion Turbine (CT) Ventilation Air……..……...39

3.1.3 Heat Recovery Steam Generator (HRSG) Exhaust…….…..……42

3.1.4 Lubrication Oil……..……. 44

3.1.5 Cooling Water…….…..……. 44

3.2 Absorption Chillers …….…..……..45

3.2.1 Modeling of components……...…….45

3.2.1.1 Absorber……...…….46

3.2.1.2 Generator……..…… 47

3.2.1.3 Condenser……...…….. 49

3.2.1.4 Evaporator…….50

3.2.1.5 Solution Heat Exchanger……...…….. 51

3.2.1.6 Solution Pump…….……...….....52

3.2.1.7 Expansion valve…….……...…...…….53

3.2.2 Absorption Cycle Assumptions……...……...54

3.2.3 Single-Effect Absorption Cycles……..…….…….....59

3.2.2.1 Single-Effect NH_3/H_2O Absorption Cycle……...…… 59

3.2.3.2 Single-Effect H_2O/LiBr Absorption Cycle……...…….... 63

Page

3.2.4 Double-Effect H_2O/LiBr Absorption Cycle…..……..... 63

3.2.5 Half-Effect Absorption Cycles……...……..... 67

3.3 Organic Rankine Cycles …….…… 69

3.3.1 Modeling of Components……..……..... 69

3.3.1.1 Condenser……..…….…...70

3.3.1.2 Pump…….……..…….…...70

3.3.1.3 Evaporator…….…….…….…...72

3.3.1.4 Expander…….……..…… 72

3.3.1.5 Heat Exchanger……..... 74

3.3.2 Organic Rankine Cycle Assumptions……..……..……..75

3.3.3 Baseline Organic Rankine Cycle……...…….77

3.3.4 Organic Rankine Cycle with Internal Regenerator……..…..……. 79

3.3.5 Two-Phase Flash Expansion Organic Rankine Cycle……...…….81

3.3.6 Organic Rankine Cycle with Multiple Heat Sources……..…..... 83

3.4 Energy Availability Utilization and Evaluation Parameter……..…….... 85

3.5 Simple Economic Analysis……..... 89

CHAPER 4. RESULTS OF MODEL ANALYSIS…….. 90

4.1 Waste Heat Capacities…… 90

4.2 Absorption Chiller Modeling Results……..……..... 92

4.3 Organic Rankine Cycle Modeling Results……..……...111

4.4 Economic Payback Periods……...……..122

CHAPTER 5. CONCLUSION AND RECOMMENDATIONS……...125

LIST OF REFERENCES..... 128

Page

APPENDICES

Appendix A. Heat Loss Analysis EES Code…….....134

Appendix B. Modeling of Absorption Chillers EES Code...…… 141

Appendix C. Modeling of Organic Rankine Cycles EES Code...…….168

Appendix D. Simple Economic Payback EES Code…...…….…….190

LIST OF TABLES

Table		Page
Table 2.1.	Waste heat sources and potential applications classified by temperature range	15
Table 2.2.	Heat engine cycles in power generation for waste heat recovery	16
Table 2.3.	Heat pump technologies for waste heat recovery	16
Table 2.4.	Summary of reviewed absorption refrigeration cycles	23
Table 2.5.	Working fluids investigated in Woodland (2013)'s study	33
Table 3.1.	Operation summary for the studied GTCC power plant	38
Table 3.2.	Exhaust gas compositions	43
Table 3.3.	Thermodynamic state points in NH_3/H_2O single-effect absorption cycle with rectifier and precooler integration	54
Table 3.4.	Thermodynamic state points in H_2O/LiBr single-effect absorption cycle	55
Table 3.5.	Thermodynamic state points in H_2O/LiBr double-effect absorption cycle	56
Table 3.6.	Thermodynamic state points in half-effect absorption cycle	57
Table 3.7.	Summary of assumptions for operating temperatures	58
Table 3.8.	Summary of concentration assumptions	58
Table 3.9.	Assumptions of components' efficiencies	58
Table 3.10.	Summary of assumptions used in ORC modeling	76
Table 3.11.	Summary of state point assumptions in ORC modeling	77
Table 4.1.	Summary of waste heat capacities and rejection temperatures	91
Table 4.2.	Presentation of results for absorption chillers	92
Table 4.3.	State points of single-effect H_2O/LiBr absorption cycle P-T diagram of lubrication oil heat source, corresponding to Figure 4.1	94

Table Page

Table 4.4. State points of single-effect H_2O/LiBr absorption cycle P-T diagram of CT room ventilation air heat source, corresponding to Figure 4.2……...96
Table 4.5. State points of single-effect NH_3/H_2O absorption cycle T-x diagram of lubrication oil heat source, corresponding to Figure 4.3……..99
Table 4.6. State points of single-effect NH_3/H_2O absorption cycle T-x diagram of CT room ventilation air heat source, corresponding to Figure 4.4…..…101
Table 4.7. State points of double-effect H_2O/LiBr absorption cycle P-T diagram of CT room ventilation air heat source, corresponding to Figure 4.5…..…103
Table 4.8. State points of half-effect H_2O/LiBr absorption cycle P-T diagram of lubrication oil heat source, corresponding to Figure 4.6…… 106
Table 4.9. State points of half-effect NH_3/H_2O absorption cycle T-x diagram of lubrication oil heat source, corresponding to Figure 4.7……..... 109
Table 4.10. Energy flows and balances of absorption cycles…… 110
Table 4.11. Summary for evaluation of absorption chiller models……....110
Table 4.12. Presentation of results for ORCs ……...….111
Table 4.13. Energy flows and balances of ORCs with single heat source of R134a working fluid……...120
Table 4.14. Energy flows and balances of ORCs with single heat source of R245fa working fluid……...120
Table 4.15. Energy flows and balances of ORCs with multiple heat sources……... 121
Table 4.16. Summary of evaluations for ORC models with single heat source..... 121
Table 4.17. Summary of evaluations for ORC models with multiple heat sources…...121
Table 4.18. Prices of waste heat recovery systems and energy…… 123
Table 4.19. Payback periods of the selected waste heat recovery systems……... 123

LIST OF FIGURES

Figure		Page
Figure 1.1.	Electricity production of Thailand (2000-2011)……..……..3	
Figure 1.2.	Primary energy sources for electricity generation of Thailand (2011)……...3	
Figure 2.1.	Three essential components required for waste heat recovery..... 10	
Figure 2.2.	The correlation between temperature differences across the heat exchanger (ΔT) and required heat exchanger area……..... 12	
Figure 2.3.	Absorption and desorption processes……..... 18	
Figure 2.4.	Pressure-temperature diagram for H_2O/LiBr…….....20	
Figure 2.5.	Simple single-effect absorption cycle……...21	
Figure 2.6.	State points of a simple single-effect absorption cycle…… 21	
Figure 2.7.	NH_3/ H_2O single-effect absorption cycle with rectifier and solution heat exchanger……..24	
Figure 2.8.	NH_3/ H_2O single-effect absorption cycle with rectifier, solution heat exchanger and precooler……... 25	
Figure 2.9.	Simple Rankine Cycle…….……. 27	
Figure 2.10.	Temperature-entropy diagram of an ideal Organic Rankine Cycle……..27	
Figure 2.11.	Pinch points in an R245fa ORC……30	
Figure 2.12.	Maximum second law effectiveness of selected working fluids in Table 2.5…….…….. 33	
Figure 3.1.	Gas-turbine combined cycle power plant……..……... 35	
Figure 3.2.	Gas turbine……....36	
Figure 3.3.	Heat recovery steam generator diagram …….. 37	
Figure 3.4.	Multi-stage steam turbines and generator…….....37	
Figure 3.5.	Half-block operation in GTCC power plant……..... 38	

Figure Page

Figure 3.6. Combustion turbine enclosure and ventilation……..... 40
Figure 3.7. Combustor energy balance diagram……..... 41
Figure 3.8. Heat-flows in a gas turbine compartment…….....42
Figure 3.9. HRSG energy balance diagram…… 42
Figure 3.10. Dew points of SO_3 at various water contents of the gas, calculated from the formula of Verhoff…….…….....43
Figure 3.11. Lubrication oil tank energy balance diagram…….... 44
Figure 3.12. Cooling tower energy balance diagram…… 45
Figure 3.13. Basic absorption cycle schematic…… 46
Figure 3.14. Absorber schematic……..... 46
Figure 3.15. Generator schematic……..... 47
Figure 3.16. Condenser schematic……..... 49
Figure 3.17. Evaporator schematic……..……..50
Figure 3.18. Solution heat exchanger schematic……..……51
Figure 3.19. Pump schematic……..... 52
Figure 3.20. Expansion valve schematic…….....53
Figure 3.21. Investigated single-effect NH_3/H_2O absorption cycle……..... 59
Figure 3.22. Rectifier and generator schematic……..……. 62
Figure 3.23. Precooler schematic……..... 62
Figure 3.24. Double-effect parallel-flow H_2O/LiBr absorption cycle on Dühring chart schematic…… 65
Figure 3.25. Low-pressure generator schematic……..…… 65
Figure 3.26. Half-effect absorption cycle schematic……..... 68
Figure 3.27. ORC condenser schematic……..…….. 70
Figure 3.28. ORC pump schematic……..……71
Figure 3.29. ORC evaporator schematic……..……72
Figure 3.30. ORC expander schematic…….…..……...73
Figure 3.31. Internal heat exchanger schematic……..……..74

Figure Page

Figure 3.32. Assumptions of temperature and pinch points plotted on R134a T-s diagram……..…….... 76
Figure 3.33. Baseline ORC schematic……..... 77
Figure 3.34. Baseline ORC T-s diagram for actual processes with heat source and heat sink temperature profiles superimposed……..... 78
Figure 3.35. ORC with regenerator schematic…….....79
Figure 3.36. ORC with regenerator T-s diagram for actual processes with heat source and heat sink temperature profiles superimposed……...…….. 80
Figure 3.37. ORC with two-phase flash expansion schematic…….....82
Figure 3.38. ORC with two-phase flash expansion T-s diagram for actual processes with heat source and heat sink temperature profiles superimposed…..... 82
Figure 3.39. Heater schematic for two-phase flash expansion ORC……...……. 83
Figure 3.40. ORC with multiple heat sources…….....84
Figure 3.41. Flow of exergy entering a closed system……..……85
Figure 3.42. Flow of exergy in a heat engine cycle……..... 87
Figure 4.1. Single-effect H_2O/LiBr absorption cycle P-T diagram of lubrication oil heat source……..... 94
Figure 4.2. Single-effect H_2O/LiBr absorption cycle P-T diagram of CT room ventilation air heat source……95
Figure 4.3. Single-effect NH_3/H_2O absorption cycle T-x diagram of lubrication oil heat source……..... 97
Figure 4.4. Single-effect NH_3/H_2O absorption cycle T-x diagram of CT room ventilation air heat source…….....100
Figure 4.5. Double-effect H_2O/LiBr absorption cycle P-T diagram of CT room ventilation air heat source……... 102
Figure 4.6. Half-effect H_2O/LiBr absorption cycle P-T diagram of lubrication oil heat source……..... 105
Figure 4.7. Half-effect NH_3/H_2O absorption cycle T-x diagram of lubrication oil heat source……...108

Figure Page

Figure 4.8. Baseline ORC T-s diagrams of lubrication oil heat source…… 113
Figure 4.9. Baseline ORC T-s diagrams of CT room ventilation air heat source...….. 114
Figure 4.10. ORC with internal regenerator T-s diagrams of lubrication oil heat source……..…115
Figure 4.11. ORC with internal regenerator T-s diagrams of CT room ventilation air heat source……..... 116
Figure 4.12. Two-phase flash expansion ORC T-s diagrams of lubrication oil heat source……..117
Figure 4.13. Two-phase flash expansion ORC T-s diagrams of CT room ventilation air heat source……118
Figure 4.14. ORC with multiple heat sources T-s diagrams……... 119

NOMENCLATURE

SYMBOL	UNIT	DESCRIPTION
A	m^2	Area
COP		Coefficient of performance
COP_{double}		Double-effect COP
COP_{half}		Half-effect COP
COP_{single}		Single-effect COP
$Cost_{fuel}$	\$/kWh	Fuel price for power plant per electrical energy generated
$Cost_{electricity}$	\$/kWh	Distributed electricity price per electrical energy consumed
C_p	kJ/kg-K	Specific heat capacity
CR		Circulation ratio
CT		Combustion turbine
ΔT	K	Temperature difference
ε_{2nd}		Second law effectiveness or exergy efficiency
ε_{cond}		Condenser effectiveness
ε_{evap}		Evaporator effectiveness
ε_{heater}		Heater effectiveness
$\varepsilon_{precooler}$		Precooler effectiveness
ε_{regen}		Regenerator effectiveness
ε_{shx}		Solution heat exchanger effectiveness

η_{pump}		Pump isentropic efficiency
η_{th}		Thermal efficiency
$\eta_{turbine}$		Turbine isentropic efficiency
$\dot{H}_{air,CT}$	kW	Enthalpy of air to compressor
$\dot{H}_{exhaust,CT}$	kW	Enthalpy of exhaust gas from gas turbine
$\dot{H}_{exhaust,hrsg}$	kW	Enthalpy of exhaust gas from HRSG
HR	kJ/kWh	Heat rate
HRSG		Heat recovery steam generator
$h_{oil,i}$	kJ/kg	Specific enthalpy of lube oil at oil tank inlet
$h_{oil,o}$	kJ/kg	Specific enthalpy of lube oil at oil tank outlet
h_s	kJ/kg	Isentropic specific enthalpy
$h_{vent,i}$	kJ/kg	Specific enthalpy of ventilation air entering CT room
$h_{vent,o}$	kJ/kg	Specific enthalpy of ventilation air leaving CT room
$h_{water,i}$	kJ/kg-K	Specific enthalpy of cooling water at cooling tower inlet
$h_{water,o}$	kJ/kg-K	Specific enthalpy of cooling water at cooling tower outlet
$\dot{I}$	kW	Irreversibility
$\dot{m}_c$	kg/s	Cold-side fluid mass flow rate
$\dot{m}_{cw}$	kg/s	Chilled water mass flow rate
$\dot{m}_h$	kg/s	Hot-side fluid mass flow rate
$\dot{m}_{oil}$	kg/s	Lubrication oil mass flow rate
$\dot{m}_{orc}$	kg/s	Organic Rankine Cycle mass flow rate

$\dot{m}_r$	kg/s	Rich solution mass flow rate
$\dot{m}_{soure}$	kg/s	Heat source mass flow rate
$\dot{m}_{vent}$	kg/s	Ventilation air mass flow rate
$\dot{m}_v$	kg/s	Vapor mass flow rate
$\dot{m}_w$	kg/s	Weak solution mass flow rate
$\dot{m}_{water}$	kg/s	Cooling water mass flow rate
MS		Multiple heat sources
P	kPa	Pressure
Φ	kW	Energy availability
$\dot{Q}$	kW	Heat transfer rate
$\dot{Q}_{abs}$	kW	Absorption heat capacity
$\dot{Q}_{cond}$	kW	Condensing heat capacity
$\dot{Q}_{cond,high}$	kW	High-pressure condenser heat
$\dot{Q}_{cond,low}$	kW	Low-pressure condenser heat
$\dot{Q}_{CT,i}$	kW	Fuel energy to combustion turbine
$\dot{Q}_{evap}$	kW	Evaporation heat capacity
$\dot{Q}_{gen}$	kW	Generator heat capacity
$\dot{Q}_{gen,high}$	kW	High-pressure generator heat
$\dot{Q}_{gen,low}$	kW	Low-pressure generator heat
$\dot{Q}_{heater}$	kW	Heater heat capacity
$\dot{Q}_{hrsg}$	kW	HRSG Heat recovery
$\dot{Q}_{max}$	kW	Maximum heat transfer rate
$\dot{Q}_{oil}$	kW	Lubrication oil heat capacity
$\dot{Q}_{precooler}$	kW	Precooler heat capacity
$\dot{Q}_{rect}$	kW	Rectifier heat capacity
$\dot{Q}_{regen}$	kW	Regenerator heat
$\dot{Q}_{shx}$	kW	Solution heat exchanger heat transfer

$\dot{Q}_{sink}$	kW	Heat sink capacity
$\dot{Q}_{source}$	kW	Heat source capacity
$\dot{Q}_{vent}$	kW	Heat capacity of combustion turbine room ventilation air
$\dot{Q}_{water}$	kW	Cooling water heat capacity
s	kJ/kg-K	Specific entropy
s_s	kJ/kg-K	Isentropic specific entropy
T	°C, K	temperature
$T_{cw,i}$	°C	Chilled water inlet temperature to evaporator
$T_{cw,o}$	°C	Chilled water outlet temperature off evaporator
T_0	°C	Surrounding temperature or dead state temperature
T_{sink}	°C	Sink temperature
U	kW/m^2-K	Heat transfer coefficient
$\dot{W}_{CT,o}$	kW	Combustion turbine work output
$\dot{W}_{net}$	kW	Net work
$\dot{W}_p$	kW	Pump work
$\dot{W}_{turbine}$	kW	Turbine work
x_r		Rich concentration
x_v		Vapor concentration
x_w		Weak concentration

ABSTRACT

Upathumchard, Ularee. M.S.M.E., Purdue University, December 2014. Waste Heat Recovery Options in a Large Gas-Turbine Combined Power Plant. Major Professor: Eckhard A. Groll, School of Mechanical Engineering.

This study focuses on power plant heat loss and how to utilize the waste heat in energy recovery systems in order to increase the overall power plant efficiency. The case study of this research is a 700-MW natural gas combined cycle power plant, located in a suburban area of Thailand. An analysis of the heat loss of the combustion process, power generation process, lubrication system, and cooling system has been conducted to evaluate waste heat recovery options. The design of the waste heat recovery options depends to the amount of heat loss from each system and its temperature. Feasible waste heat sources are combustion turbine (CT) room ventilation air and lubrication oil return from the power plant. The following options are being considered in this research: absorption chillers for cooling with working fluids Ammonia-Water and Water-Lithium Bromide (in comparison) and Organic Rankine Cycle (ORC) with working fluids R134a and R245fa. The absorption cycles are modeled in three different stages; single-effect, double-effect and half-effect. ORC models used are simple ORC as a baseline, ORC with internal regenerator, ORC two-phase flash expansion ORC and ORC with multiple heat sources. Thermodynamic models are generated and each system is simulated using

Engineering Equation Solver (EES) to define the most suitable waste heat recovery options for the power plant. The result will be synthesized and evaluated with respect to exergy utilization efficiency referred as the Second Law effectiveness and net output capacity. Results of the models give recommendation to install a baseline ORC of R134a and a double-effect water-lithium bromide absorption chiller, driven by ventilation air from combustion turbine compartment. The two technologies yield reasonable economic payback periods of 4.6 years and 0.7 years, respectively. The fact that this selected power plant is in its early stage of operation allows both models to economically and effectively perform waste heat recovery during the power plant's life span. Furthermore, the recommendation from this research will be submitted to the Electricity Generating Authority of Thailand (EGAT) for implementation. This study will also be used as an example for other power plants in Thailand to consider waste energy utilization to improve plant efficiency and sustain fuel resources in the future.

CHAPTER 1. INTRODUCTION

1.1 Background

Electric power has been one of the most important essentials driving this planet for many decades. The use of electricity spreads globally into all four energy-consumption sectors: industrial, transportation, residential, and commercial. In order to meet such high demand, sufficient amounts of electricity must be generated to supply to its load in a precise manner. While the power demand keeps increasing, fossil fuels which are the main resources for power generation, are rapidly depleting and will no longer be adequate to meet global power needs. In addition to seeking sustainable power solutions, effective use of fossil fuels is another challenging goal for power plant technology, which many research and development initiatives are focusing on.

Developed from traditional fossil-fuel fired power plants with average efficiencies of 30 to 40 percent, new power plants include heat recovery systems to increase their efficiency. Gas-turbine combined cycle power plants (GTCC) seem to be the best technology so far among all with the average efficiencies of 50 to 60 percent. Most combined cycle power plants use natural gas a primary fuel and diesel oil as a secondary. High temperature exhaust gas from the combustion process then flows through a heat recovery steam generator (HRSG) to boil water and generate steam feeding into a steam turbine. Electric power is converted from shaft power of both gas and steam turbines.

Although installation of the HRSG helps increasing power plant efficiency, GTCC power plants still have another 40 to 50 percent of heat loss throughout the power generation process. Major heat loss occurs at the steam condensers which is necessary to displace an amount of heat in order to maintain the closed feed water system to the boilers. Minor heat loss can be found at other equipments' coolers. Although not as high in temperature as the exhaust gas, this heat stream may potentially be a heat input for other low-grade heat driven systems. This idea has become a starting point of low-grade waste heat recovery (WHR) systems. Research has been carried out aiming for the best utilization of the heat source availability and highest output at the reasonable cost. However, different plant characteristics, and operation and operating conditions, make these WHR technologies challenging when finding the best way to exercise the systems for the most suitable solution for each power plant.

1.2 Motivation

Thailand is the second largest energy consumption country while Indonesia ranks first among the ten countries that are members of the Association of Southeast Asian Nations (ASEAN). The graph shown in Figure 1.1 compiles data from World Bank's Databook and presents the increase of electricity production of Thailand over ten years as well as representing the country's electricity consumption trend. Because domestic energy resources are limited to natural gas from the Gulf of Thailand and coal in the northern region, Thailand has to import energy from neighboring countries such as Myanmar, Laos and Malaysia, to serve the demand.

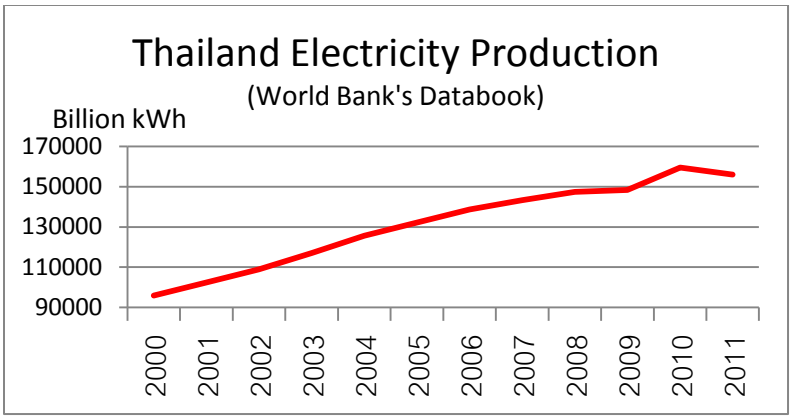

Figure 1.1. Electricity production of Thailand (2000-2011).

The energy resource chart for electricity production is provided in Figure 1.2. Due to the energy consumption growth, energy resource depletion is greatly concerned for the long run. Shown in the Southeast Asia Energy Outlook (IEA 2013), Thailand prepares its key energy policies for electricity production to gradually reduce the share of natural gas and increase renewable energy. This will maintain the availability of domestic natural gas resource for a few more decades. However, importing of coal and natural gas from other country has been planned.

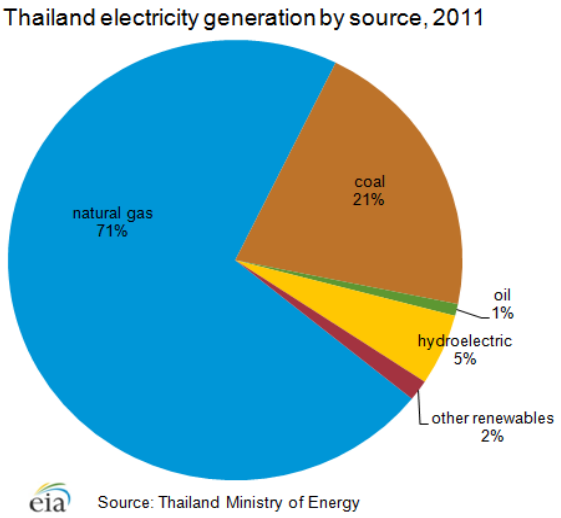

Figure 1.2. Primary energy sources for electricity generation of Thailand (2011).

While more renewable energy systems are being constructed, at the same time, power companies and researchers are working on enhancement of existing power plants efficiency. The Electricity Generating Authority of Thailand (EGAT), the largest power generation company owned by the Thai government, has the role of improving all their major power plants throughout the country, which includes 14 gas-turbine combined cycle power plants, 12 units of coal-fired thermal power plants, 11 gas-turbine power plants, and 6 hydroelectric power plants. From EGAT's company profile and mission, the total generation capacity takes up 44% of the country. EGAT's improvement policies cover maintaining high power plant reliability, increasing power availability, and development of systematic maintenance. Given the current number of GTCC power plants and a few under-construction plants that are going to start operating in the near future, it is feasible to research and implement waste heat recovery systems to these power plants.

1.3 Objective

The primary objective of this thesis is to theoretically find the best waste heat recovery options for the available waste heat streams from power plants in Thailand. The proposed options are divided into two heat utilization approaches, heat engine and heat pump systems, for the selected GTCC power plant. Models are evaluated in waste-heat utilization competency and output capacity perspectives in order to make a reasonable theoretical recommendation to EGAT. Various models of Organic Rankine Cycle (ORC) are studied and represented as the heat engine system. Utilization of the waste-heat source is thermodynamically evaluated in terms of exergy effectiveness, together with the

power output from the models, and then compared among the heat engine category. For the heat pump category with cooling aspect, models of absorption chillers are studied. The exergy effectiveness and cooling capacity are used to evaluate and compare the performance of these models. Lastly, an economic analysis is conducted to define payback period of each technology.

The secondary objective is to use this work as a pilot project for an earnest power plant WHR implementation in Thailand, and to initiate other power plants to actively analyze their heat loss and consider having WHR system to improve plant efficiency in the future.

1.4 Overview

The thesis presents the research work in five chapters, including the introduction in Chapter 1. A literature review is presented in Chapter 2, separated into three sectors as follows: current WHR technologies in industrial and power production plants, ORCs, and absorption chillers technologies.

Chapter 3 describes how the selected GTCC power plant operates including its characteristic and operating conditions that are the inputs for the proposed models. A heat loss analysis is demonstrated. Modeling of WHR systems, which are ORC and absorption chillers, is described in detail by components and put together into cycle models. Four different ORCs and five different absorption cycles are studied. Assumptions used for the analysis of both approaches are listed independently. Chapter 3 also explains how to thermodynamically evaluate the waste heat utilization of the systems and the evaluation

indicators, as well as a simple economic analysis of approximate payback calculation. Results of the models are summarized and discussed in Chapter 4. Lastly, Chapter 5 presents the conclusion of this work and proposes a recommendation of the best WHR options for the selected power plant.

CHAPTER 2. LITERATURE REVIEW AND SYSTEM DISCRIPTION

This chapter is separated into three subchapters to cover overall waste heat recovery technology, absorption chiller technology and Organic Rankine Cycles (ORC).

The first subchapter explores the literature related to waste heat recovery technologies in several areas: definition and principles of waste heat, potential waste heat sources, key opportunities for research, factors related to technology development and benefits of waste heat recovery systems. The selected method for waste heat recovery system analysis is explained and the current applicable waste heat technologies are presented.

The second subchapter describes how absorption chillers work in various heat-effected models using two pairs of working fluid, which are water - lithium bromide (H_2O/LiBr) and ammonia – water (NH_3/ H_2O). A literature review on implementations of absorption chiller technology is also included in this subchapter.

ORC technology is presented in the last subchapter. Models of traditional and modified ORCs are described. The literature review of ORC explains the selection of working fluids and current ORC applications.

2.1 Waste Heat Recovery Technologies

Reported in the Trends in Global Energy Efficiency 2011 researched by ABB and Enerdata (2011), "globally, the share of losses in energy conversion in primary energy intensity increased from 27 percent in 1990 to 31 percent in 2010. On one hand, the growth in conversion losses can be explained by the rapid development of electricity end uses and, on the other hand, by the fact that electricity is mainly generated from thermal sources, with 60-70 percent losses. At the global level, around 20 percent of energy productivity gains are counterbalanced by increasing losses in energy conversion". According to this data, there are significant amounts of waste energy discharged from most thermal power plants worldwide. This matches thermal power plant thermal efficiency of approximately 30 to 40 percent. The major loss in a thermal power plant is in the form of heat discharged from the condenser to a cooling fluid, which accounts for half of the overall energy losses, while the boiler occurs to have the most irreversibility due to the combustion process (Murehwa, Zimwara, Tumbudzuku and Mhlanga, 2012).

Besides the energy loss in power generation, enormous amounts of waste energy occur in heavy-duty industrial factories such as those in chemicals industries, petroleum refineries, mining factories, fabricated metal manufacturing and cement manufacturing. These heat losses occur in the main processes of the plants that usually involve high temperatures.

Due to the global energy crisis that first stroked the world's economics in the 1970s and has continued on until today (Behrens, 2011), many large energy-consuming countries actively put effort into energy security, release policies to sustain fossil energy

resources and invest in research and development of energy systems. It is stated in the Waste Heat Recovery Technology and Opportunities in U.S. Industry by U.S. DOE (2008) that "efforts to improve industrial energy efficiency focuses on reducing the energy consumed by the equipment used in manufacturing (e.g., boilers, furnaces, dryers, reactors, separators, motors, and pumps) or changing the processes or techniques to manufacture products."

However, capturing and reusing the energy loss, or waste heat, can be another feasible option to improve overall efficiency as well since it has no surplus in emission and energy consumption. In 2008, U.S. DOE suggested "three essential components in waste heat recovery" as shown in Figure 2.1. In order to implement waste heat recovery technology in any industries, one must have the waste heat sources, a developed heat recovery technology and an end user for the recovered heat, or in other words, this technology must be useful.

Two approaches serving these three essentials are to create new heat recovery technologies and to enhance existing ones. The benefits of both approaches are increasing recovered energy, lowering the cost to a feasible level with minimum payback period and mitigate environmental risk, as well as to improving options for end-users.

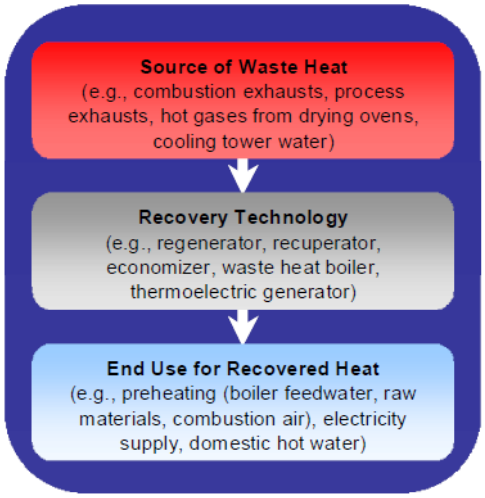

Figure 2.1. Three essential components required for waste heat recovery (U.S. DOE 2008).

The first essential component of the waste heat recovery discusses sources of waste heat. The Department of Energy, Mines and Resources of Canada defined waste heat as "the heat contained in a substance rejected from a process at a temperature higher than the ambient levels of the plant. Waste heat is any source of rejected heat having portion which may be recovered and re-used economically." Arzbaecher, Fouche, and Parmenter from Global Energy Partners (2007) suggested three key parameters used to evaluate feasibility of waste-heat profile are quantity, quality and availability. These parameters can be summarized into a thermodynamic availability equation as

$$\Phi = \dot{Q}\left(1 - \frac{T_o}{T}\right) \tag{2.1}$$

where $\dot{Q}$,which is the energy contained in the heat stream, refers to the quantity of the waste heat. T expresses as a heat stream quality or temperature, T_o is the ambient temperature, and Φ, which is the availability of energy in the heat stream, represents the

measurement of availability in the heat source. These three parameters must be taken into consideration altogether to select a heat source to be recovered.

The 2008 U.S. DOE also discussed the opportunities and challenges that focus on improving existing heat recovery systems. In the broad area of industry, waste heat streams are usually found at three different levels of temperature: high (more than 650°C), medium (230 – 650°C) and low (less than 230°C). Effective technologies, such as heat recovery steam generators (HRSGs) in gas-turbine combined cycle power plants, are used to recover waste heat at high and medium temperatures. These technologies have been successfully implemented worldwide and provide significant energy recovery. However, there are fewer systems running at low-grade waste heat, which is discharged at low temperature. According to this temperature constraint, it is challenging to enhance heat utilization in the lower range of operating temperature for waste heat recovery systems.

Cost is the major factor in the development of waste heat recovery technology. Running a system at low temperature means a smaller temperature difference between the heat source stream and the sink fluid because heat must be rejected from higher to lower temperature. This can increase the cost of heat exchangers due to the larger heat exchanged size. The correlation between temperature difference and heat exchanger area can be expressed in Equation 2.2 and Figure 2.2 as

$$\dot{Q} = UA\Delta T \tag{2.2}$$

where $\dot{Q}$ is heat transfer rate, U is the heat transfer coefficient, A is the surface area where heat is transferred and ΔT is the magnitude of difference between source and sink temperatures. Besides heat exchanger size, equipment material is another concern. Some high-efficiency systems require the expansion process to fall in the two-phase region. If the expansion process is performed by a turbine spinning at a very high rotational speed, droplets of liquid formed during the two-phase region can cause major damage to the equipment. When the systems are not operated as a continuous cycle, both heat source and heat recovery systems, load variation occurs in the system and causes vibration and stress to the equipment. High strength materials, such as titanium, must be used to build this machine. Higher strength materials lead to a much higher capital cost of the system. After all, these heat recovery technologies are evaluated in terms of economics. Industries are not willing to install long payback period systems and sometimes these systems do not return high enough profit given the total cost which includes capital, operation and maintenance costs.

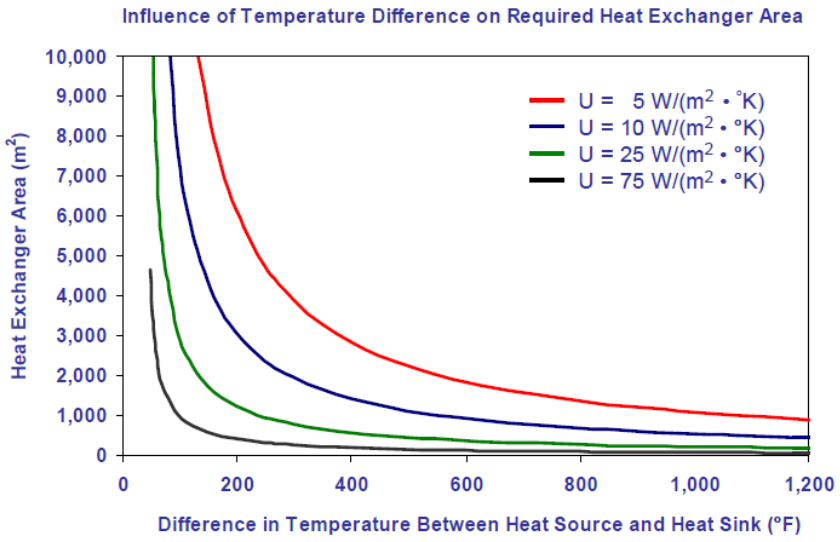

Figure 2.2. The correlation between temperature differences across the heat exchanger (ΔT) and required heat exchanger area (U.S. DOE, 2008).

Some heat recovery systems encounter temperature limits and higher cost during practical operation due to degrading, such as fouling, of the heat exchanger. This results in higher operation cost of these advantageous systems. Research can possibly be carried out to improve heat exchangers used in this application through the use of better materials, extending maintenance and cleaning intervals, and establishing effective maintenance programs.

Chemical corrosion is a limitation that makes it challenging to improve the system. Some heat source streams may contain chemical compositions that turn into toxicants at low temperature. This factor limits how far in temperature the heat stream can reach to utilize its energy availability. Losses from other waste heat sources, such as an extremely hot surface, product streams or lubricants are significant but are difficult to extract heat from because they are not accessible.

Lastly, exploring various end-use applications is a very important factor to take into consideration when developing technology. The technology itself must create benefits for the end-user to satisfy the market need. This includes industries' need as well. Industrial facilities must be able to support the installation and operation of the heat recovery systems and earn a practical benefit from them. These are the areas in need of research to decrease the system limitation.

The method being used widely to develop various waste heat recovery technologies is the pinch analysis. It was designed to optimize the systems of heat source and heat recovery pairs (Jolly, 2006). The four steps of the method are as follows (Arzbaecher et al., 2007):

- Study industry characteristics, operation data, operating conditions and plant's heat balance. Survey of space, facilities and accessibility of the potential waste heat source is necessary as well as the profit that the industry needs.
- Set the objective of the waste heat recovery system and take every restriction into account as realistically as possible.
- Make decision of systems to be designed and implemented.
- Develop and optimize the selected systems for the best performance in both technical and economic approaches

The method creates a solid structure for the development processes and leads to well organized projects. It allows researchers and users to share information and understand each other. These benefits reduce the amount of time it takes to complete the project as well as the cost.

Nowadays, applications of waste heat recovery are implemented in various industries. Table 2.1 shows levels of heat source temperatures with processes and equipment, where the heat streams are discharged, and the potential waste heat recovery systems to match those sources (U.S. DOE, 2008 and U.S. EPA CHP, 2012).

Table 2.1. Waste heat sources and potential applications classified by temperature range.

Temperature Range	Waste Heat Source	Characteristics	Waste Heat Recovery Technologies
High >650°C	Furnaces Iron cupolas Coke ovens Fume incinerators Hydrogen plants	High quality heat High heat transfer rate per area High power-generation efficiencies Chemical and mechanical contaminants	Waste heat boilers and steam turbines Pre-heaters
Medium 230 – 650°C	Steam boiler exhaust Gas turbine exhaust Reciprocating engine exhaust Heat treating furnaces Drying and baking ovens Cement kiln	Medium power-generation efficiencies Chemical and mechanical contaminants (some streams such as cement kilns)	Waste heat boilers and steam turbines (>230°C) Organic Rankine Cycle (<425°C) Kalina Cycle (<540°C) Pre-heaters
Low <230°C	Exhaust gas exiting recovery devices in gas-fired boilers Ethylene furnaces Steam condenser Cooling water Low-temperature ovens Hot process liquids or solids	Energy contained in numerous small sources Low-power generation efficiencies Recovery of combustion streams limited due to acid concentration if temperature reduced too low	Organic Rankine Cycle (>150°C gaseous streams, >80°C liquid streams) Kalina Cycle (>90°C) Heat pump cycles Space heating Domestic water heating

Waste heat recovery options can be described in three approaches, heating and cooling, heat engine and heat pumps. Heating and cooling applications refer to passive heating and direct cooling such as a pre-heater using waste heat to warm up working fluid and a condenser in which the waste heat stream acts as a sink medium. Waste heat recovery heat engine systems' main purpose is to produce electric power. Options and range of operating temperatures for these systems are shown in Table 2.2 (U.S. DOE 2008).

Table 2.2. Heat engine cycles in power generation for waste heat recovery.

Heat Engine Cycles	Waste Heat Sources Temperature Level	Sources of Waste Heat
Traditional steam cycle	High, Medium	Exhaust from gas turbine, reciprocating engines, incinerators and furnaces
Kalina cycle	Medium, Low	Gas turbine exhaust, boiler exhaust, cement kilns
Organic Rankine cycle (ORC)	Medium, Low	Gas turbine exhaust, boiler exhaust, heated water, cement kilns
Thermoelectric generation	High, Medium	Not yet demonstrated in industrial applications
Piezoelectric generation	Low	Not yet demonstrated in industrial applications
Thermal photovoltaic	High, Medium	Not yet demonstrated in industrial applications

While heat pump cycles tend to provide cooling capacity for refrigeration and air conditioning applications, heat pumps can either use waste heat as an input energy to drive the cycles or can be used to lift up the temperature level of the waste heat stream. The options for heat pump cycles are shown in Table 2.3 (IEA HPC and U.S. DOE, 2008).

Table 2.3. Heat pump technologies for waste heat recovery.

Heat Pump Technologies	Temperature Lift	Output Temperature	Waste Heat Sources Temperature Level
Mechanical vapor recompression systems (MVRs)	30 – 80°C	110 – 150°C	Low
Closed-cycle compression heat pumps	40 – 50°C	≤ 120°C	Low
Absorption heat pumps (Type I)	50 – 65°C	100 – 250°C	Medium, Low
Heat transformer (Type II)	50 – 60°C	≤ 150°C	Low

In addition to direct benefit of reducing fuel cost, waste heat recovery helps reduce environmental impacts. It reduces discharge temperature from industries to a lower level. This leads to high quality of cooling air, water, ecosystem around the plant areas, and lastly, green house gas emissions (GHG) are reduced because less fuel is used for the combustion process.

2.2 Absorption Chiller

Absorption technology is one of the common technologies used for low-grade waste heat recovery with the heat source temperature range of 75 - 200°C. There are various waste heat sources used to drive absorption cycles such as power plant's rejected heat (Garimella, Brown and Nagavarapu, 2011), waste heat from diesel engine (Keinath, Delahanty, Garimella and Garrabrant, 2012), internal combustion engine' exhaust (Longo, Gasparella and Zilio, 2002) and hot water (Ohuchi, Aizawa, Kawakami, Nishiguchi, Hatada and Kunugi, 1994). Waste heat is used in place of traditional thermal energy as an input energy for the system. This technology has been developed in two approaches which are absorption refrigeration (Type I) and absorption heat transformer or reverse absorption heat pump (Type II). However, the literature review will only cover the refrigeration approach.

2.2.1 Absorption and Desorption Processes

Absorption systems use a binary solution which consists of refrigerant and absorbent together as a working fluid. Figure 2.3(a) describes the absorption processes. In the absorption processes, refrigerant vapor, which is evaporated from the cooling load

(Q_L) in the evaporator, flows into the absorber and is absorbed into the high-concentration absorbent solution. During this process, heat (Q_I) must be rejected in order to absorb refrigerant because it is an exothermic process (Srikhirin, Aphornratana and Chungpaibulpatana, 2001). The desorption process occurs in the generator or desorber. Refrigerant is boiled out of the solution by the heat input (Q_H). Low absorbent-concentration solution leaves the desorber at the highest temperature in the cycle. The exiting refrigerant vapor is then condensed and rejects heat (Q_I) to the surroundings. The desorption process is shown in Figure 2.3(b)

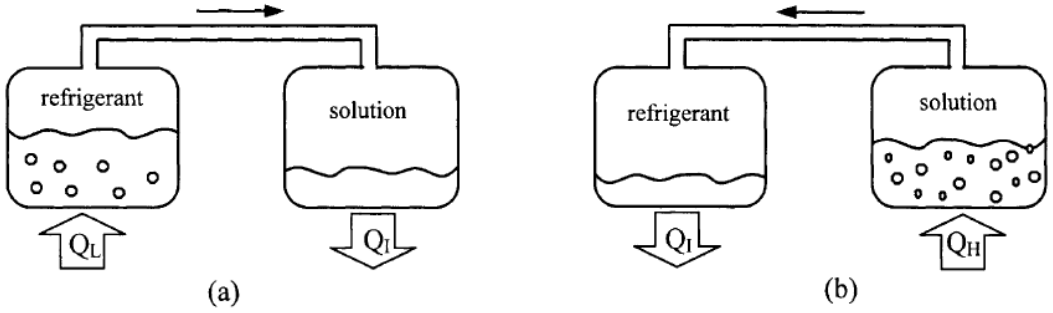

Figure 2.3. Absorption and desorption processes.

2.2.2 Working Fluids

Perez-Blanco (1984) revealed that chemical and thermodynamic properties of working fluids have a major effect on the performance of absorption systems. Srikhirin et al. (2001) stated that an important property of working fluids is the liquid working-fluid solution, which must mix homogeneously within the operating temperature range of the cycle. The mixture must also be chemically stable, non-toxic, non-explosive and non-flammable. Holmberg and Berntsson (1990) added the requirement to working fluid properties that the pure refrigerant and the absorbent must have a large difference of

boiling point at a certain pressure. Refrigerant should have high heat of vaporization in order to maintain low circulation ratio between absorber and generator. Both refrigerant and absorbent must have favorable transport properties and should be non-corrosive, environmental friendly and low-cost.

There are many working fluid pairs mentioned in the literature (Marcriss, Gutraj and Zawacki, 1988). However, the most common pairs of working fluid are water - lithium bromide water (H_2O/LiBr) and ammonia – water (NH_3/ H_2O). For NH_3/ H_2O, NH_3 acts as a refrigerant with water acting as an absorbent. For H_2O/LiBr, water performs as a refrigerant with LiBr as an absorbent.

Each of the two working fluid pairs has different outstanding advantages. NH_3/ H_2O pair was used first. Srikhirin et al. (2001) mentioned in the literature that NH_3/ H_2O can be used in a wide range of operating temperatures due to the high latent heat of vaporization and low freezing point (-77 °C) of NH_3. The fluids are environmental friendly and not expensive. However, due to volatility of both fluids, water vapor is carried out with NH_3 vapor during the desorption process. To address this, a rectifier must be included in the system to purify the NH_3 refrigerant. This prevents the water from freezing and causing damage to the pipe and expansion components as they operate at subzero degree-Celsius temperatures. In addition, cumulated water in the evaporator can lower performance.

H_2O/LiBr was developed later to eliminate rectifier from the system. Salt LiBr does not volatilize and it solutes in water during absorption - desorption process. Water is boiled out from the LiBr solution during desorption and generates pure water vapor

which leads to better cooling performance at the evaporator. Nevertheless, the cooling temperature is limited due to the freezing point of water refrigerant at 0°C (32°F). This means the cooling application using H_2O/LiBr cannot operate below this temperature and the system must be operated under vacuum pressure conditions. H_2O/LiBr also has a crystallization issue as high concentration and low operating pressure can cause LiBr to crystallize from the solution into salt. The crystallization chart for H_2O/LiBr is plotted in a pressure-temperature diagram, shown in Figure 2.4. To avoid crystallization during the absorption process, the highest salt concentration should be further to the left of crystallization line.

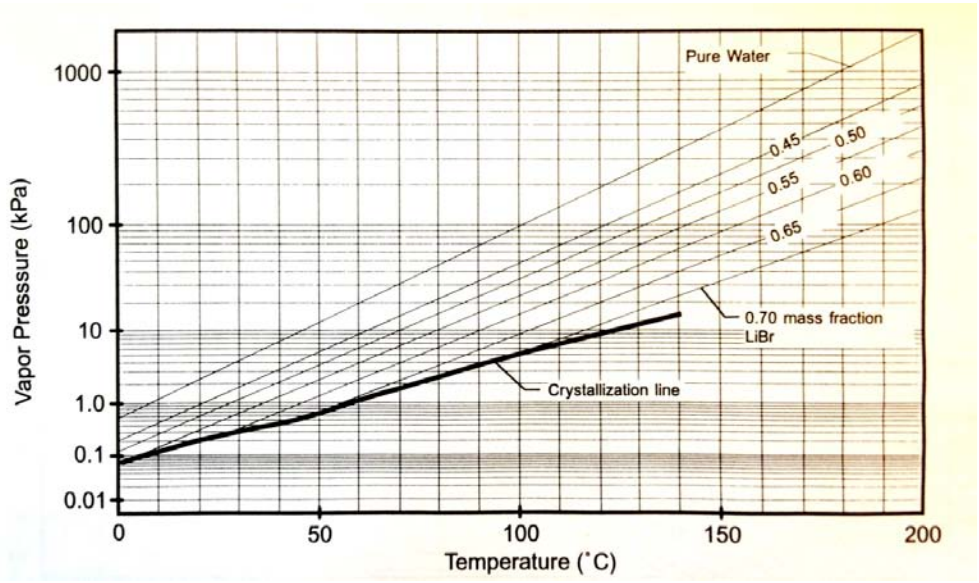

Figure 2.4. Pressure-temperature diagram for H_2O/LiBr (Herold et al., 1996).

2.2.3 Thermodynamic Principles of the Absorption Refrigeration Cycle

Single-effect absorption refrigeration is referred here as a simple cycle. Figure 2.5 illustrates the cycle configuration and Figure 2.5 shows the state points in a temperature-concentration diagram for NH_3/H_2O cycle (Groll, 2011). Rich solution is named for a

solution with a high concentration of refrigerant. The solution with low concentration of refrigerant is referred to as a weak solution. Groll (2011) explained Figure 2.5 and Figure 2.6 with thermodynamic principles the seven processes as follows;

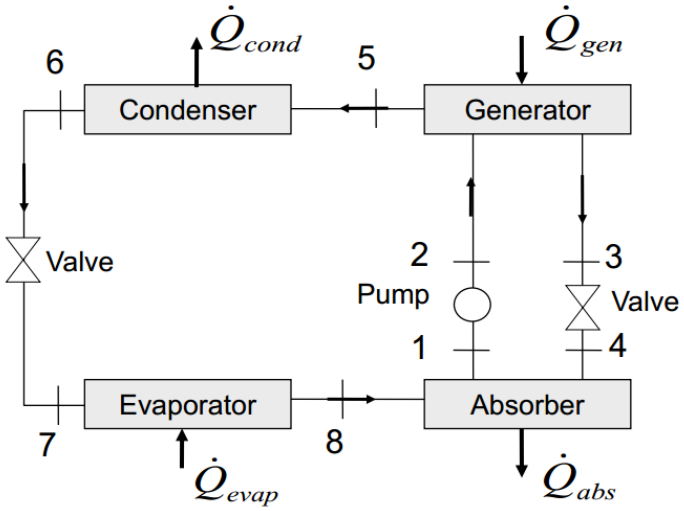

Figure 2.5. Simple single-effect absorption cycle (Groll, 2011).

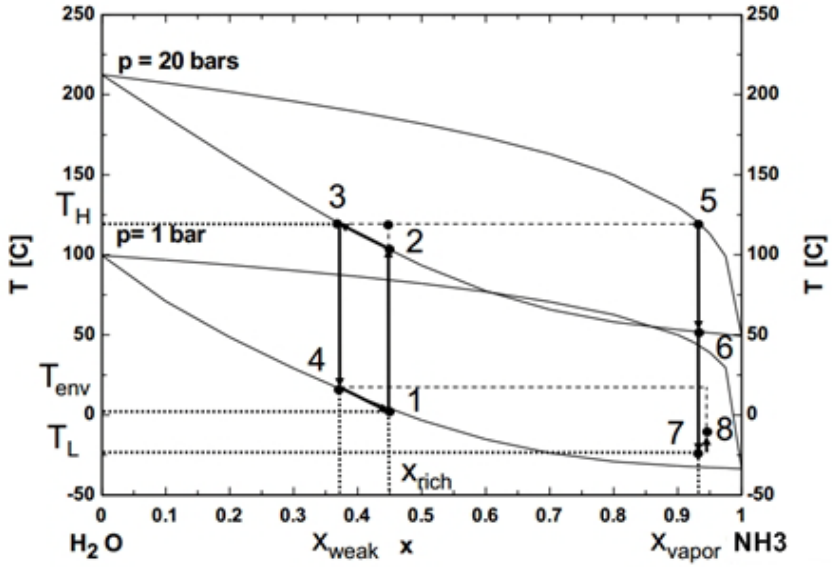

Figure 2.6. State points of a simple single-effect absorption cycle (Groll, 2011).

1. Pumping process (1 – 2) increases the pressure of saturated-liquid rich solution. Heat is usually added to bring state point 2 closer to saturated liquid.

2. Isobaric heat addition process (2 – 3 and 5) obtains additional heat from an external heat source. During this process, vapor (5) is simultaneously extracted from liquid rich solution (2) and leaves a saturated-liquid weak solution to state point 3. Vapor at state point 5 is ideally pure refrigerant or extremely concentrated refrigerant.

3. Isenthalpic expansion process (3 – 4) reduces the pressure to the lower operating pressure.

4. Isobaric heat rejection process (8 – 1 and 4) rejects heat to sink fluid or environment. Extremely concentrated refrigerant vapor, or ideally pure refrigerant vapor from state point 8, is simultaneously absorbed into liquid (occasionally two-phase) weak solution (4). The solution then becomes richer in refrigerant when it becomes saturated liquid at state point 1.

5. Isobaric condensation (5 – 6) rejects heat to sink fluid or environment from the vapor with extremely high refrigerant concentration. The exit state point 6 is saturated liquid.

6. Isenthalpic expansion (6 – 7) reduces the pressure to the lower operating pressure. State point 7 usually exits in two-phase region.

7. Isobaric evaporation (7 – 8) receives heat which is the cooling load of the cooling space or chilled water. Heat is obtained evaporate refrigerant or the two-phase solution of high-concentration refrigerant.

Various designs of absorption refrigeration cycles are used for waste heat recovery. A summary of cycles studied in this thesis is shown in Table 2.4.

Table 2.4. Summary of reviewed absorption refrigeration cycles.

System	Pressure Level	Operating Temperature (°C)		Working Fluid	Cooling Capacity (ton)	COP	Current Status	Remark
		Heat Source	Cooling					
Single-effect cycle	2	80–100	5–10	H_2O/ LiBr	10–100	0.5–0.7	Large water chiller	1. Simplest and widely use 2. Using water as a refrigerant, cooling temperature is above 0°C 3. Negative system pressure 4. Water cooled absorber is required to prevent crystallization at high concentration
	2	120–150	< 0	NH_3/H2O	3–25	0.5	Commercial	1. Rectification of refrigerant is required 2. Working solution is environmental friendly 3. Operating pressure is high as using NH_3 4. No crystallization problem 5. Suitable for using as heat pump due to wide operating range
Double-effect cycle	3	120–150	5–10	H_2O/ LiBr	Up to 1000	0.8–1.2	Large water chiller	1. High performance cycle which is available (series chiller commercially flow) 2. Heat of condensation from the first effect is used as heat input for the second stage
Half-effect cycle	3	Low	< 0	H_2O/ LiBr	N/A	0.2–0.3	Computer model	1. Poor efficiency and complicate 2. Suitable when driving heat is cheap or free, COP is claimed to be better than a single absorber-heat-model effect by 10%
	3	Low	5–10	NH_3/H2O	N/A	0.2–0.35		

Source: A Review of Absorption Refrigeration Technologies (Srikhirin et al., 2001) and CAC (1985)

2.2.4 Modification of Absorption Refrigeration Cycles

This literature survey will only cover modified NH_3/ H_2O single-effect absorption cycles. The original absorption cycle for NH_3/ H_2O is presented as Figure 2.5. However, extra components are designed and added to the original cycle in order to enhance its efficiency, which is indicated by an increase of the coefficient of performance (COP). Figure 2.7 illustrates the NH_3/ H_2O single-effect cycle with rectifier and solution heat exchanger. The purpose of the rectifier is to purify ammonia from the solution as much as possible. The higher concentration of ammonia helps the cycle to obtain more cooling load and increase refrigerating ability, hence reduce water accumulated in the evaporator. However, heat must be rejected during rectification. The solution heat exchanger reduces the amount of heat rejection at the absorber by transfer some heat from warm weak solution to heat up the cooler rich solution (Herold et al., 1996). Up to 60 percent of the coefficient of performance (COP) of the cycle can be increased when internal heat exchanger is used (Aphornratana, 1995).

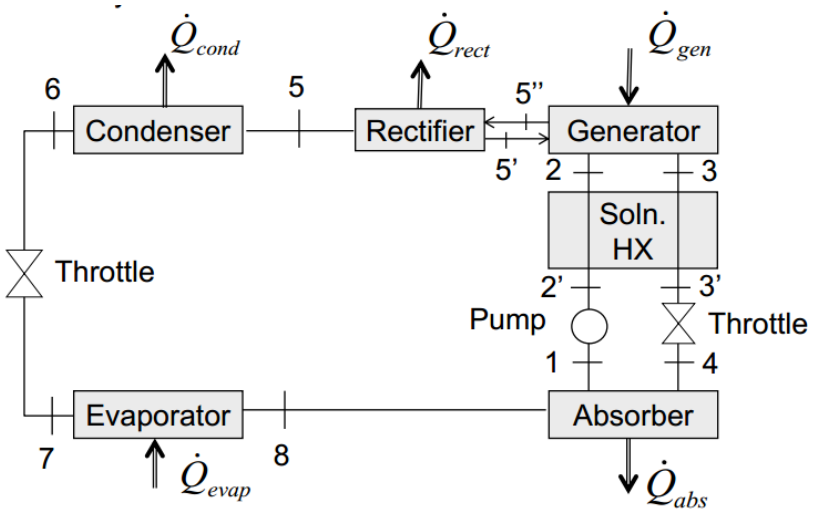

Figure 2.7. NH_3/ H_2O single-effect absorption cycle with rectifier and solution heat exchanger (Groll, 2011).

Another modified cycle is illustrated in Figure 2.8. Groll (2011) described the advantage and disadvantage of the cycle in Figure 2.8 as the precooler helps increase evaporator refrigerating ability with overall performance increases by approximately 10 percent. However, it forces the absorber to reject more heat to the environment. The cycle in Figure 2.8 can have additional modification, which falls in the heat utilization of rectifier heat rejection. The rich solution is heated up twice. The subcooled rich solution is pumped first to the rectifier to receive heat rejected from the rectifier and then into the solution heat exchanger to obtain heat transferred from the warm weak solution. The COP of the cycle shown in Figure 2.8 further increases by 2 percent.

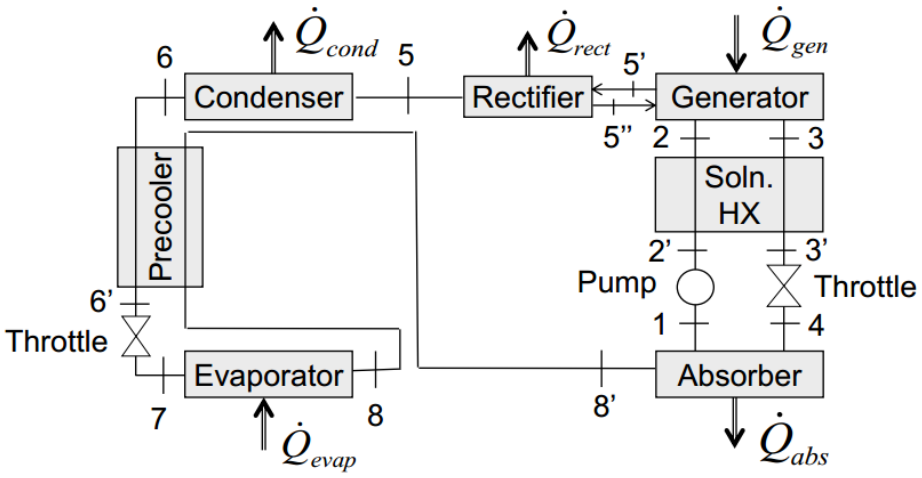

Figure 2.8. NH_3/ H_2O single-effect absorption cycle with rectifier, solution heat exchanger and precooler (Groll, 2011).

Besides modifications described above, there are a few more absorption cycles that are designed to be driven by higher and lower ranges of heat source temperatures. Herold et al. (1996) brought up an example of a certain operating condition of a half-effect absorption cycle which required a very low minimum heat input temperature of 74°C. However, Groll (1997) noted that heat rejected from a half-effect cycle is

approximately 50% more than a single-effect cycle and this causes a relatively low COP in the half-effect cycle performance.

Invention of double-effect absorption cycle started in the mid nineteenth century (Vilet, Lawson and Lithgow, 1982) and was proposed as a higher efficiency system compared to the single-effect. Because the double-effect cycle is designed to increase the utilization ability in energy availability, the cycle can operate at higher temperature heat input. Srikhirin et al. (2001) simply explained the double-effect cycle as a combination of two single-effect cycles, therefore gave an approximate COP correlation between the overall double-effect cycle and its corresponding single-effect cycles as Equation 2.3. According to this equation, the COP of double-effect cycle is higher than that of a single-effect cycle due to

$$COP_{double} = COP_{single} + (COP_{single})^2. \quad (2.3)$$

Moreover, multi-effect cycles have also been developed with more complexity. However, the double-effect cycle is the most commercially available technology in the current market (Ziegler, Kahn, Summerer and Alefeld, 1993).

2.3 Organic Rankine Cycle

Typically, a Rankine Cycle is designed to operate as a heat engine. The cycle uses water as a working fluid and generates steam for a power turbine. A high temperature (> 650°C) heat source such as coal-fired, gas turbine exhaust, biomass and nuclear reaction can be input energy to boil water. Superheated steam leaves the boiler and enters the steam turbine. Partial thermal energy in the steam is converted to mechanical shaft

power. The rest of the energy remains in the low-energy stream entering the condenser. Saturated water exiting the condenser is then pumped up as feed water back to the boiler, and closes the cycle. This type of cycle usually has a thermal efficiency up to 40 percent. Figure 2.9 shows a simple Rankine Cycle schematic and a temperature-entropy diagram of the cycle is shown in Figure 2.10.

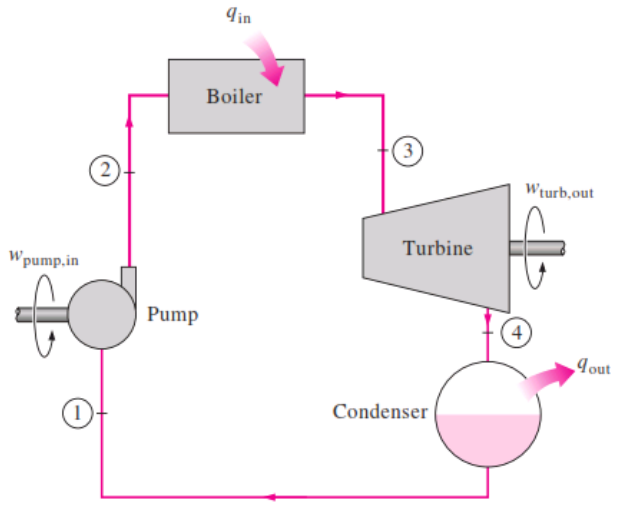

Figure 2.9. Simple Rankine Cycle (Bhattacharjee, 2012).

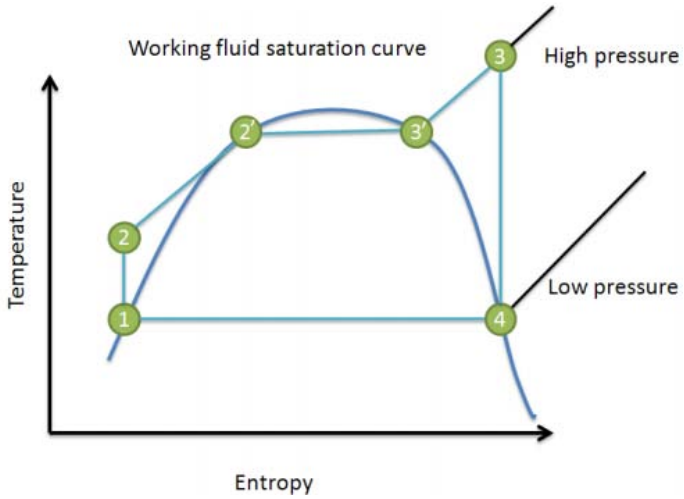

Figure 2.10. Temperature-entropy diagram of an ideal Organic Rankine Cycle (Poles and Venturin, Opengineering).

2.3.1 Thermodynamic Principles of Organic Rankine Cycle

Referring to Figure 2.9 and Figure 2.10, Quoilin (2008) described the ideal Rankine Cycle using the following four processes:

1. Isobaric evaporation (2 – 3) occurs in the evaporator without pressure drops in the heat exchanger. Range of temperatures in evaporating process can be divided into three steps which are preheating (2-2'), evaporation (2'-3') and superheating (3'-3).

2. Isentropic expansion (3 – 4) occurs across an adiabatic reversible turbine where there is no energy loss from heat transfer between the components and the environment. In other words, the energy difference between turbine inlet and outlet is completely converted to turbine work output.

3. Isobaric condensation (4 – 1) occurs in the condenser, condensing saturated vapor to saturated liquid. However, the condensation process may begin in the superheated region if the turbine releases vapor at a temperature higher than the saturated temperature of the exiting pressure. Likewise, the condensation process may end in the subcooled region if the working fluid is condensed to a temperature lower than the saturated temperature of the condensing pressure. The condensation process can be divided into three steps which are de-superheating, condensation and subcooling.

4. Isentropic pumping (1 – 2) occurs at an adiabatic reversible pump to increase the pressure of working fluid, in order to evaporate at the heat source temperature.

As stated by the second law of thermodynamics, irreversibility must occur in the cycle and causes the real cycle to experience lower thermal efficiency than the Carnot limit. Various forms of irreversibility can be found in every process.

An Organic Rankine Cycle (ORC) shares the same principle in cycle operation as the steam Rankine Cycle; however an organic substance, refrigerant or fluorocarbon, is used as a working fluid in place of water. The properties of the organic substances and refrigerants used as working fluids allow the ORC to perform at a lower heat source temperature (<425°C).

There are three types of ORCs, which are subcritical ORC and transcritical, ORC. These cycles are defined by the thermodynamic states of their working fluids. If both the heat input and the heat rejection processes of the working fluid occur at subcritical pressures, the cycle is called subcritical ORC. If heat input process occurs at a supercritical pressure and the heat rejection process occurs at a subcritical pressure, the cycle is called transcritical ORC. Although Kestin, DiPippo, Khalifa and Ryley (1980) proved that the transcritical cycle has more advantages than the subcritical cycle at medium heat source temperature (>200°C), its drawback is the larger size of components, such as heat exchanger and pipelines, which leads to higher system cost. This thesis will only investigate the subcritical ORCs due to limitations of the software used in the cycle analysis.

2.3.2 Pinch Point Analysis

The design of ORCs requires heat exchanger pinch points to limit cooling and heating processes in the cycles to make the systems closest to practical. Figure 2.11 illustrates temperature profiles in the heat exchangers and minimal pinch points on a temperature-entropy diagram. The pinch points are defined to give the heat exchangers a limit of heat transfer.

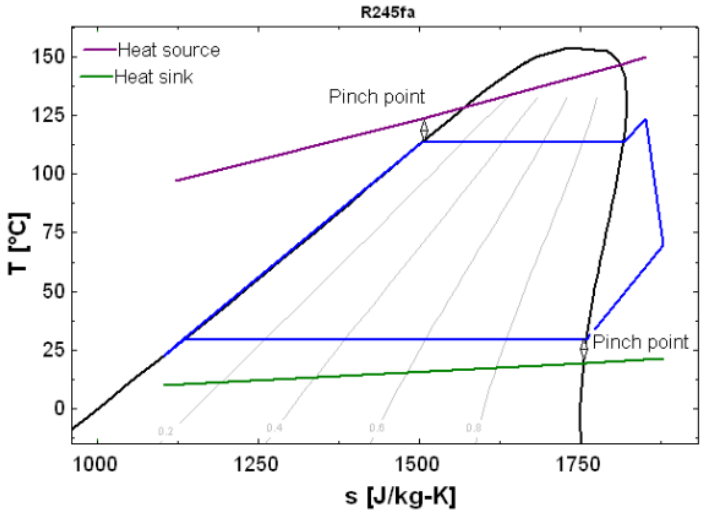

Figure 2.11. Pinch points in an R245fa ORC (Quoilin, 2008).

Quoilin (2008) explained that the heat source stream can only be cooled down to a certain temperature and cannot cut across the evaporation line to reach lower temperature as indicated in Figure 2.11; otherwise the heat exchanger will malfunction. This limitation also applies to the condenser. In order to cool the heat source stream down to a lower temperature, the evaporating pressure must be reduced which also decreases the cycle efficiency. Only by achieving a positive value at the pinch point can the heat exchanger operate properly. However, setting pinch points affects the size of heat exchangers. Smaller pinch points increases the amount of heat transferred and lead to larger heat exchangers, while higher pinch points allow smaller heat transfers which means only a smaller heat exchanger is required which helps reduce the cost. Quoilin (2008) also mentioned that pinch point values of 5 to 10 K will give an optimum economic performance in refrigeration. For ORCs, the pinch point value depends on the system configuration and heat sink and heat source temperatures.

2.3.3 Past and Current Research on Organic Rankine Cycles

Currently, ORC and modified ORCs are considered waste heat recovery technologies for which much research has been carried out (Liu et al., 2012). Most of the performance analysis of ORCs in waste heat recovery applications focuses on the thermal efficiency, availability utilization or exergy efficiency and cost effectiveness. Teng and Regner (2009) gave the result of up to a 20 percent increase in power efficiency of heavy-duty diesel engines after using an ORC to recover heat rejected from the Exhaust Gas Recirculation (EGR) cooler. Bombarda, Invernizzi and Pietra (2010) compared the performance of an ORC with the Kalina Cycle in utilization of waste energy from a diesel engine's exhaust gas. Although the generated power outputs were similar, the ORC performed with less cycle complexity and the installation of a smaller heat exchanger reduced cycle cost. Recently, Algieri and Morrone (2014) studied the performance of a biomass-fired power plant operating by ORCs in Italy. Various types of cycles were investigated including a modified ORC with equipped regenerative internal heat exchanger. Because biomass has such a low heating value, the results show that ORCs generate acceptable power output and the attached regenerator notably affects cycle performance.

2.3.4 Working Fluids

Apart from the ORC configuration, selecting a suitable working fluid is another key factor in order to achieve high cycle performance. ORC working fluids should have low boiling points to allow subcritical operation for the low-grade heat sources. Their critical temperatures and pressures should be significantly lower than that of water

(Lukawski, 2009). High density working fluid can help reduce the size of components and lower the system cost. Working fluids must be thermally and chemically stable (Quoilin, 2011), safe for the user, non-toxic and non-flammable.

Another important concern regarding working fluids is their environmental impact. Candidates for ORC working fluids are usually hydrocarbons and fluorocarbons (Kestin et al., 1980), which may have a strong impact to ozone depletion and global warming. According to regulations related to the ozone depletion potential (ODP) and global warming potential (GWP) of working fluids, many fluorocarbons are eliminated and replaced. Research is still ongoing towards the invention of new working fluids to improve properties and eventually replace the current use of high ODP and GWP fluids with zero impact.

Based on the previously described characteristics, the heat source temperature is another variable for choosing the best working fluid for an ORC to achieve high performance. Woodland (2013) investigated selected working fluids based on the commercially used criteria mentioned earlier.

The studied fluids represented wet, dry and isentropic fluids. Wet fluids are those with negative-slop saturated vapor line on a temperature-entropy diagram, dry fluids have positive-slop, and isentropic fluids have their saturated vapor line perpendicular to the entropy-axis. Properties of selected working fluids in Woodland (2013)'s work are presented in Table 2.5. Woodland (2013) plotted the maximum Second Law effectiveness (η_{II},finite) of the selected fluids in Table 2.5 as a function of heat source inlet temperature over an optimum simple ORC shown in Figure 2.9, with the assumption of neglecting

condenser fan power input. Figure 2.12 shows the result that R134a and R245fa are the best two working fluids for the studied ORC.

Table 2.5. Working fluids investigated in Woodland (2013)'s study (Woodland, 2013).

Working Fluid	Chemical Formula	Molecular Weight	Saturated Vapor Line	Critical Temperature (°C)	Critical Pressure (kPa)	Normal Boiling Point (°C)	Condensing Pressure at 35°C (kPa)
CO_2 (R744)	CO_2	44	wet (trans-critical)	31.0	7377	-78.4	N/A
R134a	$C_2H_2F_4$	102	isentropic (wet)	101	4059	-26.1	887
Ammonia (R717)	NH_3	17	Wet	132	11330	-33.3	1350
R245fa	$C_3H_3F_5$	134	isentropic (dry)	154	3651	15.1	212
Pentane (R601)	C_5H_{12}	72.1	dry	197	3370	36.1	97.7
Acetone	C_3H_6O	58.1	isentropic (wet)	235	4700	56	46.5
Water (R718)	H_2O	18	wet	374	22060	100	5.63

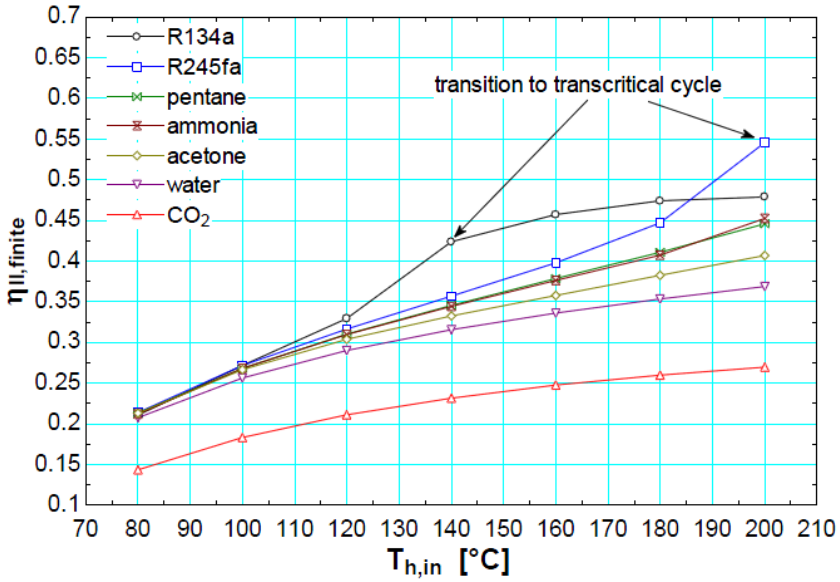

Figure 2.12. Maximum second law effectiveness of selected working fluids in Table 2.5 (Woodland, 2013).

CHAPTER 3. MODELING OF THE WASTE HEAT RECOVERY SYSTEMS

This chapter provides calculation of waste heat analysis and modeling of each waste heat recovery (WHR) cycle. It is divided into four subchapters. The first subchapter covers the investigation of waste heat from the selected gas-turbine combined cycle (GTCC) power plant in Thailand. Subchapter 2 covers absorption cycle analyses for absorption chillers. It provides theoretical modeling of components, explains different absorption cycles with H_2O/LiBr and NH_3/H_2O working fluid pairs. Theoretical modeling of Organic Rankine Cycle (ORC) is presented in Subchapter 3. Concepts of energy availability and availability utilization, analytical calculations, and evaluation of availability utilization are compiled in Subchapter 4. All models investigated are implemented in Engineering Equation Solver (EES) (Klein, 2013). Fluid properties and reference points are based on the EES software. Optimum performances of the cycles are selected from parametric studies conducted in EES. Subchapter 5 shows the calculation method of a simple economic payback period.

3.1 Heat Loss Analysis

The investigation of waste heat is conducted for a GTCC power plant in Thailand. This power plant is located in a suburban area surrounded by a residential area, office buildings and plant facility offices. There are two gas turbine units, each unit couples

with a heat recovery steam generator (HRSG) which consists of preheater (optional), economizers, superheated steam and reheated steam pipelines. Steam from both HRSGs feeds to a steam turbine, and then is condensed in the condenser. Condensate water is fed back to the HRSGF to start another cycle. Electric power is generated from the shaft power of the two gas turbines and a steam turbine. Figure 3.1 shows an illustration of a GTCC power plant as described. On the left-hand side of the picture, two gas-turbine units are presented in green and their HRSGs are in orange. Steam pipelines are located on the right-hand side where the steam turbine is presented in lime green. Referring to Figure 3.1, only two generators out of three can be seen and they are presented in dark blue.

Figure 3.1. Gas-turbine combined cycle power plant (Alstom.com).

3.1.1 Power Plant Operation and Characteristic

The GTCC power plant is considered one of the most common waste heat recovery technologies for high-grade waste heat. Most of GTCC power plants in

Thailand operate to serve as base-load. Natural gas is used as primary fuel while diesel oil is a back-up fuel. A gas turbine unit, shown in Figure 3.2, consists of the compressor, combustor and turbine. The compressor increases pressure and temperature of the intake air as it passes through each stage of the compressor and into the combustion chamber. Natural gas is fed into the combustor and ignited to burn with the compressed air. Exhaust gas from the combustion process that is extremely high in energy, pressure and temperature (>1000°C) enters the turbine parts, which creates propulsion forces and rotates the turbine. The whole gas turbine shaft, which connects to the generator shaft, rotates and then, electricity is produced. Although the energy and temperature of the exhaust gas leaving the gas turbine has dropped significantly, it is high enough to be recovered in the HRSG at temperatures of approximately more than 600°C.

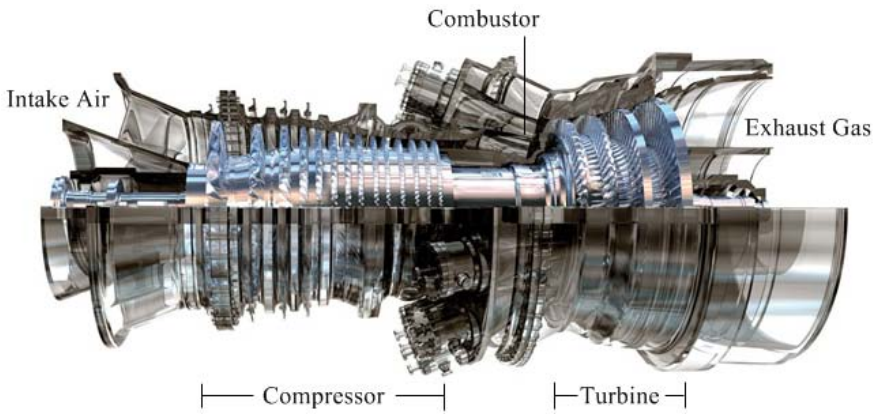

Figure 3.2. Gas turbine (GE-Flexibility.com).

The HRSG recovers heat from exhaust gas by using it to boil feed water. Figure 3.3 illustrates the water evaporating loops in the HRSG. Hot exhaust gas flows vertically from the bottom to the top of the HRSG and gradually transfer heat to every loop located in this recovery component. High-grade steam from the superheater loop flows to the

high-pressure steam turbine. The exiting steam returns to the HRSG to be reheated and fed to the intermediate-pressure and low-pressure turbines, respectively. Three stages of steam turbines are presented in Figure 3.4.

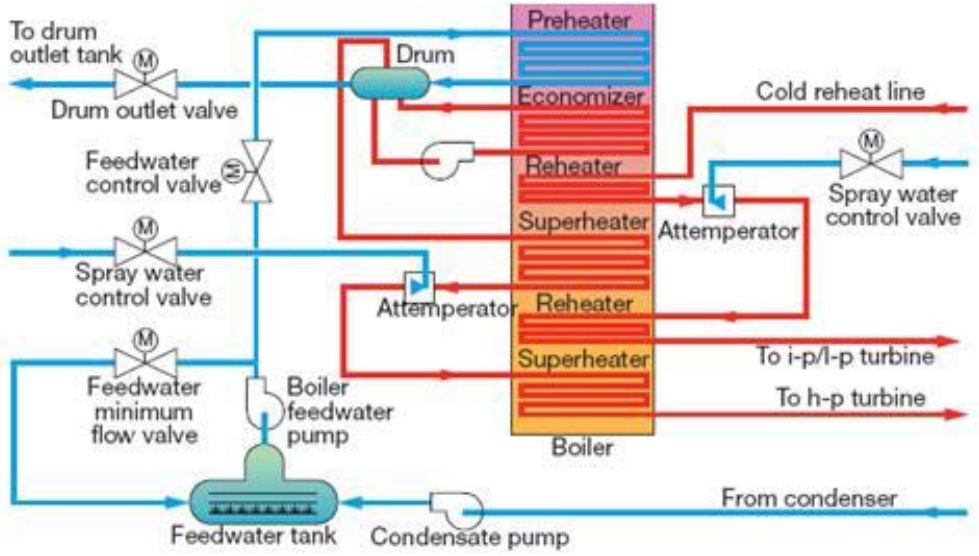

Figure 3.3. Heat recovery steam generator diagram (Combined Cycle Journal Online).

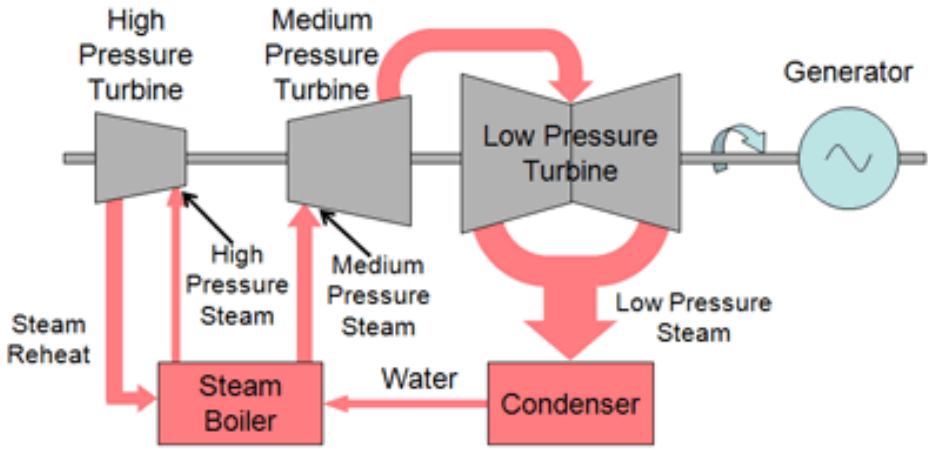

Figure 3.4. Multi-stage steam turbines and generator (mpoweruk.com).

Most GTCC power plants that serve as base load usually operate with both gas turbines and steam turbine together; this is called full-load operation. Moreover, GTCC

power plants have the flexibility to operate with a single gas turbine and steam turbine; this is called half-load operation. Half-load operation allows each gas turbine to have its maintenance separately while the rest of the power plant is still running. However, if the steam turbine is shut down for maintenance, both gas turbines are not in operation due to economic constrains. Figure 3.5 shows the GTCC half-block operation. The operation summary of the investigated GTCC power plant is presented in Table 3.1.

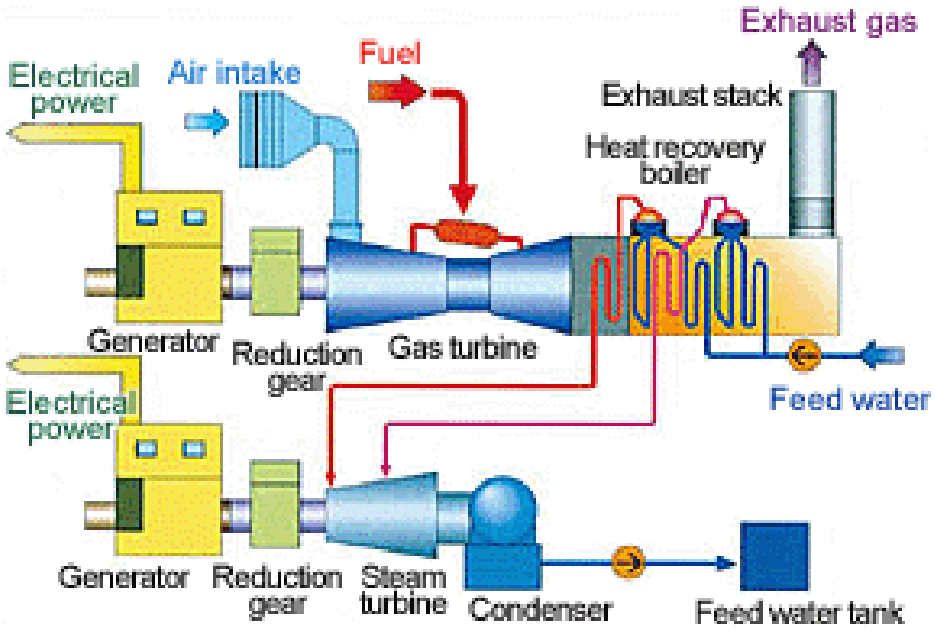

Figure 3.5. Half-block operation in GTCC power plant (Kawasaki TechnoBox).

Table 3.1. Operation summary for the studied GTCC power plant.

Operation duty	Full-load
Number of gas turbine	2
Number of steam turbine	1
HRSG Type	Vertical exhaust flow
Plant net capacity	703.6 MW
Combustion turbine (CT) gross capacity	227.4 MW
Steam turbine (ST) gross capacity	268.6 MW
CT gross generation (daily)	4,100 MWh

Table 3.1. continued.

ST gross generation (daily)	5,450 MWh
Plant net generation (daily)	13,300 MWh
Net efficiency	49 %
Net heat rate	7,350 kJ/kWh
CT gross heat rate	11,950 kJ/kWh
Total generation hours (as of July 2014)	28,820 hours
Primary fuel	Natural gas
CT fuel consumption	109.4 MMscf
CT exhaust gas temperature	620°C
HRSG exhaust gas temperature	101°C
Ambient temperature	32-33°C
Cooling water temperature inlet/outlet condenser (maximum)	27°C / 40°C
Cooling water mass flow rate	11,600 kg/s
Lubrication oil temperature inlet/outlet tank (design)	82°C / 54°C
Lubrication oil mass flow rate	40 kg/s
CT compartment air temperature	150°C

3.1.2 Combustion Turbine Ventilation Air

A gas turbine unit is usually located in a room with enclosed walls for safety and noise control. When the gas turbine is running, heat is generated in the compression and combustion processes. Some of the generated heat is transferred to the environment in forms of heat conduction through gas turbine case itself, heat convection to the ventilation air, and radiation. This heat rejected to the environment is considered heat loss.

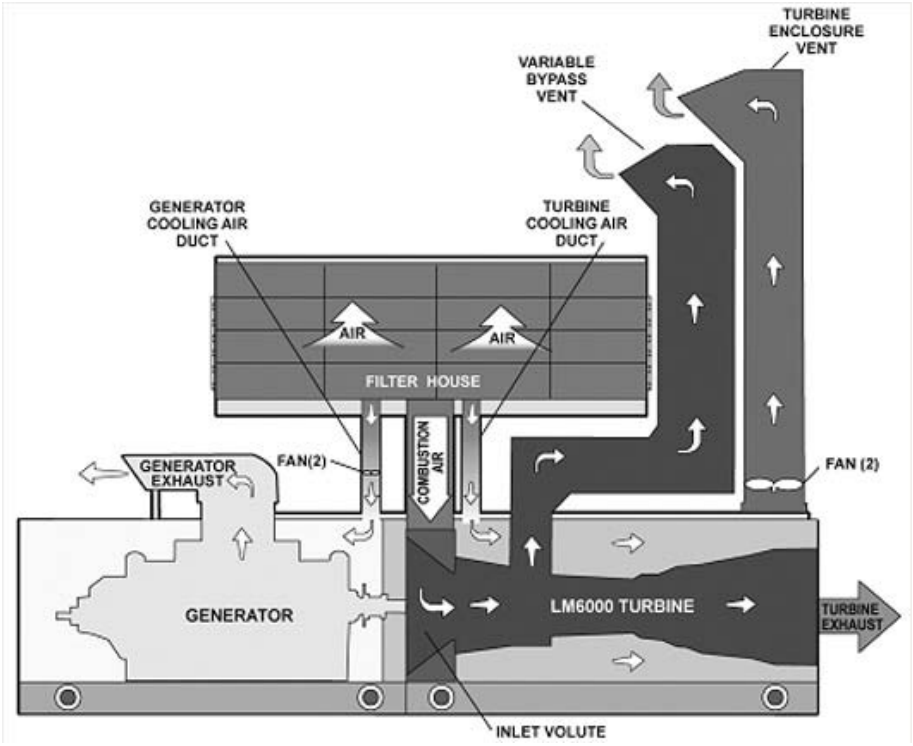

Figure 3.6. Combustion turbine enclosure and ventilation (grupogeinca.com).

However, ventilation air is necessary for the gas turbine compartment. When heat convection is transferred from the gas turbine surface to the air inside the room, without ventilation; temperature of the air increases as heat is accumulated, and causes damage to gas turbine case, material and the enclosure walls. Ventilation air helps rejecting this abandoned heat to the outside environment and keeps a constant room temperature. A fan is installed to accelerate the air-flow and increase the heat transfer coefficient. Figure 3.6 shows how the ventilation air flows from the gas turbine room through the fan and leaves at the turbine enclosure vent stack. The amount of heat loss to the ventilation air ($\dot{Q}_{vent}, kW$) can be calculated from combustion heat rate and energy balance. Figure 3.7 shows the combustor heat balance diagram.

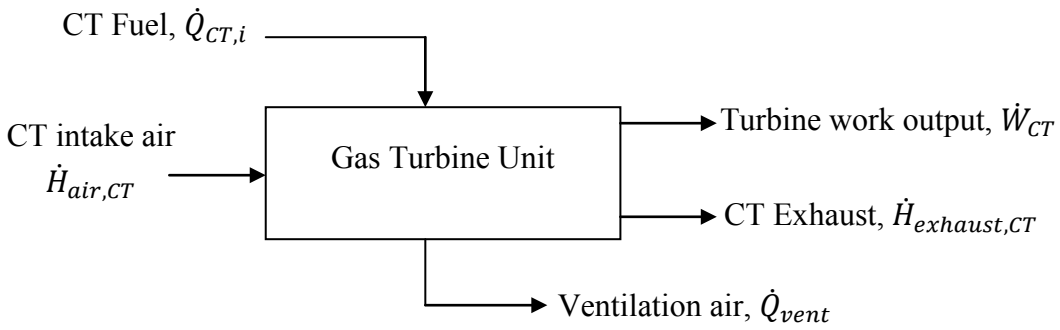

Figure 3.7. Combustor energy balance diagram.

The heat rate (HR, kJ/kWh) is presented in Equation 3.1 as a ratio of input fuel energy and turbine work output. A conversion of daily combustion turbine heat input to power is shown in Equation 3.2. Steady state and steady flow (SSSF) is assumed and changes in kinetic energy (KE) and potential energy (PE) are neglected,

$$HR = \frac{Q_{CT,i}}{W_{CT,o}} \tag{3.1}$$

$$\dot{Q}_{CT,i} = \frac{Q_{CT,i}}{24*60*60}. \tag{3.2}$$

The energy balance of the combustion process is shown Equation 3.3 and heat loss to ventilation ($\dot{Q}_{vent}$) can be calculated,

$$\dot{H}_{air,CT} + \dot{Q}_{CT,i} = \dot{H}_{exhaust,CT} + \dot{W}_{CT} + \dot{Q}_{vent}. \tag{3.3}$$

In order to maintain a constant room temperature, a mass flow rate of ventilation air can be calculated by obtaining the gas turbine room as a control volume. An energy balance over this control volume is presented in Equation 3.4 and a diagram is shown in Figure 3.8. The same assumptions as applied to Equation 3.3 are being used. In addition, it is

assumed that the heat loss from the gas turbine is completely transferred to the ventilation air. The energy balance equation can be defined as

$$\dot{Q}_{vent} = \dot{m}_{vent}(h_{vent,o} - h_{vent,i}). \quad (3.4)$$

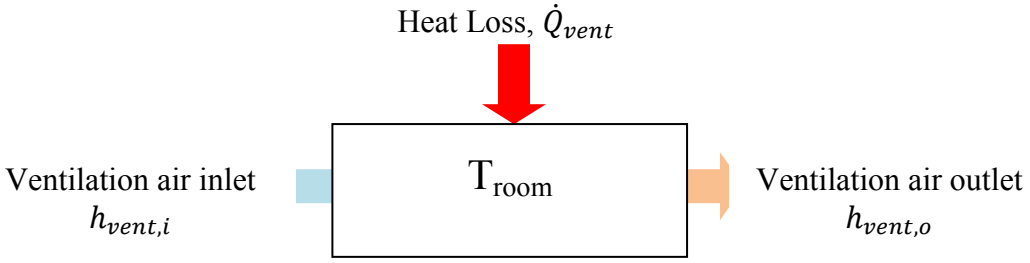

Figure 3.8. Heat-flows in a gas turbine compartment.

3.1.3 Heat Recovery Steam Generator (HRSG) Exhaust

The gas turbine's exhaust gas has its energy recovered by the HRSG and leaves the stack at a temperature of 100 to 110 °C. An energy flow diagram is illustrated in Figure 3.9. The exhaust gas compositions are listed in Table 3.2. The energy balance is given in Equation 3.5,

$$\dot{Q}_{HRSG} = \dot{m}_{exhaust}(h_{exhaust,i} - h_{exhuast,o}). \quad (3.5)$$

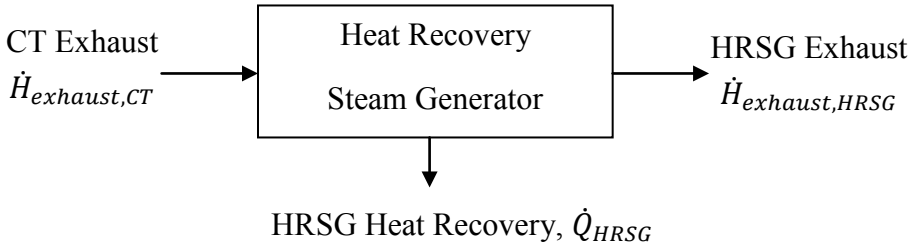

Figure 3.9. HRSG energy balance diagram.

Table 3.2. Exhaust gas compositions.

Argon (Ar)	0.86 %volume
Nitrogen (N_2)	72.55 %volume
Oxygen (O_2)	11.97 %volume
Carbon dioxide (CO_2)	4.04 %volume
Water (H_2O)	10.59 %volume
Mono nitrogen oxides (NO_x)	30 vppm
Sulfur dioxide (SO_2)	0.90 vppm
Sulfur trioxide (SO_3)	0.5 vppm

Although the HRSG exhaust gas has a potential of medium temperature for heat recovery, it is limited by the final flue gas temperature, which must be above acid dew points when it is released to the environment. As the amount of SO_3 appears to be the most significant acid compared to other acids, the acid dew point of SO_3 is taken into consideration. The selected plant's operation has an SO_3 acid dew point at 105 to 110 °C, as shown in Figure 3.10. Based on strict regulations for health and safety, and corrosion concerns, the use of this waste heat source is impossible at this stage.

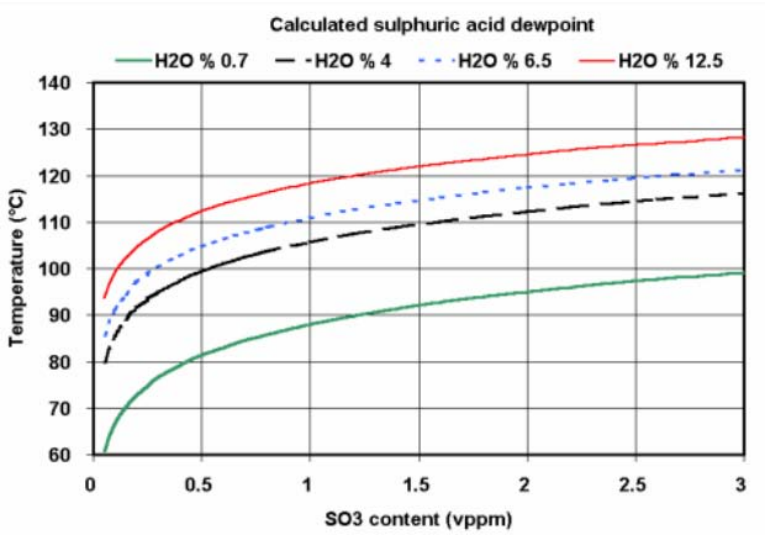

Figure 3.10. Dew points of SO_3 at various water contents of the gas, calculated from the formula of Verhoff (Sinha and NETRA, 2012).

3.1.4 Lubrication Oil

Besides lubrication, the lubrication oil, or lube oil, also acts as a cooling fluid and removes excessive heat from the components when it flows through the macinery. With almost 30°C of temperature difference between return and supply lube oil, the rejected heat can be thermodynamically calculated by Equation 3.6. Figure 3.11 shows the energy fow diagram across the lube oil tank. Steady state and steady flow is assumed and kinetic and potential energy changes are neglected. Lube oil heat rejection is calculated by

$$\dot{Q}_{oil} = \dot{m}_{oil}(h_{oil,i} - h_{oil,o}). \tag{3.6}$$

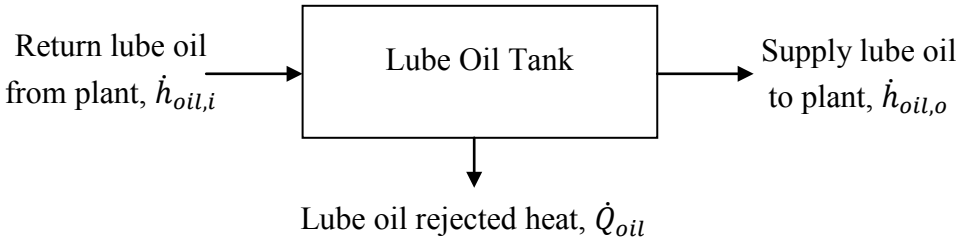

Figure 3.11. Lubrication oil tank energy balance diagram.

3.1.5 Cooling Water

The cooling water used in the condensers and in other coolant loops of the power plant is fed to the cooling tower to reject the heat. An energy balance diagram of the cooling water is presented in Figure 3.12 and the calculation of the rejected heat is expressed in Equation 3.7 by assuming steady state and steady flow and neglecting changes in kinetic and potential energies.

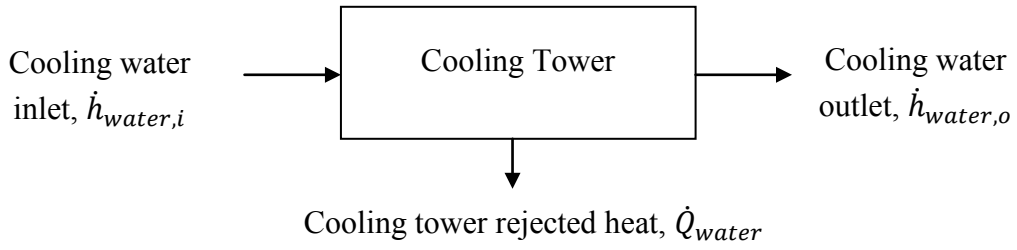

Figure 3.12. Cooling tower energy balance diagram.

Heat rejected from the cooling tower is calculated from

$$\dot{Q}_{water} = \dot{m}_{water}(h_{water,i} - h_{water,o}). \quad (3.7)$$

However, the cooling water exiting temperature has a small difference from the ambient temperature, which makes this waste heat source insufficient for energy utilization cycles.

3.2 Absorption Chillers

3.2.1 Modeling of Components

A basic absorption cycle, as shown in Figure 3.13, consists of fundamental components necessary for the cycle to operate. The schematic is superimposed on a Dühring chart of working fluid properties corresponded to pressure and temperature. State points in the cycles are labeled and connected with arrows. This schematic also shows energy obtained externally from the heat source ($\dot{Q}_{gen}$) and cooling space or chilled water ($\dot{Q}_{evap}$), and energy rejected externally to the environment ($\dot{Q}_{abs}$ and $\dot{Q}_{cond}$). Modeling of each component is presented in the following subchapters. The rich

solution term refers to a high-refrigerant concentration solution, and weak solution refers to a low refrigerant-concentration solution.

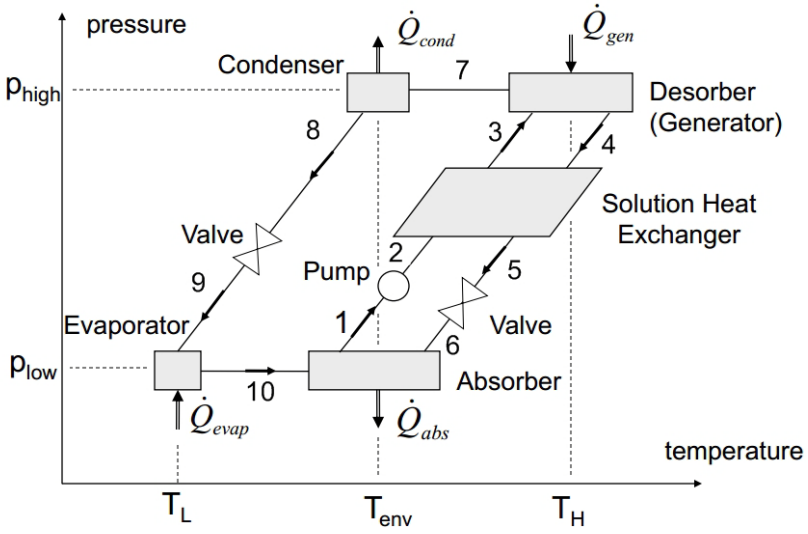

Figure 3.13. Basic absorption cycle schematic (Groll, 2011).

3.2.1.1 Absorber

An absorber is considered a mixing chamber of refrigerant vapor from state point 10 and saturated liquid weak solution from state point 6. The absorption process occurring in the absorber causes the rejection of heat and releases saturated liquid rich solution at state point 1. A schematic is illustrated in Figure 3.14.

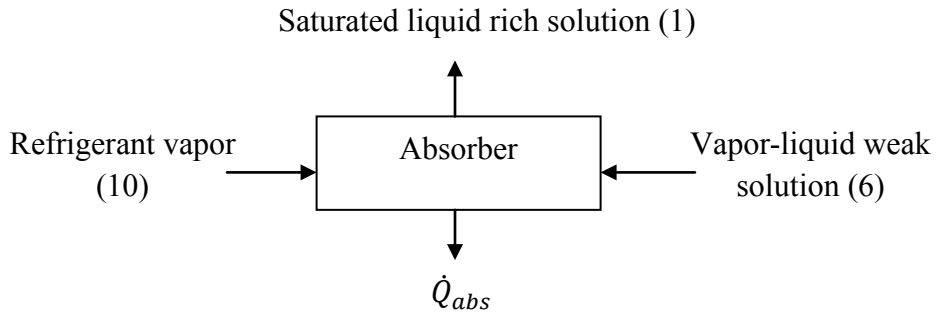

Figure 3.14. Absorber schematic.

Assuming SSSF, KE = 0, PE = 0 and W = 0, the mass balance and energy balance are presented in the following equations,

$$\dot{m}_1 = \dot{m}_r \text{ (3.8)}, \qquad \dot{m}_6 = \dot{m}_w \text{ (3.9)}, \qquad \dot{m}_{10} = \dot{m}_v \text{ (3.10)}$$

$$\dot{m}_1 = \dot{m}_{10} + \dot{m}_6 \tag{3.11}$$

$$x_r \dot{m}_r = x_w \dot{m}_w + x_v \dot{m}_v \tag{3.12}$$

$$\dot{Q}_{abs} = \dot{m}_{10} h_{10} + \dot{m}_6 h_6 - \dot{m}_1 h_1. \tag{3.13}$$

3.2.1.2 Generator

Similar to an absorber, a generator is another mixing chamber. However, a desorption process occurs instead of an absorption process. External heat is required during this process to evaporate saturated vapor from the saturated solution. A schematic is shown in Figure 3.15.

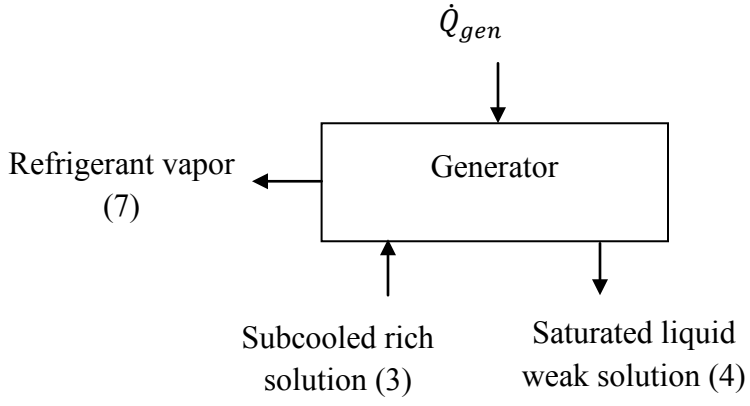

Figure 3.15. Generator schematic.

Assuming SSSF, neglecting changes in KE and PE, and applying no work output to the calculations, the mass and energy balances across the generator are given next. Equation 3.14 provides the mass balance,

$$\dot{m}_3 = \dot{m}_4 + \dot{m}_7 . \tag{3.14}$$

The refrigerant mass balance is shown as Equation 3.12 and the concentrations are as followings,

$$x_r = x_3 \text{ (3.15)}, \qquad x_w = x_4 \text{ (3.16)}, \qquad x_v = x_7 \text{ (3.17)}.$$

After dividing by $\dot{m}_v$, a circulation ratio (CR) can be defined as shown in Equation 3.18,

$$CR = \frac{\dot{m}_r}{\dot{m}_v} . \tag{3.18}$$

According to the fraction above, the value of CR must always be more than 1,

$$CR - 1 = \frac{\dot{m}_w}{\dot{m}_v} . \tag{3.19}$$

Equation 3.19 can be rewritten as follows and CR can be expressed by Equation 3.21,

$$CR \cdot x_r = (CR - 1) \cdot x_w + x_v \tag{3.20}$$

$$CR = \frac{x_v - x_w}{x_r - x_w} . \tag{3.21}$$

The energy balance is given by Equations 3.22 and 3.23,

$$\dot{Q}_{gen} = \dot{m}_4 h_4 + \dot{m}_7 h_7 - \dot{m}_3 h_3 \tag{3.22}$$

$$\dot{Q}_{gen} = \dot{m}_7 [(CR - 1) \cdot h_4 + h_7 - CR \cdot h_3]. \tag{3.23}$$

3.2.1.3 Condenser

The condenser is a heat exchanger component where refrigerant vapor is condensed and exits the condenser as saturated liquid refrigerant condensate. In some cases, the condensate can be in forms of subcooled liquid or two-phase vapor, depending on design of the system. Heat is rejected from this process to the environment or to drive another system. Figure 3.16 shows schematic of condenser.

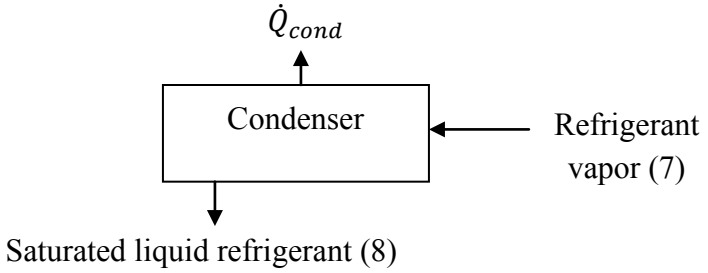

Figure 3.16. Condenser schematic.

The mass balance, refrigerant mass balance and energy balance across the condenser can be expressed in the following equations, respectively, with the same assumptions as for the generator,

$$\dot{m}_7 = \dot{m}_8 = \dot{m}_v \tag{3.24}$$

$$x_7\dot{m}_7 = x_8\dot{m}_8 = x_v\dot{m}_v \tag{3.25}$$

$$\dot{Q}_{cond} = \dot{m}_v(h_7 - h_8). \tag{3.26}$$

3.2.1.4 Evaporator

A schematic of the evaporator is illustrated in Figure 3.17. A cooling load is supplied as heat input to evaporate two-phase refrigerant from state point 9 to saturated vapor at state point 10. The evaporator can release the refrigerant in forms of saturated vapor or vapor-liquid refrigerant or possibly superheated.

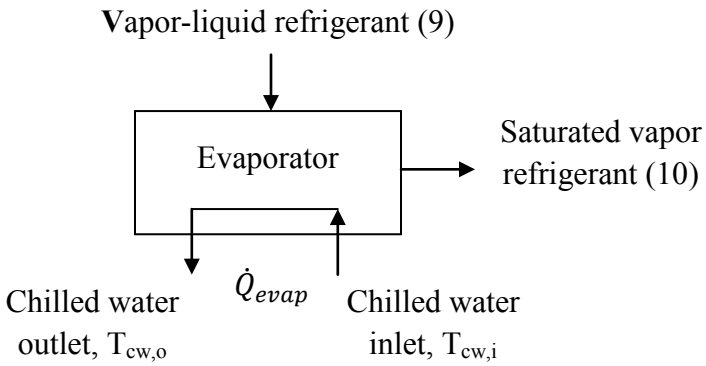

Figure 3.17. Evaporator schematic.

The mass balance, refrigerant mass balance and energy balance across the evaporator can be expressed in the following equations, respectively, with the same assumptions as used before. The energy transferred from the chilled water is shown in Equation 3.30,

$$\dot{m}_9 = \dot{m}_{10} = \dot{m}_v \tag{3.27}$$

$$x_9\dot{m}_9 = x_{10}\dot{m}_{10} = x_v\dot{m}_v \tag{3.28}$$

$$\dot{Q}_{evap} = \dot{m}_v(h_{10} - h_9) \tag{3.29}$$

$$\dot{Q}_{evap} = \dot{m}_{cw} \cdot C_{p,cw}(T_{cw,i} - T_{cw,o}). \tag{3.30}$$

3.2.1.5 Solution Heat Exchanger

The internal heat exchanger in the absorption cycle is also called solution heat exchanger, as two solution streams exchange energy. Heat is transferred from higher temperature weak solution to the lower temperature rich solution. This heats up the subcooled rich solution from state point 2 to state point 3. This process aims to bring the temperature of state point 3 closer to saturated liquid in order to reduce the amount of heat source necessary during the desorption process; by utilizing the heat in the weak solution stream, which would otherwise be rejected in the absorber. Figure 3.18 shows a solution heat exchanger schematic.

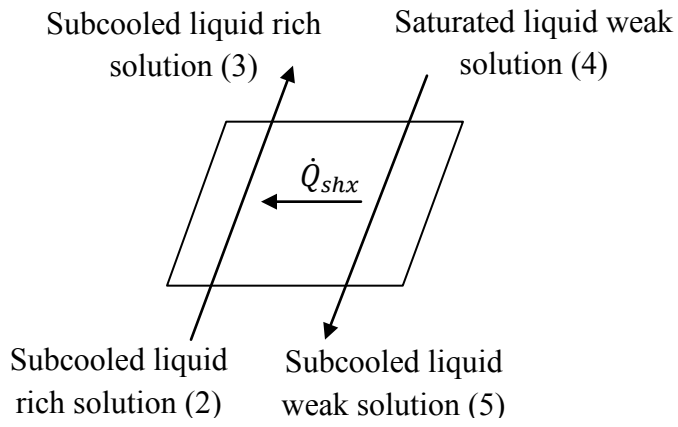

Figure 3.18. Solution heat exchanger schematic.

The mass balance and refrigerant mass balance of the solution heat exchanger can be expressed by the following set of equations, respectively, using the same assumptions as before,

$$\dot{m}_2 = \dot{m}_3 = \dot{m}_r \tag{3.31}$$

$$\dot{m}_4 = \dot{m}_5 = \dot{m}_w \tag{3.32}$$

$$x_2\dot{m}_2 = x_3\dot{m}_3 = x_r\dot{m}_r \tag{3.33}$$

$$x_4\dot{m}_4 = x_4\dot{m}_4 = x_w\dot{m}_w. \tag{3.34}$$

The energy balance equations using the heat exchanger effectiveness are presented as,

$$\dot{Q}_{shx} = \varepsilon_{shx} \cdot \min\left(\dot{m}_w c_{p,w}, \dot{m}_r c_{p,r}\right) \cdot (T_4 - T_2) \tag{3.35}$$

$$\dot{Q}_{shx} = \dot{m}_w(h_4 - h_5) \tag{3.36}$$

$$\dot{Q}_{shx} = \dot{m}_r(h_3 - h_2). \tag{3.37}$$

3.2.1.6 Solution Pump

A pump is necessary in order to increase the pressure of the rich solution from the absorber to generator pressure. The pumping process is assumed to be adiabatic, at SSSF, and with no changes in KE and PE. The rich solution is assumed to be an incompressible liquid. The pump has a certain efficiency. Figure 3.19 shows a pump schematic.

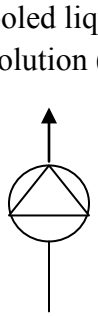

Figure 3.19. Pump schematic.

The mass balances are presented by:

$$\dot{m}_1 = \dot{m}_2 = \dot{m}_r \tag{3.38}$$

$$x_1\dot{m}_1 = x_2\dot{m}_2 = x_r\dot{m}_r \tag{3.39}$$

and the energy balance yields the following:

$$\dot{W}_p = \dot{m}_r(h_2 - h_1) \quad \text{or} \quad w_p = (h_2 - h_1) \tag{3.40}$$

$$w_p = \frac{v_1(P_2 - P_1)}{\eta_p}. \tag{3.41}$$

3.2.1.7 Expansion Valve

Expansion valves are used in the throttling processes of the weak solution in the absorption cycle, and the throttling process of the refrigerant. The same principles of mass balance and energy balance are applied to both processes. The throttling process is assumed to be adiabatic, at SSSF, and the changes of KE and PE are neglected. A schematic is drawn as Figure 3.20.

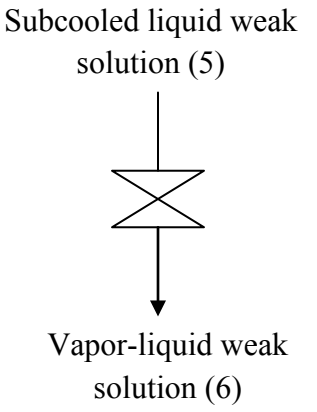

Figure 3.20. Expansion valve schematic.

The throttling process of the weak solution can be expressed by the following equations:

$$\dot{m}_5 = \dot{m}_6 = \dot{m}_w \tag{3.42}$$

$$x_5\dot{m}_5 = x_6\dot{m}_6 = x_w\dot{m}_w \tag{3.43}$$

$$h_5 = h_6. \tag{3.44}$$

The throttling process of the refrigerant can be expressed using the following equations:

$$\dot{m}_8 = \dot{m}_9 = \dot{m}_v \tag{3.45}$$

$$x_8\dot{m}_8 = x_9\dot{m}_9 = x_v\dot{m}_v \tag{3.46}$$

$$h_8 = h_9. \tag{3.47}$$

3.2.2 Absorption Cycle Assumptions

Assumptions are categorized into three groups which are thermodynamic state points in the cycle, operating temperatures and conditions, and components' efficiencies. Table 3.3 summarizes the thermodynamic state points of the NH_3/H_2O single-effect absorption cycle, while those of the H_2O/LiBr single-effect absorption cycle are presented in Table 3.4. The thermodynamic state points of the H_2O/LiBr double-effect and half-effect absorption cycles are shown in Table 3.5 and Table 3.6, respectively.

Table 3.3. Thermodynamic state points in NH_3/H_2O single-effect absorption cycle with rectifier and precooler integration (Herold et al., 1996).

Point	State	Notes
1	Saturated liquid solution	Vapor quality set to 0 as assumption
2	Subcooled liquid solution	State calculated from pump model
3	Subcooled liquid solution	State calculated from rectifier model

Table 3.3. continued.

4	Two-phase or Subcooled liquid solution	State calculated from solution heat exchanger model
5	Saturated liquid solution	State calculated from solution heat exchanger model
6	Subcooled liquid solution	State calculated from solution heat exchanger model
7	Two-phase solution	Vapor flashes as liquid passes through expansion valve
8	Saturated vapor solution	Assumed to be in thermal equilibrium with state point 9, vapor quality set to 1 as assumption
9	Saturated liquid solution	Assumed to be in thermal equilibrium with saturated liquid rich solution, vapor quality set to 0 as assumption
10	Saturated vapor solution	Assumed extremely high in ammonia concentration (x_v), vapor quality set to 1 as assumption
11	Saturated liquid solution	Vapor quality set to 0 as assumption
12	Subcooled liquid solution	State calculated from precooler heat exchanged model
13	Two-phase solution	Vapor flashes as liquid passes through expansion valve
14	Two-phase solution	Assumed high vapor quality (Qu_{evap})
15	Saturated vapor solution	Vapor quality set to 1 as assumption

Table 3.4. Thermodynamic state points in H_2O/LiBr single-effect absorption cycle (Herold et al., 1996).

Point	State	Notes
1	Saturated liquid solution	Vapor quality set to 0 as assumption
2	Subcooled liquid solution	State calculated from pump model
3	Subcooled liquid solution	State calculated from solution heat exchanger model
4	Saturated liquid solution	Vapor quality set to 0 as assumption
5	Subcooled liquid solution	State calculated from solution heat exchanger model

Table 3.4. continued.

6	Two-phase solution	Vapor flashes as liquid passes through expansion valve
7	Superheated water vapor	Assumed to have zero salt content
8	Saturated liquid water	Vapor quality set to 0 as assumption
9	Vapor-liquid water	Vapor flashes as liquid passes through expansion valve
10	Saturated water vapor	Vapor quality set to 1 as assumption

Table 3.5. Thermodynamic state points in H_2O/LiBr double-effect absorption cycle (Herold et al., 1996).

Point	State	Notes
1	Saturated liquid solution	Vapor quality set to 0 as assumption
2	Subcooled liquid solution	State calculated from pump model
3	Subcooled liquid solution	State calculated from solution heat exchanger model
4	Saturated liquid or subcooled liquid solution	State calculated from heat exchanged model between high-pressure condenser and intermediate-pressure generator, pinch point is assumed
5	Subcooled liquid solution	State calculated from solution heat exchanger model
6	Two-phase solution	Vapor flashes as liquid passes through expansion valve
7	Superheated water vapor	Assumed to have zero salt content
8	Saturated liquid water	Vapor quality set to 0 as assumption
9	Vapor-liquid water	Vapor flashes as liquid passes through expansion valve
10	Saturated water vapor	Vapor quality set to 1 as assumption
11	Saturated liquid solution	Vapor quality set to 0 as assumption
12	Subcooled liquid solution	State calculated from pump model
13	Subcooled liquid solution	State calculated from solution heat exchanger model
14	Saturated liquid solution	Vapor quality set to 0 as assumption
15	Subcooled liquid solution	State calculated from solution heat exchanger model
16	Two-phase solution	Vapor flashes as liquid passes through expansion valve
17	Superheated water vapor	Assumed to have zero salt content
18	Saturated liquid water	Vapor quality set to 0 as assumption
19	Vapor-liquid water	Vapor flashes as liquid passes through expansion valve

Table 3.6. Thermodynamic state points in half-effect absorption cycle (Herold et al., 1996).

Point	State	Notes
1	Saturated liquid solution	Vapor quality set to 0 as assumption
2	Subcooled liquid solution	State calculated from pump model
3	Subcooled liquid solution	State calculated from solution heat exchanger model
4	Saturated liquid solution	Vapor quality set to 0 as assumption
5	Subcooled liquid solution	State calculated from solution heat exchanger model
6	Two-phase solution	Vapor flashes as liquid passes through expansion valve
7	Saturated liquid solution	Vapor quality set to 0 as assumption
8	Subcooled liquid solution	State calculated from pump model
9	Subcooled liquid solution	State calculated from solution heat exchanger model
10	Saturated liquid solution	Vapor quality set to 0 as assumption
11	Subcooled liquid solution	State calculated from solution heat exchanger model
12	Two-phase solution	Vapor flashes as liquid passes through expansion valve
13	Superheated water vapor (H_2O/LiBr)	Assumed to have zero salt content, in thermal equilibrium with saturated liquid rich solution of state point 9
	Superheated solution (NH_3/H_2O)	Assumed extremely high in ammonia concentration ($x_{v,2}$), in thermal equilibrium with saturated liquid rich solution of state point 9
14	Saturated liquid water (H_2O/LiBr)	Vapor quality set to 0 as assumption
	Saturated liquid solution (NH_3/H_2O)	
15	Vapor-liquid water (H_2O/LiBr)	Vapor flashes as liquid passes through expansion valve
	Two-phase solution (NH_3/H_2O)	
16	Saturated water vapor (H_2O/LiBr)	Vapor quality set to 1 as assumption
	Saturated vapor solution (NH_3/H_2O)	
17	Superheated water vapor (H_2O/LiBr)	Assumed to have zero salt content, in thermal equilibrium with saturated liquid rich solution of state point 3
	Saturated vapor solution (NH_3/H_2O)	Vapor quality set to 1 as assumption, in thermal equilibrium with saturated liquid rich solution of state point 3

Operating temperatures assumed in modeling are listed in Table 3.7, and concentration and efficiency assumptions are listed in Table 3.8 and 3.9, respectively.

Table 3.7. Summary of assumptions for operating temperatures.

Sink fluid temperature	27°C
Ambient temperature (dead state)	32°C
Required chilled water temperature for office space	12.8°C (55°F)
Chilled water temperature difference	5 K
Temperature difference between heat source stream and operating temperature of the generator	10 K
Temperature difference between sink fluid and evaporating temperature of the evaporator	5 K
Pinch temperature (double-effect H_2O/LiBr cycle)	5 K
Temperature difference of CT room ventilation air at generator	50 K

Table 3.8. Summary of concentration assumptions.

Single-effect (H_2O/LiBr)	x_v (salt content)	0
Single-effect (NH_3/H_2O)	x_v (ammonia content)	0.9996
	Qu_{evap}	0.98
Double-effect (H_2O/LiBr)	x_r (salt content)	0.65
	x_v (salt content)	0
Half-effect (H_2O/LiBr)	$x_{r,1}$ (salt content)	0.65
	$x_{v,1}$ (salt content)	0
	$x_{v,2}$ (salt content)	0
Half-effect (NH_3/H_2O)	$x_{v,2}$ (ammonia content)	0.9999

Table 3.9. Assumptions of components' efficiencies.

Single-effect	Pump efficiency	0.60
	Solution heat exchanger effectiveness	0.45
Double-effect	Pump efficiency	0.60
	LP Solution heat exchanger effectiveness	0.25
	HP Solution heat exchanger effectiveness	0.60
Half-effect	Pump efficiency	0.60
	LP Solution heat exchanger effectiveness	0.60
	HP Solution heat exchanger effectiveness	0.80
All heat exchangers are counter-flow heat exchangers.		

3.2.3 Single-Effect Absorption Cycle

The study of the single-effect cycle has been conducted with the working fluids NH_3/H_2O and $H_2O/LiBr$. The cycle for each working fluid has a different configuration and requires a slightly different modeling approach. This subchapter will present the details of the modeling approach for both working fluids.

3.2.3.1 Single-Effect NH_3/H_2O Absorption Cycle

The configuration in Figure 3.21 presents the NH_3/H_2O cycle that has been selected to investigate in this study according to its potential for high COPs. The cycle is equipped with an absorber and evaporator operating at low pressure level, a generator and condenser operating at high pressure, an internal heat exchanger, a pump and two expansion valves. The additional components in this cycle are the rectifier and precooler.

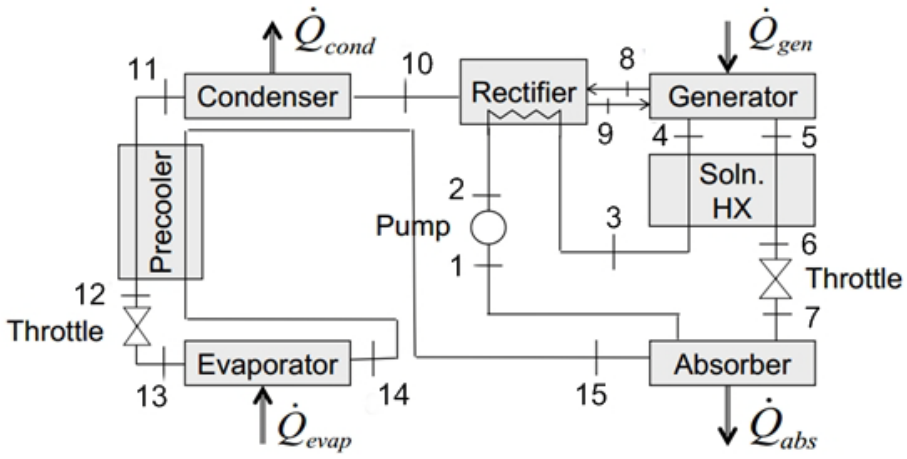

Figure 3.21. Investigated single-effect NH_3/H_2O absorption cycle (Groll, 2011).

Refrigerant, which is evaporated at the evaporator flows through the precooler and is heated up by subcooling the saturated refrigerant solution flowing towards the

expansion valve. Higher vapor quality refrigerant then flows to the absorber and is absorbed into the highly concentrated absorbent solution or weak solution of refrigerant. At state point 1, so called the rich solution leaves the absorber. The rich solution exits the absorber as a saturated liquid and is pumped up to the high operating pressure at state point 2 as a subcooled liquid solution. As it flows through the rectifier, it is heated by the heat rejection from rectification process. It continues to the solution heat exchanger and is heated up once again by the warmer weak solution leaving the generator. Rich solution from state point 4 may enter the generator for desorption process as warm subcooled liquid or saturated liquid or at most two-phase solution. Heat is supplied to the generator to boil the refrigerant out of the solution and leave a weak solution to exit the generator at saturated liquid at state point 5. This weak solution exchanges heat in the internal heat exchanger, then expands to lower pressure by the expansion valve, and flows back to the absorber. NH_3 refrigerant vapor leaves the generator at state point 8 with very small water content and enters the rectifier to condense water out of this vapor. Saturated water flows back to the generator at state point 9. Saturated vapor that is extremely high in ammonia concentration leaves the rectifier. It is then condensed in the condenser and leaves the condenser as saturated liquid. It is further subcooled in the precooler. Its pressure and temperature are reduced as it flows through a refrigerant expansion valve; this is in order to prepare the refrigerant to be able to pull out the heat from the cooling load in the evaporator. Modeling of the fundamental components is already given in Chapter 3.2.

The rectifier schematic is illustrated in Figure 3.22. Mass balance and energy balance calculations of the rectifier and generator are shown in the following equations,

$$\dot{m}_4 = \dot{m}_r \text{ (3.48)}, \qquad \dot{m}_5 = \dot{m}_w \text{ (3.49)}, \qquad \dot{m}_{10} = \dot{m}_v \text{ (3.50)}$$

$$\dot{m}_4 = \dot{m}_5 + \dot{m}_{10} \tag{3.51}$$

$$x_4\dot{m}_4 = x_5\dot{m}_5 + x_{10}\dot{m}_{10} \tag{3.52}$$

$$\dot{Q}_{gen} = \dot{m}_v[h_{10} + (CR-1)\cdot h_5 - CR\cdot h_4] + \dot{Q}_{rect}. \tag{3.53}$$

The rectifier mass balance is presented by,

$$\dot{m}_8 = \dot{m}_9 + \dot{m}_{10} \tag{3.54}$$

$$x_8\dot{m}_8 = x_9\dot{m}_9 + x_{10}\dot{m}_{10} \tag{3.55}$$

$$\dot{m}_9 = \dot{m}_{10}\left(\frac{x_{10}-x_8}{x_8-x_9}\right) \tag{3.56}$$

and the energy balance yields:

$$\dot{Q}_{rect} = (\dot{m}_{10} + \dot{m}_9)h_8 - \dot{m}_{10}h_{10} - \dot{m}_9h_9 \tag{3.57}$$

$$\dot{Q}_{rect} = \dot{m}_{10}[(h_8 - h_{10}) + \left(\frac{x_{10}-x_8}{x_8-x_9}\right)(h_8 - h_9)]. \tag{3.58}$$

A complete heat transfer from the rectifier heat rejection to the rich solution is assumed,

$$\dot{Q}_{rect} = \dot{m}_r(h_3 - h_2). \tag{3.59}$$

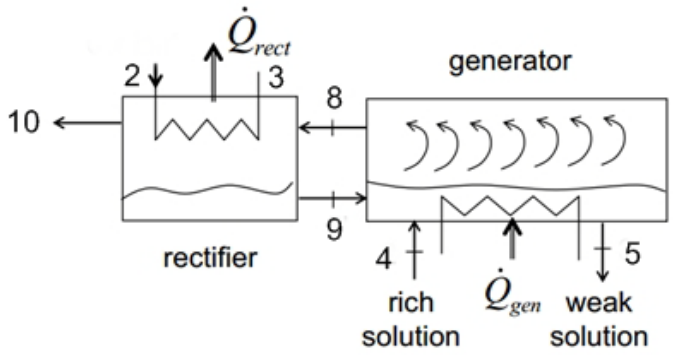

Figure 3.22. Rectifier and generator schematic (Groll, 2011).

A schematic of the precooler is provided in Figure 3.23. The mass and energy balances are provided in the set of equations below,

$$\dot{m}_{11} = \dot{m}_{12} = \dot{m}_{14} = \dot{m}_{15} = \dot{m}_v \tag{3.60}$$

$$x_{11} = x_{12} = x_{14} = x_{15} = x_v \tag{3.61}$$

$$\dot{Q}_{precooler} = \varepsilon_{precooler} \cdot \dot{m}_v \cdot (h_{11} - h_{14}) \tag{3.62}$$

$$\dot{Q}_{precooler} = \dot{m}_v (h_{11} - h_{12}) \tag{3.63}$$

$$\dot{Q}_{percooler} = \dot{m}_v (h_{15} - h_{14}). \tag{3.64}$$

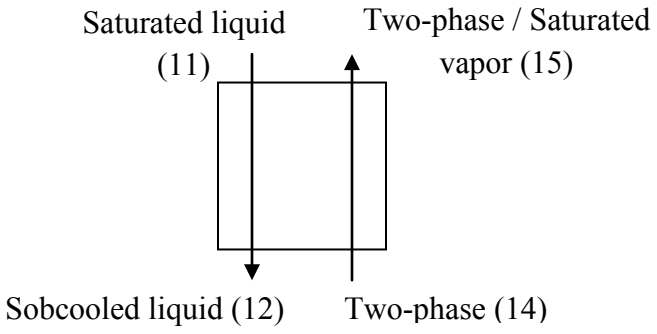

Figure 3.23. Precooler schematic.

The absorption cycle performance and overall energy balances are presented in the following set of equations,

$$\dot{Q}_{evap} = \dot{m}_v(h_{14} - h_{13}) \tag{3.65}$$

$$\dot{W}_{pump} = \dot{m}_r(h_2 - h_1) \tag{3.66}$$

$$COP = \frac{\dot{Q}_{evap}}{\dot{Q}_{gen} + \dot{W}_{pump}}. \tag{3.67}$$

3.2.3.2 Single-Effect H_2O/LiBr Absorption Cycle

The configuration of the single-effect H_2O/LiBr absorption cycle was previously shown in Figure 3.13. The cycle operation is simpler than the NH_3/H_2O cycle due to fewer components, and its refrigerant vapor is purely desorbed from the generator as superheated steam. Typically, the rich solution in the H_2O/LiBr cycle refers to the solution with high LiBr-salt concentration, and the weak solution refers to the solution with low LiBr-salt concentration, in other words, high in refrigerant. Basically, they are called conversely from NH_3/H_2O cycle. The performance of the cycle can be expressed in the same manner as those of NH_3/H_2O single-effect cycle.

3.2.4 Double-effect H_2O/LiBr Absorption Cycle

The study of the double-effect absorption cycle focuses only on the parallel-flow configuration as illustrated in Figure 3.24. This cycle operates at three different pressure levels in which absorber and evaporator operate at the low pressure level, low generator or low desorber and low condenser operate at an intermediate pressure level, and high generator or high desorber and high condenser operate at the high pressure level. Heat

received from external heat source ($\dot{Q}_{gen,high}$) only supplies to the high generator and the low generator is driven by heat rejected from high condenser. Considering these heat flows, heat from the original source has been used twice in this configuration, and in other words, it has double up its effect to the overall system (Herold et al., 1996). Driven by the heat rejected from the high condenser ($\dot{Q}_{cond,high}$), a portion of the refrigerant water is desorbed from LiBr solution at the low generator and flows to the low condenser. The left-out salt solution becomes richer in the low generator. It mixes with the rich solution throttling down from high generator and releases two solution streams, one is the weak solution to the high-pressure pump and another is the rich solution back to the absorber. Since there are only two LiBr-concentrations for the solution streams, the two pressure-level cycles share same circulation ratio. The cycle also allows the use of higher heat source temperature at the high-pressure generator.

Most of the components in the double-effect H_2O/LiBr cycle are similar to single-effect H_2O/LiBr cycle, except for the heat exchanged between the high-pressure condenser and the low generator at an intermediate pressure that makes the cycle more complex. The low generator must be modeled differently. A schematic of the low generator is presented in Figure 3.25. Another difference is at the low condenser, which operates at intermediate pressure.

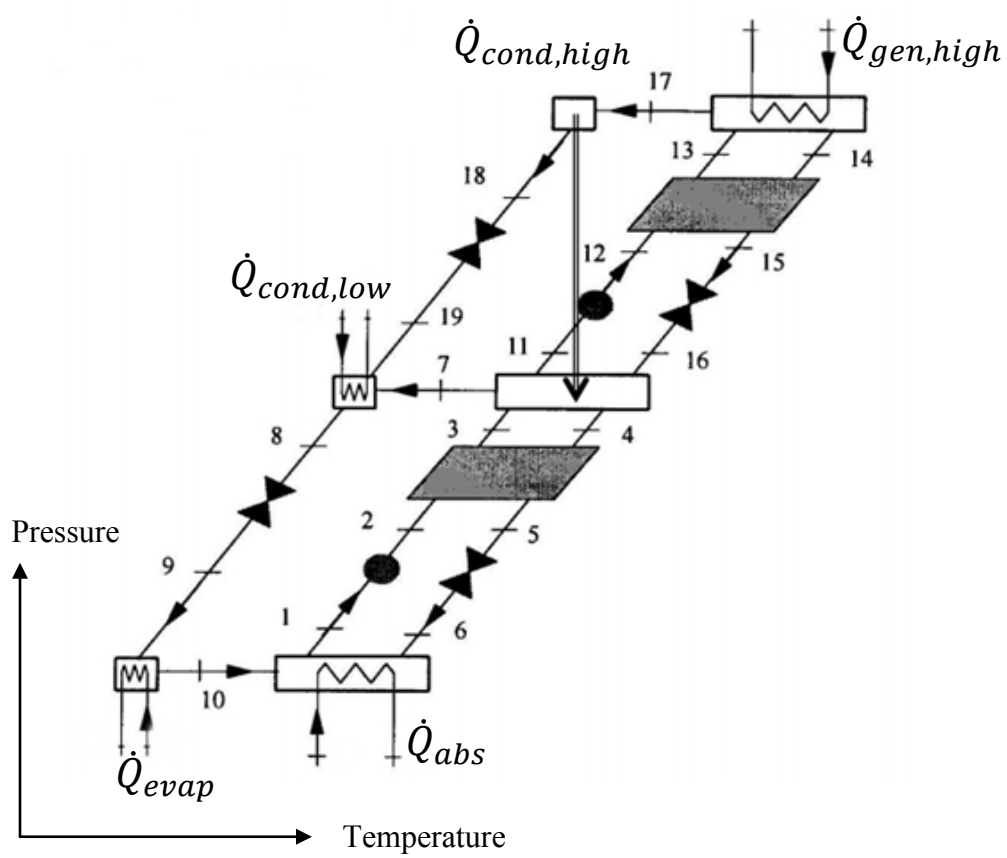

Figure 3.24. Double-effect parallel-flow H_2O/LiBr absorption cycle on Dühring chart schematic (Groll, 2011).

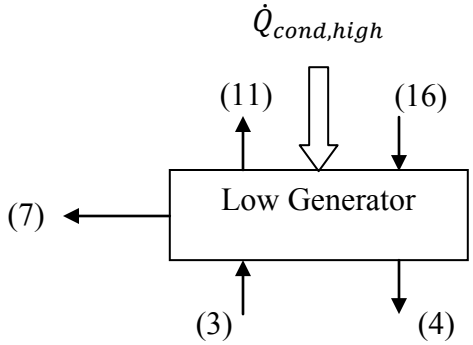

Figure 3.25. Low-pressure generator schematic.

The mass balances of the generator can be written as:

$$\dot{m}_3 = \dot{m}_{w,1} \text{ (3.68)}, \quad \dot{m}_4 = \dot{m}_{r,1} \text{ (3.69)}, \quad \dot{m}_7 = \dot{m}_{v,1} \text{ (3.70)}$$

$$\dot{m}_{11} = \dot{m}_{w,2} \text{ (3.71)}, \quad \dot{m}_{16} = \dot{m}_{r,2} \text{ (3.72)}, \quad \dot{m}_{17} = \dot{m}_{v,2} \text{ (3.73)}$$

$$\dot{m}_3 + \dot{m}_{16} = \dot{m}_4 + \dot{m}_{11} + \dot{m}_7. \tag{3.74}$$

Equation 3.77 represents the effect of heat rejection from the high condenser to the low generator as

$$\dot{Q}_{cond,high} = \dot{m}_{v,2}(h_{17} - h_{18}) \tag{3.75}$$

$$\dot{Q}_{gen,low} = \dot{m}_{v,1}h_7 + \dot{m}_{r,1}h_4 + \dot{m}_{w,2}h_{11} - \dot{m}_{w,1}h_3 - \dot{m}_{r,2}h_{16} \tag{3.76}$$

$$\dot{Q}_{cond,high} = \dot{Q}_{gen,low}. \tag{3.77}$$

The mass and energy balances of the low-pressure condenser are:

$$\dot{m}_8 = \dot{m}_{v,1} + \dot{m}_{v,2} = \dot{m}_v \tag{3.78}$$

$$\dot{m}_8 = \dot{m}_7 + \dot{m}_{19} \tag{3.79}$$

$$\dot{Q}_{cond,low} = \dot{m}_{v,2}h_{19} + \dot{m}_{v,1}h_7 - \dot{m}_v h_8. \tag{3.80}$$

Due to additional components, the cycle performance yields

$$COP_{double} = \frac{\dot{Q}_{evap,double}}{\dot{Q}_{gen,high} + \dot{W}_{pump,total}} \tag{3.81}$$

$$\dot{Q}_{evap,double} = \dot{m}_v(h_{10} - h_9) \tag{3.82}$$

$$\dot{Q}_{gen,high} = \dot{m}_{v,2}h_{17} + \dot{m}_{r,2}h_{14} - \dot{m}_{w,2}h_{13} \tag{3.83}$$

$$\dot{W}_{pump,total} = \dot{m}_{w,1}(h_2 - h_1) + \dot{m}_{w,2}(h_{12} - h_{11}). \tag{3.84}$$

A pinch point analysis is applied to the temperature difference between the high condenser outlet at state point 18 and the highest exiting temperature of the low-generator, which occurs at state point 4.

3.2.5 Half-Effect Absorption Cycle

Although the half-effect cycle is relatively complex and has lower efficiencies, it allows heat recovery to perform with low-grade waste heat at relatively low temperatures. The configuration of the half-effect cycle is shown in Figure 3.26. It can be realized with both H_2O/LiBr and NH_3/H_2O working fluids.

Referring to the schematic shown in Figure 3.26, the solutions in the low cycle have higher absorbent concentration than those in the high cycle. The main heat source stream is split evenly to two heat streams, $\dot{Q}_{gen,high}$ and $\dot{Q}_{gen,high}$, this is why the cycle is called half-effect cycle. The first half of the main heat source drives high generator or high desober, while the other half drives the low generator or low desorber. Evaporated refrigerant vapor is first absorbed in the low absorber, mixed with absorbent, and then leaves the low cycle at the low generator, which operates at the intermediate pressure. It is absorbed once again at the high absorber, mixed and exits the absorption circuits at the high generator. After the condensing process, saturated liquid refrigerant is throttled from the highest to lowest pressure of the cycle.

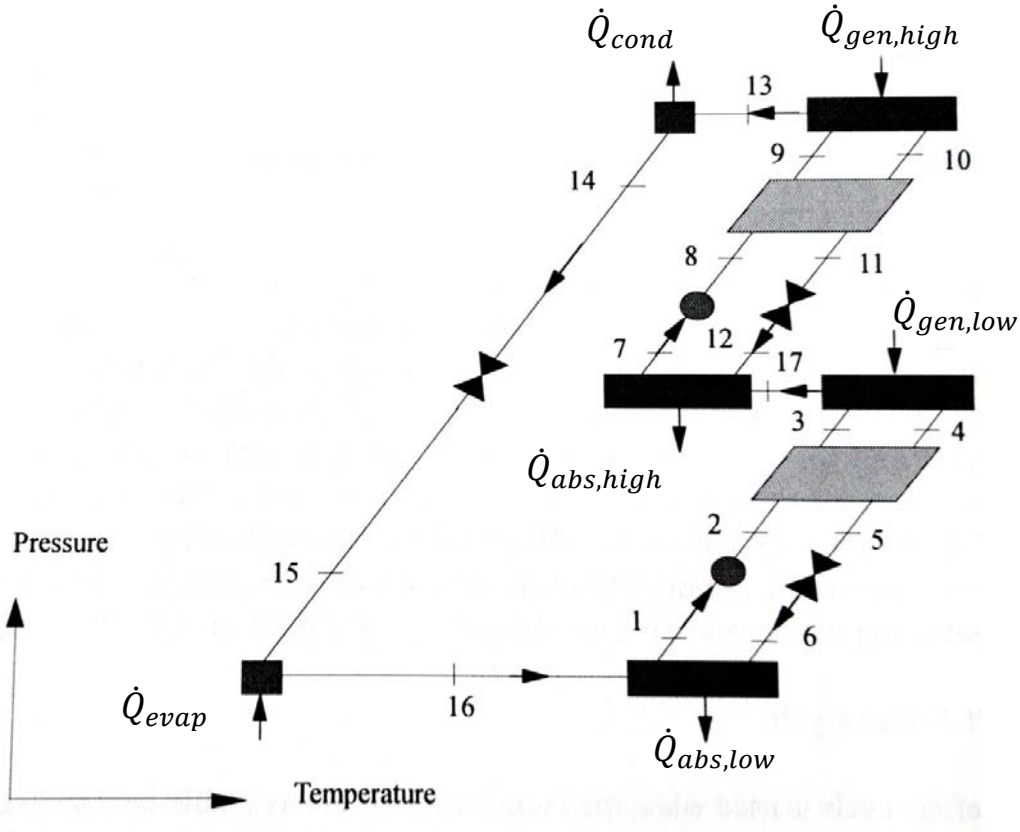

Figure 3.26. Half-effect absorption cycle schematic (Herold et al. 1996).

Modeling of each component of the half-effect cycle is similar to what is described in Subchapter 3.2. The main challenge in optimizing the cycle falls into the selection of the concentration for each solution stream, which makes a difference in circulation ratios. A parametric study was conducted to find the optimum concentrations. The rich solution refers to a solution with high refrigerant concentration. Weak solution refers to a solution with low refrigerant concentration. The mass flow rates can be defined by the following set of equations,

$$\dot{m}_1 = \dot{m}_2 = \dot{m}_3 = \dot{m}_{r,1} \tag{3.85}$$

$$\dot{m}_4 = \dot{m}_5 = \dot{m}_6 = \dot{m}_{w,1} \tag{3.86}$$

$$\dot{m}_{17} = \dot{m}_{v,1} \tag{3.87}$$

$$\dot{m}_{7} = \dot{m}_{8} = \dot{m}_{9} = \dot{m}_{r,2} \tag{3.88}$$

$$\dot{m}_{10} = \dot{m}_{11} = \dot{m}_{12} = \dot{m}_{w,2} \tag{3.89}$$

$$\dot{m}_{13} = \dot{m}_{14} = \dot{m}_{15} = \dot{m}_{16} = \dot{m}_{v,2}. \tag{3.90}$$

There is a slight difference in performance calculation. The cycle performance can be expressed as,

$$COP_{half} = \frac{\dot{Q}_{evap,half}}{\dot{Q}_{gen,total} + \dot{W}_{pump,total}} \tag{3.91}$$

with corresponding energy equations of

$$\dot{Q}_{evap,half} = \dot{m}_{v,2}(h_{16} - h_{15}) \tag{3.92}$$

$$\dot{Q}_{gen,total} = \dot{Q}_{gen,high} + \dot{Q}_{gen,low} \tag{3.93}$$

$$\dot{W}_{pump,total} = \dot{m}_{r,1}(h_2 - h_1) + \dot{m}_{r,2}(h_8 - h_7). \tag{3.94}$$

3.3 Organic Rankine Cycle

3.3.1 Organic Rankine Cycles Components

As described in the literature review, ORCs generally consist of five fundamental components, which are condenser, pump, evaporator or boiler, and expander or turbine. An additional heat exchanger may be installed in the cycle in order to enhance the efficiency and heat utilization.

3.3.1.1 Condenser

The condensing process is assumed to be at SSSF and the changes in KE and PE are neglected. There is no work done by the condenser. A schematic is shown in Figure 3.27.

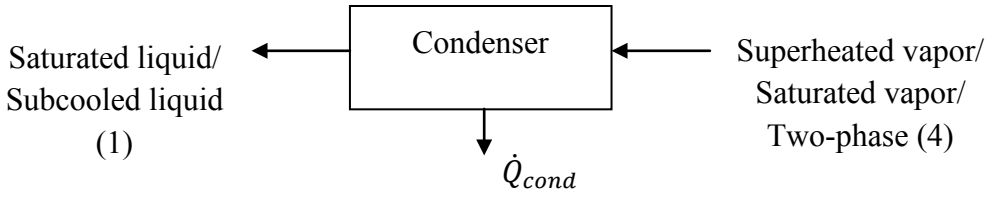

Figure 3.27. ORC condenser schematic.

The mass balance and energy balance across the condenser are defined as:

$$\dot{m}_1 = \dot{m}_4 = \dot{m}_{orc} \tag{3.95}$$

$$\dot{Q}_{cond} = \dot{m}_{orc}(h_4 - h_1). \tag{3.96}$$

3.3.1.2 Pump

The pumping process is assumed to be adiabatic, at SSSF, and the changes in KE and PE are neglected. During the process, the working fluid is assumed to be an incompressible liquid. The pump increases the operating pressure from condensing pressure to evaporating pressure. The pump is modeled using an isentropic pumping efficiency. A parametric study is conducted to find the optimum pressure ratio. Figure 3.28 shows pump schematic.

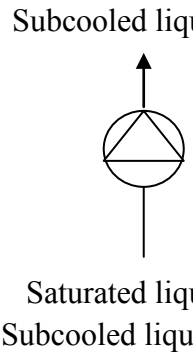

Figure 3.28. ORC pump schematic.

The mass balance across the pump is defined as

$$\dot{m}_1 = \dot{m}_2 = \dot{m}_{orc}. \tag{3.97}$$

Isentropic pumping yields:

$$s_{2s} = s_1. \tag{3.98}$$

The isentropic enthalpy (h_{2s}) at state point 2 is defined as a function of isentropic entropy and high side pressure. The pump efficiency is expressed by Equation 3.99, and the actual enthalpy at state point 2 is computed from

$$\eta_{pump} = \frac{h_{2s}-h_1}{h_{2a}-h_1}. \tag{3.99}$$

The actual pump work yields

$$\dot{W}_{pump} = \dot{m}_{orc}(h_{2a} - h_1). \tag{3.100}$$

3.3.1.3 Evaporator

Waste energy from the heat source stream is obtained in the evaporator to preheat, evaporate and superheat the working fluid. The process is also assumed to be at SSSF, changes in KE and PE are neglected, and the evaporator is a no work device. The highest temperature in the evaporator is defined by an assumed pinch point. The evaporating temperature corresponds with the evaporating pressure. A parametric study yields the optimum evaporation pressure, and the effectiveness can be calculated.

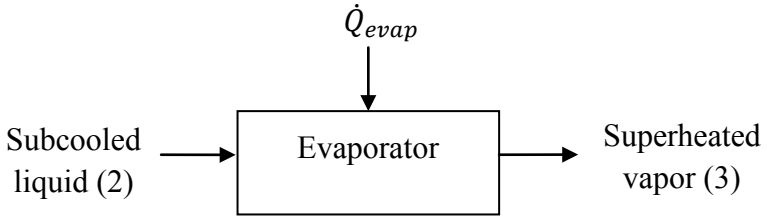

Figure 3.29. ORC evaporator schematic.

The mass balance and energy balance can be expressed in the following equations,

$$\dot{m}_2 = \dot{m}_3 = \dot{m}_{orc} \tag{3.101}$$

$$\dot{Q}_{evap} = \dot{m}_{orc}(h_3 - h_2). \tag{3.102}$$

Modeling of the effectiveness will be described in heat exchanger Subchapter 3.3.1.5.

3.3.1.4 Expander

A schematic of the expander is shown in Figure 3.30. The expansion process is assumed to be adiabatic, at SSSF, and the changes in KE and PE are neglected. The expansion process provides work output of the cycle. The expander or turbine works

between high and low pressures of the cycle and has an isentropic efficiency. The expander discharge flows back to the condenser to complete the cycle.

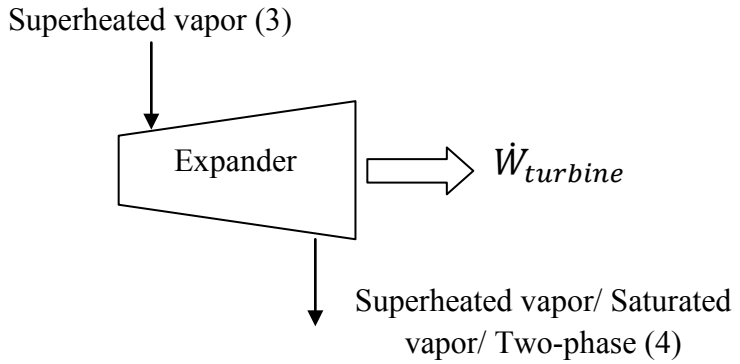

Figure 3.30. ORC expander schematic.

The mass balance across the expander is defined by

$$\dot{m}_3 = \dot{m}_4 = \dot{m}_{orc} . \tag{3.103}$$

Isentropic expansion yields

$$s_{4s} = s_3. \tag{3.104}$$

The isentropic enthalpy (h_{4s}) at state point 4 is defined as a function of isentropic entropy and low side pressure. The turbine efficiency is expressed by Equation 3.105, and the actual enthalpy at state point 4 is computed from

$$\eta_{turbine} = \frac{h_3 - h_{4a}}{h_3 - h_{4s}}. \tag{3.105}$$

Actual turbine work yields

$$\dot{W}_{turbine} = \dot{m}_{orc}(h_3 - h_{4a}). \tag{3.106}$$

3.3.1.5 Internal Heat Exchanger

An internal heat exchanger may be an important component of the ORC depending on the thermodynamic characteristics of the working fluid. This subchapter will present theoretical modeling of heat exchanger in general. A pinch point analysis is applied in the model. A schematic of the heat exchanger with heat source or heat sink stream is shown in Figure 3.31.

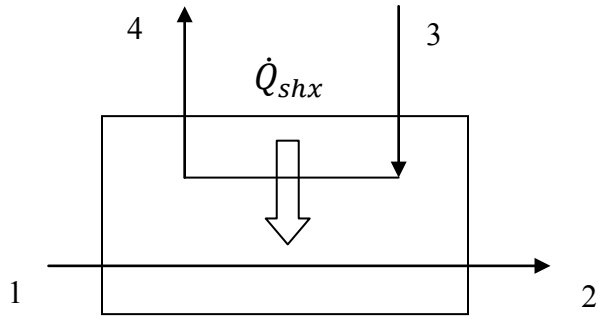

Figure 3.31. Internal heat exchanger schematic.

The schematic illustrates a heat transfer rate, $\dot{Q}_{shx}$, from the heat-source stream (4 – 3) to the heat-sink stream (1 – 2). The analysis assumes a counter-flow heat exchanger, where $T_3 > T_2 > T_1$, SSSF, and changes KE and PE are neglected;

$$T_3 = T_{h,in} \text{ (3.107)}, \qquad T_4 = T_{h,out} \text{ (3.108)}$$

$$T_1 = T_{c,in} \text{ (3.109)}, \qquad T_2 = T_{c,out} \text{ (3.110)}$$

$$\dot{m}_1 = \dot{m}_2 = \dot{m}_c \text{ (3.111)}, \qquad \dot{m}_3 = \dot{m}_4 = \dot{m}_h \text{ (3.112)}.$$

The maximum heat transfer rate is expressed as

$$\dot{Q}_{max} = \min\left(\dot{m}_c\left(h_c(T_{h,in}, P_c) - h_c(T_{c,in}, P_c)\right), \dot{m}_h\left(h_h(T_{h,in}, P_h) - h_h(T_{c,in}, P_h)\right)\right). \tag{3.113}$$

The actual heat transfer rate can be calculated from

$$\dot{Q}_{shx} = \dot{m}_c(h_2 - h_1) = \dot{m}_h(h_4 - h_3). \tag{3.114}$$

The heat exchanger effectiveness yields

$$\varepsilon_{shx} = \frac{\dot{Q}_{shx}}{\dot{Q}_{max}}. \tag{3.115}$$

3.3.2 Organic Rankine Cycle Assumptions

Certain assumptions are made in the analysis of the ORC. These assumptions relate to the operating environment, pinch points, efficiency of components and certain state points of the cycle. They are applied constant over all cycles in the model. These assumptions are made based on the literature review, experiments done in the literature, and the power plant operating environment. Table 3.10 gives the assumed parameters. Figure 3.32 indicates the temperature and pinch points used in the assumptions in a temperature-entropy diagram of R-134a. Lastly, Table 3.11 summarizes the state point assumptions.

Table 3.10. Summary of assumptions used in ORC modeling.

Sink fluid inlet temperature	27°C
Ambient temperature (dead state)	32°C
Temperature difference between sink fluid inlet and condensing temperature	10 K
Temperature difference between heat-source fluid inlet and working fluid outlet across the evaporator	5 K
Pinch temperature	5 K
Pump isentropic efficiency	0.60
Expansion turbine isentropic efficiency	0.80
Regenerative heat exchanger effectiveness	0.80
All cycles are modeled under subcritical limitation.	
Heat source and heat sink streams have constant specific heat capacities.	
Incompressible heat source and heat sink fluid	
Negligible pressure changes in heat source and heat sink fluids	
SSSF is applied with negligible of KE and PE.	
Only counter-flow heat exchangers are equipped in the cycles.	
Heater outlet state point is saturated liquid for two-phase flash expansion ORC.	

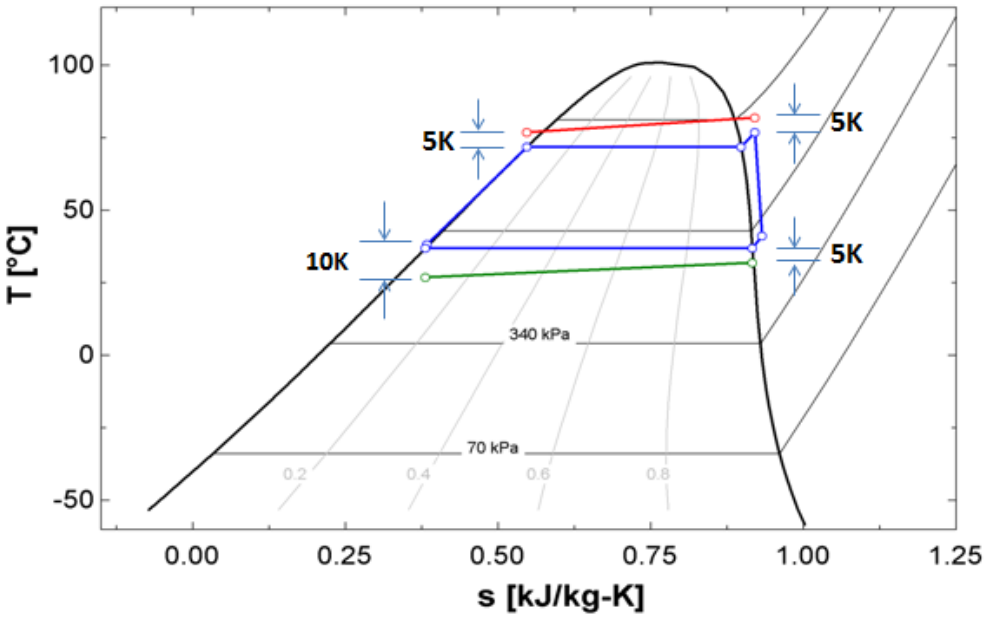

Figure 3.32. Assumptions of temperature and pinch points plotted on R134a T-s diagram.

Table 3.11. Summary of state point assumptions in ORC modeling.

Point	State	Notes
1 (Condenser outlet)	Saturate liquid	Vapor quality set to 0 as assumption
2 (Pump outlet)	Subcooled liquid	State calculated from pump model
3 (Evaporator outlet)	Superheated vapor	State calculated from evaporating pressure, source temperature and temperature assumption
4 (Expander outlet)	Superheated vapor or saturated liquid	State calculated from ORC modeling

3.3.3 Baseline Organic Rankine Cycle

A simple ORC is considered to be the baseline cycle in this thesis. A schematic is illustrated in Figure 3.33. Figure 3.34 shows the actual state points of the cycle in a temperature-entropy diagram for the working fluid R245fa.

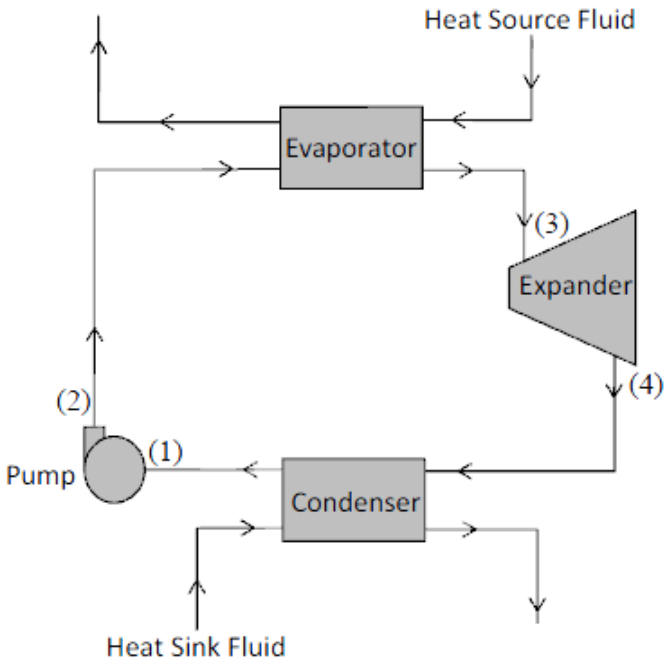

Figure 3.33. Baseline ORC schematic (Woodland, 2013).

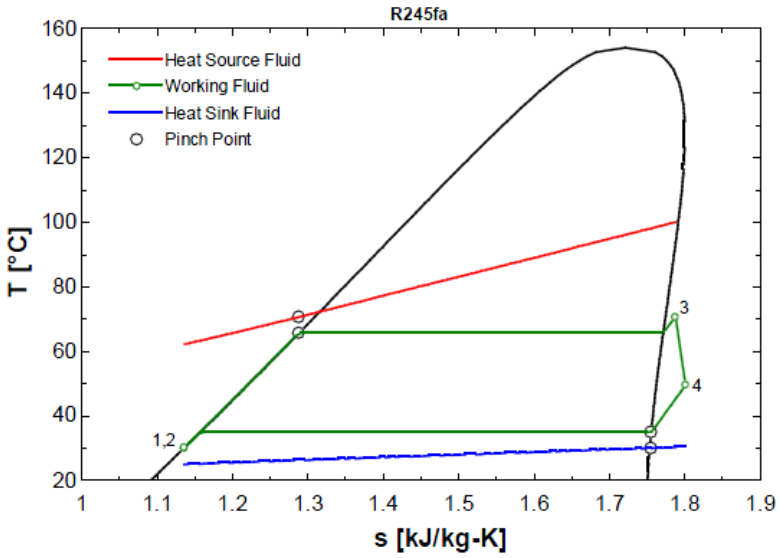

Figure 3.34. Baseline ORC T-s diagram for actual processes with heat source and heat sink temperature profiles superimposed (Woodland, 2013).

The mass balance of the cycle can be written as

$$\dot{m}_1 = \dot{m}_2 = \dot{m}_3 = \dot{m}_4 = \dot{m}_{orc} . \tag{3.116}$$

The net work output is defined as

$$\dot{W}_{net} = \dot{W}_{turbine} - \dot{W}_{pump}. \tag{3.117}$$

The thermal efficiency of the cycle yields

$$\eta_{th} = \frac{\dot{W}_{net}}{\dot{Q}_{evap}}. \tag{3.118}$$

The evaporator heat exchanger effectiveness can be calculated from the following equations,

$$\dot{Q}_{source,max} = \dot{m}_{soure} \cdot C_{p,source}(T_{source,i} - T_2) \tag{3.119}$$

$$\varepsilon_{evap} = \frac{\dot{Q}_{evap}}{\dot{Q}_{source,max}}. \tag{3.120}$$

Also, the condenser heat exchanger effectiveness can be calculated from

$$\dot{Q}_{sink,max} = \dot{m}_{sink} \cdot C_{p,sink}(T_4 - T_{sink,i}) \tag{3.121}$$

$$\varepsilon_{cond} = \frac{\dot{Q}_{cond}}{\dot{Q}_{sink,max}}. \tag{3.122}$$

3.3.4 Organic Rankine Cycle with Internal Regenerator

A regenerative internal heat exchanger is added to the baseline ORC in order to modify the configuration for better efficiency (Woodland, 2013). The regenerator is added for heat exchanged between expander exit stream and pumped stream as shown in Figure 3.35.

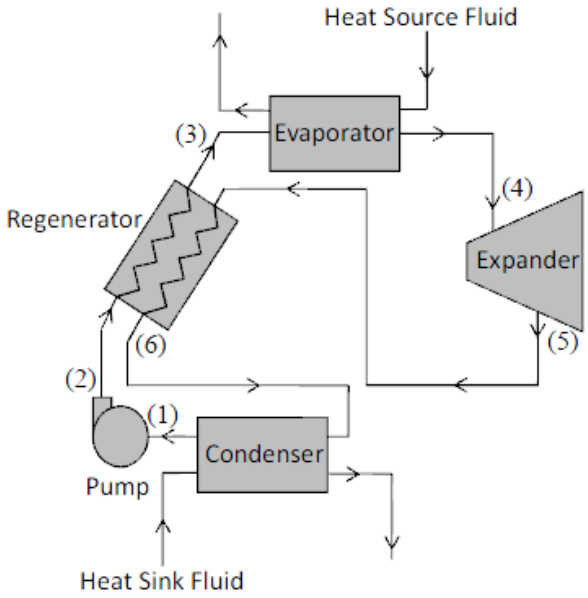

Figure 3.35. ORC with regenerator schematic (Woodland, 2013).

The expander discharges superheated vapor having sufficiently high energy. This stream has a potential to preheat the subcooled liquid working fluid from the pump before it enters the evaporator. This additional regenerator helps reducing the heat input to the

evaporator and let the heat source stream exits the cycle at higher temperature compared to a regular baseline ORC. As a result, the thermal efficiency of the cycle is increased. A temperature-entropy diagram for the working fluid R245fa, indicating the state points of the ORC with regenerator, is provided as Figure 3.36, where the regenerator exchanges heat from state point 5 to 6 to heat up the pumped stream from state point 2 to 3.

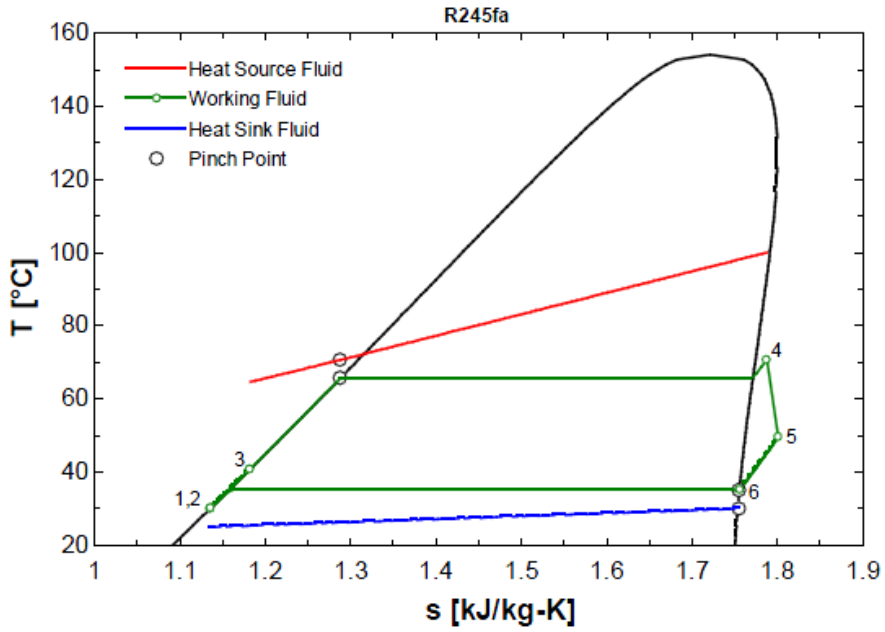

Figure 3.36. ORC with regenerator T-s diagram for actual processes with heat source and heat sink temperature profiles superimposed (Woodland, 2013).

This application is advantageous for heat streams containing acid substances such as combustion exhaust gases. The exhaust stream has a specific discharge temperature limited to the acid dew point temperature. If the discharge temperature is lower than the acid dew point, acids contained in the flue gas will condense and cause corrosion damage to the equipment.

The mass balance of the regenerator is defined as

$$\dot{m}_2 = \dot{m}_3 = \dot{m}_5 = \dot{m}_6 = \dot{m}_{orc} . \tag{3.123}$$

The energy balance across the regenerator can be expressed as

$$\dot{Q}_{regen} = \dot{m}_{orc}(h_5 - h_6) = \dot{m}_{orc}(h_3 - h_2). \tag{3.124}$$

The regenerator effectiveness governs as

$$\dot{Q}_{regen,max} = \dot{m}_{orc}(h_5 - h_2) \tag{3.125}$$

$$\varepsilon_{regen} = \frac{\dot{Q}_{regen}}{\dot{Q}_{regen,max}}. \tag{3.126}$$

3.3.5 Two-Phase Flash Expansion Organic Rankine Cycle

A schematic of an ORC with two-phase flash expansion, whose expansion process starts from saturated liquid or two-phase mixture instead of saturated vapor or superheated vapor, is shown in Figure 3.37. The inlet stream is flashed into the two-phase region by the pressure drops across the expander and the outlet state has more vapor fraction than its inlet as shown in Figure 3.38 of the cycle state points in a temperature-entropy diagram for the working fluid R245fa. A detailed schematic of the heater is shown in Figure 3.39.

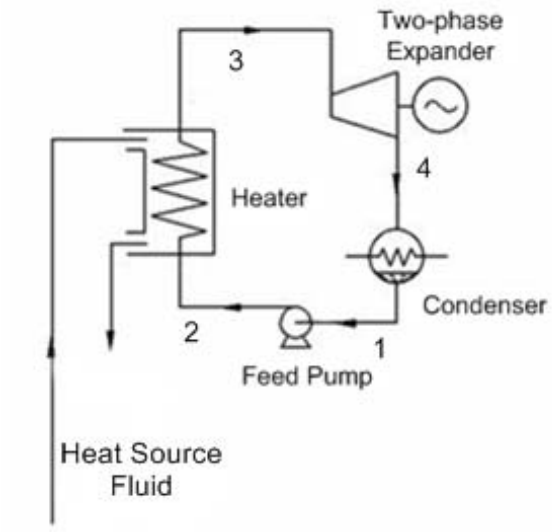

Figure 3.37. ORC with two-phase flash expansion schematic (Edited from Smith, Stosic and Kovacevic, 2001).

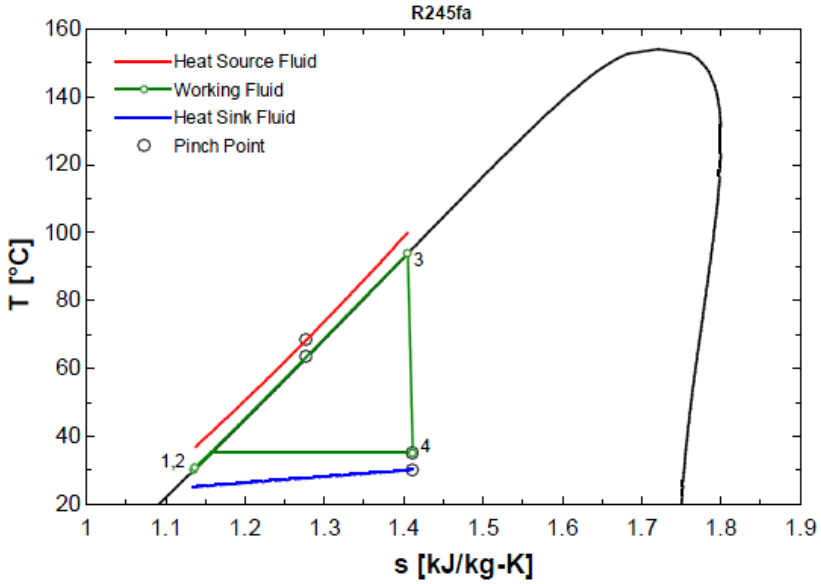

Figure 3.38. ORC with two-phase flash expansion T-s diagram for actual processes with heat source and heat sink temperature profiles superimposed (Woodland, 2013).

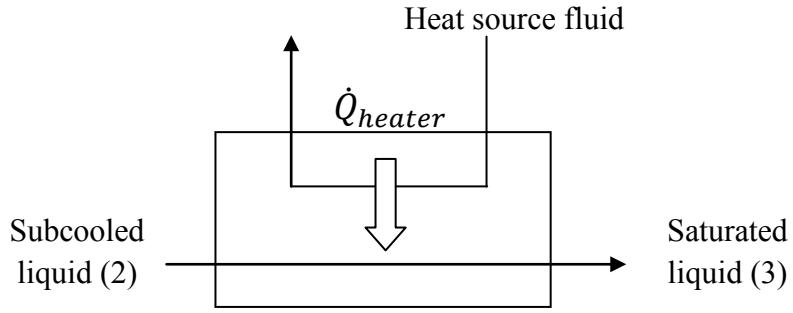

Figure 3.39. Heater schematic for two-phase flash expansion ORC.

The mass balance of the working fluid in the heater is defined as

$$\dot{m}_2 = \dot{m}_3 = \dot{m}_{orc}. \tag{3.127}$$

The energy balance across the regenerator can be expressed as

$$\dot{Q}_{heater} = \dot{m}_{orc}(h_3 - h_2) = \dot{m}_{source}(h_{source,i} - h_{source,o}). \tag{3.128}$$

The maximum heat transfer rate in the heater and heater effectiveness are calculated as

$$\dot{Q}_{heater,max} = \dot{m}_{source} \cdot C_{p,source}(T_{source,i} - T_2) \tag{3.129}$$

$$\varepsilon_{heater} = \frac{\dot{Q}_{heater}}{\dot{Q}_{heater,max}}. \tag{3.130}$$

3.3.6 Organic Rankine Cycle with Multiple Heat Sources

The model of the ORC with multiple heat sources is developed to utilize multiple potential waste heat sources from the power plant at different temperature levels. The lower-grade heat source is obtained to a heat exchanger for preheating of the working fluid before flowing to the evaporator. A schematic of the cycle is illustrated in Figure 3.31, where the heat source fluid 2 has a higher temperature than the heat source fluid 1.

The lower-grade heat source or heat source fluid 1 can be referred to as a secondary heat source.

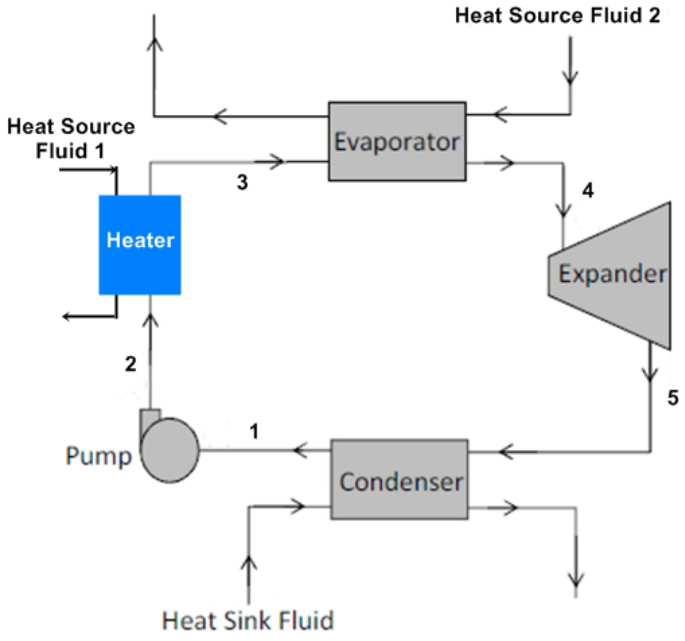

Figure 3.40. ORC with multiple heat sources (modified from Woodland, 2013).

The heat transfer rate in the heater can be expressed as

$$\dot{Q}_{heater,MS} = \dot{m}_{orc}(h_3 - h_2) = \dot{m}_{source,1}(h_{source,1,i} - h_{source,1,o}). \quad (3.131)$$

The maximum heat transfer rate in the heater and heater effectiveness are calculated as

$$\dot{Q}_{heater,MS,max} = \dot{m}_{source,1} \cdot C_{p,source,1}(T_{source,1,i} - T_2) \quad (3.132)$$

$$\varepsilon_{heater} = \frac{\dot{Q}_{heater,MS}}{\dot{Q}_{heater,MS,max}}. \quad (3.133)$$

The total heat input to the cycle is calculated by

$$\dot{Q}_{total,MS} = \dot{Q}_{evap,MS} + \dot{Q}_{heater,MS} \quad (3.134)$$

$$\dot{Q}_{evap,MS} = \dot{m}_{orc}(h_4 - h_3). \quad (3.135)$$

The thermal efficiency yields

$$\eta_{th,MS} = \frac{\dot{W}_{net,MS}}{\dot{Q}_{total,MS}}. \quad (3.136)$$

3.4 Energy Availability Utilization and Evaluation Parameter

Energy availability, or so called exergy, of a heat source stream is the maximum useful work possible that could be obtained in a cycle or a process, which brings the stream from its initial state into equilibrium with surroundings (Perrot, 1998 and Groll, 2012). Figure 3.41 illustrates the flow of exergy as an availability transfer rate enters a closed system.

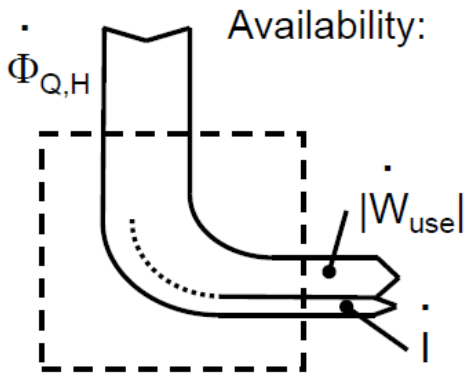

Figure 3.41. Flow of exergy entering a closed system (Groll, 2012).

The balance of availability for a closed system under the assumption of steady state conditions can be expressed as

$$\dot{\Phi}_{Q_H} = \dot{W}_{use} + \dot{I} \quad (3.137)$$

where $\dot{\Phi}_{Q_H}$ is the availability transfer rate or exergy rate to the system due to the heat transfer of the heat stream, $\dot{W}_{use}$ refers to the actual or useful work of the stream, and $\dot{I}$ represents the irreversibility. By assuming steady state and steady flow conditions with negligible changes in kinetic and potential energy, the availability transfer rate can be calculated from

$$\dot{\Phi}_Q = \dot{m} \int (1 - \frac{T_o}{T}) \delta q = \dot{m}[(h - h_o) - T_o(s - s_o)]. \qquad (3.138)$$

T_o is the surrounding temperature or dead state temperature. T is the temperature of the heat stream. $\dot{Q}$ is the energy capacity contained in the heat stream and the mass flow rate of the heat stream is indicated as $\dot{m}$. Specific enthalpy, *h* and specific entropy, *s* are presented as functions of T and T_o.

A cycle is a combination of processes and the energy flow. Figure 3.42 illustrates energy flow in a general heat engine cycle with uniform temperatures under SSSF conditions. The heat source stream enters the cycle at temperature T_H. The cycle is presented by the control mass, CM. The input energy flowing into cycle which operates at the high-side temperature of T_A is considered the remaining energy of the source stream after irreversibility ($\dot{I}_{Q_H}$) occurred. Once the input energy which has the availability transfer rate of $\dot{\Phi}_{Q_{H,A}}$ drives the cycle, it provides useful power, $\dot{W}_{use}$, as the cycle temperature drops from T_A to T_B, and at the same time produces irreversibility ($\dot{I}_{CM}$). Heat rejected from the cycle also has an availability transfer rate of $\dot{\Phi}_{Q_{B,o}}$. This availability transfer rate reaches zero if the stream is brought down to dead state conditions within the surrounding. In this case, the availability transfer rate of the

rejected heat can be implied as irreversibility ($\dot{I}_{Q_L}$). At dead state, there is no availability transfer rate left and $\dot{\Phi}_{Q_{0,0}} = 0$.

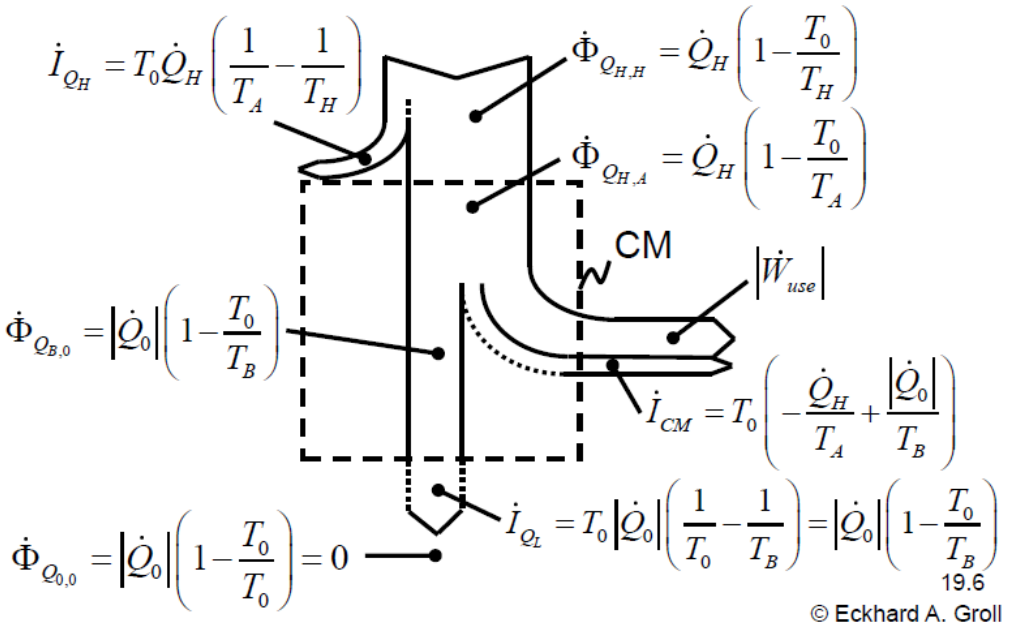

Figure 3.42. Flow of exergy in a heat engine cycle (Groll, 2012).

Exergy efficiency can be used as one of the methods to evaluate the availability utilization of a cycle. It represents the ability of the cycle in producing exergy rate output from the initial exergy rate input. The performance of the cycle is defined by the Second Law of Thermodynamics and can be expressed as the Second Law effectiveness as shown in Equation 3.139,

$$\varepsilon_{2nd} = \frac{Exergy\ Rate_{output}}{Exergy\ Rate_{input}}. \tag{3.139}$$

The Second Law effectiveness of an absorption heat pump cycle for cooling application can be expressed in the set of equations as

$$\varepsilon_{HP,cooling} = \frac{\dot{\Phi}_{Q_L}}{\Phi_{Q_{input}} + \dot{W}_{input}} = \frac{COP_{actual,cooling}}{COP_{Carnot,cooling}} \tag{3.140}$$

$$\dot{\Phi}_{Q_L} = \dot{m}_L \int (\frac{T_o}{T_L} - 1)\delta q = \dot{m}_L[T_o(s_o - s_L) - (h_o - h_L)] \tag{3.141}$$

where $\dot{Q}_L$is the cooling capacity at the evaporator, $\dot{Q}_{input}$is the heat capacity of the heat source stream and $\dot{W}_{input}$ is the work supplied to pumps. The mass flow rate of the chilled water or cooling air is presented as $\dot{m}_L$.

For incompressible fluids at constant pressure, the difference of specific entropy is expressed as

$$\Delta s = s_1 - s_2 = C_p \ln (\frac{T_1}{T_2}) . \tag{3.142}$$

For Organic Rankine cycles, the Second Law effectiveness yields

$$\varepsilon_{HE} = \frac{\dot{W}_{output,net}}{\dot{\Phi}_{Q_{input}}} = \frac{\eta_{th,actual}}{\eta_{th,Carnot}} \tag{3.143}$$

$$\dot{\Phi}_{Q_{input}} = \dot{m}_H \int (1 - \frac{T_o}{T_H})\delta q = \dot{m}_H[(h_H - h_o) - T_o(s_H - s_o)]. \tag{3.144}$$

The net power output of the cycle represents the turbine power minus the pump and other auxiliary power input and the exergy input lies in the heat source stream. When the cycles are driven by the same heat source stream, the denominator is constant and the Second Law effectiveness only depends on the net power output produced by the cycle. Higher net power output results in a higher effectiveness, which means the cycles can better utilize the heat source. This indicator can be used to evaluate the performance of the given systems.

3.5 Simple Economic Analysis

An economic analysis is another important tool in making a decision to invest in a system. The payback period of the system is one of the economic indicators, which presents the period of time when the system's inflows or savings can breakeven its investment cost. Shorter payback periods appeal to investors to put money into waste heat recovery technologies. Along with exergy efficiency, a simple payback method is selected in this work to evaluate the different systems. The results aim to help investors making decision. The calculation of payback period is expressed as

$$Payback\ Period = \frac{Investment\ Cost}{Annual\ Savings}. \tag{3.145}$$

Considering a waste heat recovery system that generates electricity, the recovered power output does not consume any input fuel. $Cost_{fuel}$ is the price of the input primary energy per unit of electrical energy produced. The savings can be calculated by:

$$Annual\ Savings_{power\ gen} = Annual\ WHR\ Power\ Production \cdot Cost_{fuel} \tag{3.146}$$

For absorption chillers driven by waste heat, the savings relates to the cooling load achieved by the system and cost of electricity spent to provide the cooling load if WHR is not installed. $Cost_{electricity}$ refers to the price of distributed electricity per unit of electrical energy consumed. The savings can be calculated by:

$$Annual\ Savings_{chiller} = Annual\ Cooling\ load\ achieved\ by\ WHR \cdot Cost_{electricity}. \tag{3.147}$$

The payback period is usually presented in number of years. This is the reason why yearly savings are taken into consideration.

CHAPTER 4. RESULTS OF MODEL ANALYSIS

This work has been conducted to theoretically compare two waste heat recovery technologies; absorption chillers and ORCs. Four different absorption-chiller models are studied with two different working-fluid pairs, which are H_2O/LiBr and NH_3/H_2O. For ORCs, four different cycles are modeled with two selected working fluids, which are R134a and R245fa. Feasible waste heat sources are applied to the applicable models. Thermodynamic modeling was performed in EES. Amounts of heat rejected from the power plant from different components are revealed in Subchapter 4.1. Results of the model analysis and summaries of the evaluations are discussed in Subchapter 4.2 and Subchapter 4.3, for absorption chillers and ORCs, respectively. The calculated simple economic payback periods are presented in Subchapter 4.4.

4.1 Waste Heat Capacities

As mentioned earlier in Chapter 3, four potential waste heat streams are rejected from this power plant in forms of CT room ventilation air, exhaust gas leaving HRSG, lubrication oil heat rejection, and cooling tower heat rejection. With the equations of energy balance demonstrated in Chapter 3, heat capacities of the waste heat streams can be calculated and the results are summarized in Table 4.1.

Table 4.1. Summary of waste heat capacities and rejection temperatures.

Waste Heat Source	Rejected Heat Capacity (kW)	Heat Rejection Temperature (°C)	Mass Flow Rate (kg/s)
CT room ventilation air	145,200	150	1,200
Exhaust gas leaving HRSG	74,910	100	915
Lubrication oil	2,355	82	40
Cooling tower water	631,000	40	11,600

From Table 4.1, the ventilation air heat stream has significantly high heat capacity due to its high temperature and a large mass flow rate. This heat stream is an excellent heat input for both systems; absorption chillers and ORCs. Especially for absorption chillers, this hot air stream shows great promise as the heat source to the double-effect H_2O/LiBr cycle and may have the potential to provide a large cooling capacity. For the exhaust gas leaving HRSG stack, there is a strong evidence of acid-condensation potential due to the acid dew point of sulfur trioxide (SO_3) substance that is contained in the exhaust gas, as shown in Chapter 2. Unfortunately, this amount of heat must be thrown away with the flue gas to protect HRSG components and pipelines from corrosive damage. Although heat rejection from lubrication oil tank does not give as high heat capacity as the first two streams, its rejecting temperature is enough to drive the studied WHR technologies. This heat stream can be used as a heat source for either single-effect or half-effect absorption cycles, or ORCs. Cooling water or cooling tower's circulating water contains the largest amount of heat among all the waste heat candidates. However, it has insufficiently low temperature to drive the bottoming WHR cycles and thus; this waste heat stream is not feasible to be the input energy of any cycles in this study.

In summary, the only useful waste heat streams for the investigated models are the CT room ventilation air and the heat stream rejected from lubrication oil tank.

4.2 Absorption Chiller Modeling Results

The lubrication oil heat stream at 82°C and the CT room ventilation air heat stream at 150°C are applied to the single-effect absorption cycles for both working fluids. It is evident that only the CT room ventilation air heat stream can possibly drive the double effect H_2O/LiBr absorption cycle as it requires a higher temperature heat source. On the other hand, only the lubrication oil heat stream is applied to the half-effect cycles, since the half-effect cycle requires a lower temperature heat source. Results of all the absorption chiller models will be discussed as of the order shown in Table 4.2.

Table 4.2. Presentation of results for absorption chillers.

Model	Working Fluid	Heat Source
Single-effect cycle	H_2O/LiBr	Lubrication oil
		CT room ventilation air
	NH_3/H_2O	Lubrication oil
		CT room ventilation air
Double-effect cycle	H_2O/LiBr	CT room ventilation air
Half-effect cycle	H_2O/LiBr	Lubrication oil
	NH_3/H_2O	Lubrication oil

Figure 4.1 shows the P-T diagram of the single-effect H_2O/LiBr absorption cycle driven by heat rejected from the lubrication oil tank. Saturated water vapor is evaporated by the cooling load of 1,947 kW and leaves the evaporator at state point 10. The absorber rejects heat of 2,294 kW in order to absorb this water vapor into the absorption cycle while having a temperature glide in the range of 27°C to 49.7°C. The weak solution with

LiBr-concentration (x_w) of 49% exits the absorber at state point 1 and is pumped up to a higher pressure at state point 2. This subcooled weak solution is then heated up to state point 3 after flowing through the solution heat exchanger. The warm subcooled weak solution enters the generator and has a temperature glide from 48.5°C to 72°C which is the range in which the heat input must occur. As the hot lubrication oil stream flows through the generator, heat is being transferred causing a temperature drop in the oil from 82°C to 54°C, at the lowest. The generator receives a 2,355-kW heat input by the heat rejected from the lube oil and boils the water off from the weak solution. Following this, the superheated water steam leaves the generator at state point 7. This forces the remaining solution to become a rich solution with a LiBr-concentration (x_r) of 61%. This rich solution exits the generator at 72°C as saturated liquid and enters the solution heat exchanger to reject an amount of heat to the weak solution as explained earlier. It then becomes subcooled and is then expanded through the throttling valve before it returns to the absorber. After evaporating out of the generator, superheated refrigerant enters the condenser and is condensed to saturated liquid refrigerant during which a condensing heat of 2,008 kW is rejected. This cycle operation conforms to other typical single-effect absorption cycles and thus, gives a COP of 0.83 with an exergy efficiency of 79%. The state points corresponding to this cycle are shown in Table 4.3.

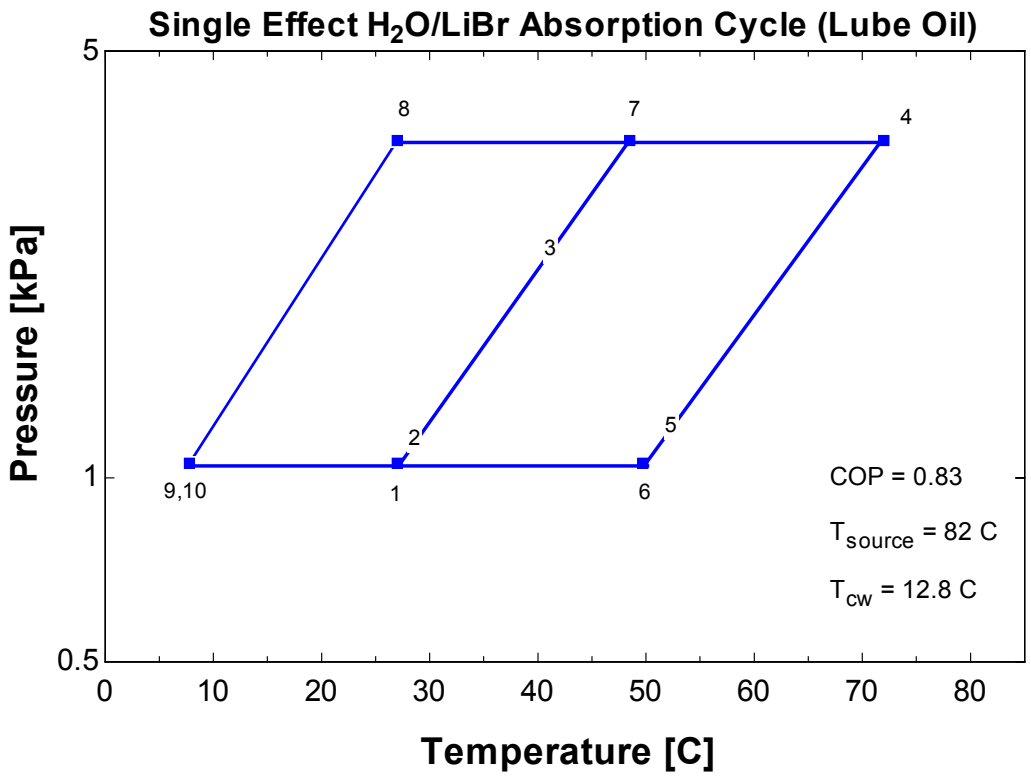

Figure 4.1. Single-effect H_2O/LiBr absorption cycle P-T diagram of lubrication oil heat source.

Table 4.3. State points of single-effect H_2O/LiBr absorption cycle P-T diagram of lubrication oil heat source, corresponding to Figure 4.1.

State Point	Enthalpy	Pressure	Quality	Temperature	LiBr concentration	Mass flow rate
	[kJ/kg]	[kPa]	[-]	[C]	[-]	[kg/s]
1	53.48	1.057	0	27	0.4879	4.08
2	53.48	3.567	-100	27	0.4879	4.08
3	84.51	3.567	-100	41.13	0.4879	4.08
4	183.5	3.567	0	72	0.6089	3.269
5	144.8	3.567	-100	51.75	0.6089	3.269
6	144.8	1.057	0.001198	49.7	0.6089	3.269
7	2590	3.567	100	48.5	0	0.8107
8	113.1	3.567	0	27	0	0.8107
9	113.1	1.057	0.03241	7.778	0	0.8107
10	2515	1.057	1	7.778	0	0.8107

The P-T diagram in Figure 4.2 shows a single-effect H_2O/LiBr absorption cycle driven by waste heat contained in the 150°C-CT room ventilation air. Table 4.4 presents the corresponding state points.

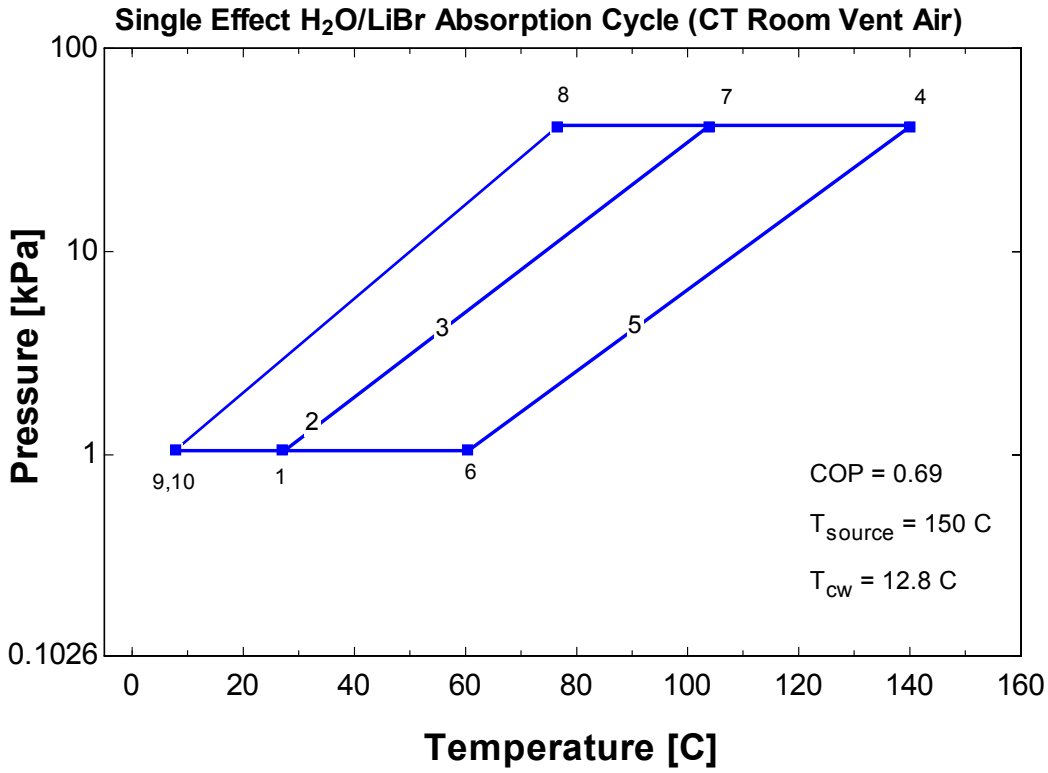

Figure 4.2. Single-effect H_2O/LiBr absorption cycle P-T diagram of CT room ventilation air heat source.

In this cycle, the absorber rejects 57,508 kW of heat to the environment and has a temperature glide from 27°C to 60.3°C. The CT room ventilation air stream provides heat input of 60,858 kW to the generator which covers the range of generator temperature glide from 104°C to 140°C. This cycle has a similar operation to that of the single-effect H_2O/LiBr absorption cycle driven by the lubrication oil heat stream. With higher heat source temperature, the rich solution results in higher LiBr-concentration. However, the rich solution concentration is limited to 65% due to the crystallization limit, forcing the

high-side pressure to be increased in order for the cycle to operate at 150°C-heat input. This limitation causes higher pressure ratio compared to the lube-oil-driven cycle, hence causing a lower COP of 0.69 and a lower exergy efficiency of 24%. Despite having a lower COP and exergy efficiency, the massive hot-air heat source allows the cycle to provide a large cooling capacity of up to 41,839 kW to the chilled water. Nevertheless, in order to achieve this higher cooling capacity the sizes of the components in the ventilation-air-driven model must be increased, which could result in a higher cost.

Table 4.4. State points of single-effect H_2O/LiBr absorption cycle P-T diagram of CT room ventilation air heat source, corresponding to Figure 4.2.

State Point	Enthalpy	Pressure	Quality	Temperature	LiBr concentration	Mass flow rate
	[kJ/kg]	[kPa]	[-]	[C]	[-]	[kg/s]
1	53.48	1.057	0	27	0.4879	76.44
2	53.52	40.98	-100	27.02	0.4879	76.44
3	124.6	40.98	-100	59.08	0.4879	76.44
4	332.7	40.98	0	140	0.65	57.38
5	238	40.98	-100	89.16	0.65	57.38
6	238	1.057	0.01708	60.33	0.65	57.38
7	2691	40.98	100	103.8	0	19.06
8	320.1	40.98	0	76.46	0	19.06
9	320.1	1.057	0.1158	7.778	0	19.06
10	2515	1.057	1	7.778	0	19.06

The state points of a single-effect NH_3/H_2O absorption cycle are presented on the temperature-concentration diagram since the NH_3-refrigerant leaving the rectifier is usually not pure.

Figure 4.3 illustrates the T-x diagram of a single-effect NH_3/H_2O absorption model with a precooler and a rectifier heat exchanger. The cycle uses rejected heat from the lubrication oil of 2,355 kW as the heat input.

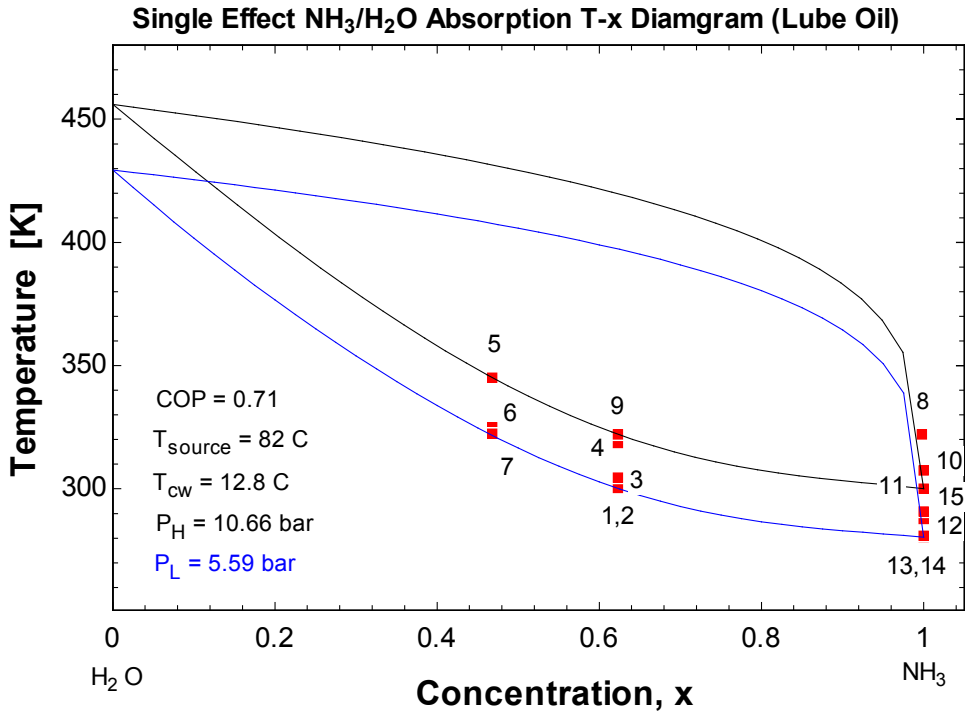

Figure 4.3. Single-effect NH_3/H_2O absorption cycle T-x diagram of lubrication oil heat source.

The temperature glide of the absorber ranges from 300 K to 322.4 K (27°C to 49.3°C). After absorbing saturated vapor of extremely strong refrigerant solution with NH_3-concentration of 99.96%, the absorber rejects 2,344 kW of heat to the environment. The exiting solution at state point 1 still has a high NH_3-concentration, which is 62.3%. This solution is called the rich solution. This rich solution leaves the absorber as saturated liquid and is pumped up to state point 2. Now, the high-pressure rich solution is first preheated by heat rejected from the rectifier, following which it is heated up while flowing through the solution heat exchanger. This heated rich solution at state point 4

enters the generator, which has a temperature glide covering from 322.1 K to 345.1 K (49°C to 72°C). Due to the desorbing process in the generator, most NH_3 is boiled out to state point 8 and the weak solution leaves the generator as saturated liquid at state point 5. Superheated NH_3 of a concentration of 99.78% at state point 8 must be purified at the rectifier before entering the condenser to a concentration of 99.96% at state point 10. Water-dominant solution with a NH_3-concentration of 62.3% as saturated liquid returns to the generator at state point 9. Purification process at the rectifier must reject some heat to the environment; thus, the cycle is modeled to utilize this heat by preheating the pumped rich solution as mentioned earlier. The warm weak solution flows through the solution heat exchanger and is expanded down to the absorber to complete the absorption circuit. The refrigerant solution is condensed to saturated liquid at the condenser. Then, it is cooled down at the precooler and throttled down to the evaporator. Because the refrigerant solution that leaves the evaporator usually has some quality, the heat rejected from the precooler is utilized to heat this two-phase solution. This process lets the refrigerant solution enter the absorber as saturated vapor. Table 4.5 shows the corresponding state points, which theoretically conform to literature.

Due to the contamination of water in the refrigerant vapor, this cycle can only provide 1,690 kW of cooling capacity with the COP of 0.71 and an exergy efficiency of 67.4%. Also, as more heat exchangers have to be used, the cycle becomes more complex.

Table 4.5. State points of single-effect NH_3/H_2O absorption cycle T-x diagram of lubrication oil heat source, corresponding to Figure 4.3.

State Point	Enthalpy [kJ/kg]	Mass flow rate [kg/s]	Pressure [bar]	Quality [-]	Temperature [K]	NH3-Concentration [-]
1	-99.33	4.995	5.588	0	300.1	0.6229
2	-98.25	4.995	10.66	-0.001	300.3	0.6229
3	-78.96	4.995	10.66	-0.001	304.5	0.6229
4	-14.11	4.995	10.66	-0.001	318.6	0.6229
5	84.96	3.537	10.66	0	345.1	0.4677
6	-6.613	3.537	10.66	-0.001	325	0.4677
7	-6.613	3.537	5.588	0.008199	322.4	0.4677
8	1355	1.464	10.66	1	322.1	0.9978
9	2.357	0.007149	10.66	0	322.1	0.6229
10	1296	1.457	10.66	1	307.5	0.9996
11	127	1.457	10.66	0	300.1	0.9996
12	94.64	1.457	10.66	-0.001	293.4	0.9996
13	94.64	1.457	5.588	0.04936	280.4	0.9996
14	1252	1.457	5.588	0.98	280.9	0.9996
15	1284	1.457	5.588	1	290.8	0.9996

For the single-effect NH_3/H_2O absorption cycle driven by CT room ventilation air heat source, all state points are plotted in a T-x diagram as shown in Figure 4.4. This cycle has a similar operation as compared to the single-effect NH_3/H_2O absorption cycle driven by the lube oil heat source, except for the higher operating temperatures at the generator. Pressure ratios of both cycles are the same since NH_3-concentrations are not constrained by crystallization.

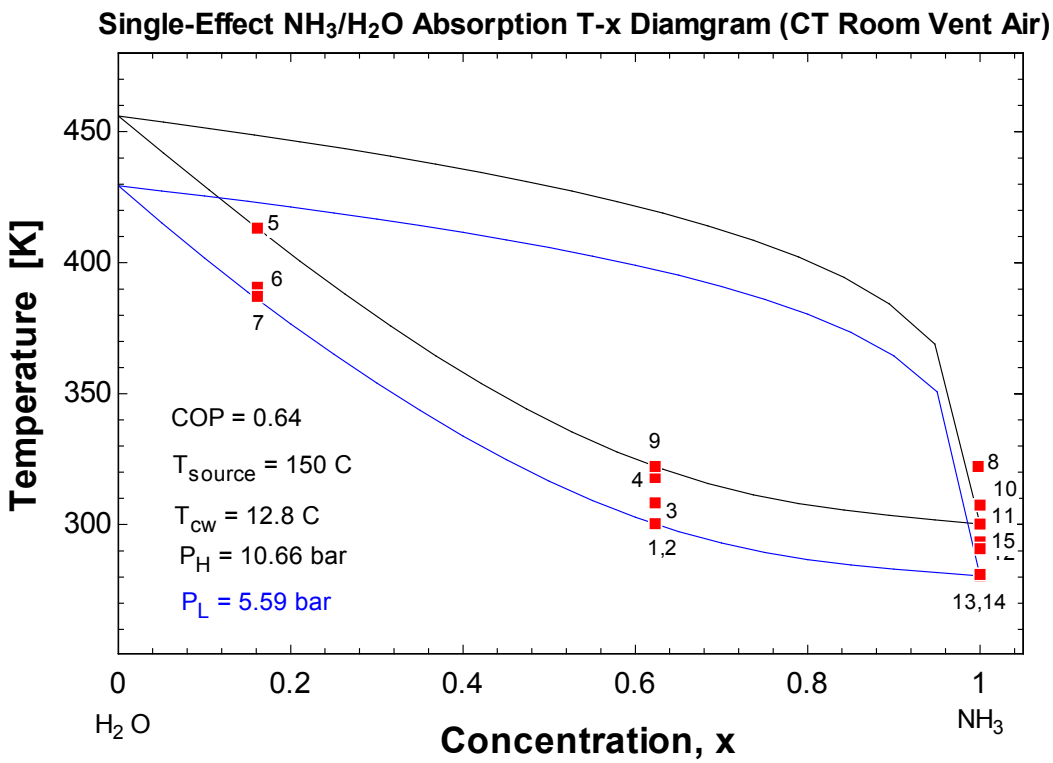

Figure 4.4. Single-effect NH_3/H_2O absorption cycle T-x diagram of CT room ventilation air heat source.

The absorber temperature glide ranges from 300K to 387.2K (27°C to 114°C) and 60,534-kW heat is rejected from the absorption process. The generator receives heat input from the hot ventilation air of 60,858 kW to cover the range of generator temperature glide of 322.1K to 413.1K (89°C to 140°C). With the heat input temperature of 150°C, this cycle can provide cooling capacity of 39,285 kW with the COP of 0.64 and an exergy efficiency of 22.2%. Properties of all the state points are shown in Table 4.6.

Table 4.6. State points of single-effect NH_3/H_2O absorption cycle T-x diagram of CT room ventilation air heat source, corresponding to Figure 4.4.

State Point	Enthalpy	Mass flow rate	Pressure	Quality	Temperature	NH3-Concentration
	[kJ/kg]	[kg/s]	[bar]	[-]	[K]	[-]
1	-99.33	61.65	5.588	0	300.1	0.6229
2	-98.25	61.65	10.66	-0.001	300.3	0.6229
3	-61.85	61.65	10.66	-0.001	308.2	0.6229
4	-16.65	61.65	10.66	-0.001	318	0.6229
5	491	27.7	10.66	0	413.1	0.1614
6	390.4	27.7	10.66	-0.001	390.6	0.1614
7	390.4	27.7	5.588	0.008525	387.2	0.1614
8	1355	34.11	10.66	1	322.1	0.9978
9	2.357	0.1665	10.66	0	322.1	0.6229
10	1296	33.95	10.66	1	307.5	0.9996
11	127	33.95	10.66	0	300.1	0.9996
12	94.64	33.95	10.66	-0.001	293.4	0.9996
13	94.64	33.95	5.588	0.04936	280.4	0.9996
14	1252	33.95	5.588	0.98	280.9	0.9996
15	1284	33.95	5.588	1	290.8	0.9996

At this point, it can be seen that the H_2O/LiBr cycles has higher efficiencies than the NH_3/H_2O cycles which conforms to the literature reviewed. When comparing the performance of single-effect cycles by heat source temperatures, the cycles driven by CT room ventilation air tends to have lower COP and relatively lower exergy efficiencies than the cycles driven by lubrication oil. These results support the statement that the single-effect absorption cycles are suitable for low heat source temperatures, whereas the high heat source temperatures are better to drive the double-effect absorption cycles.

The state points of the double-effect H2O/LiBr absorption cycle are indicated in a P-T diagram as presented in Figure 4.5. The double-effect cycle operates at three pressure levels, where the two pumps and the two solution heat exchangers are independent from

each other. The effectiveness of each heat exchanger is adjusted to theoretically satisfy the state point temperatures. Properties of all state points are shown in Table 4.7.

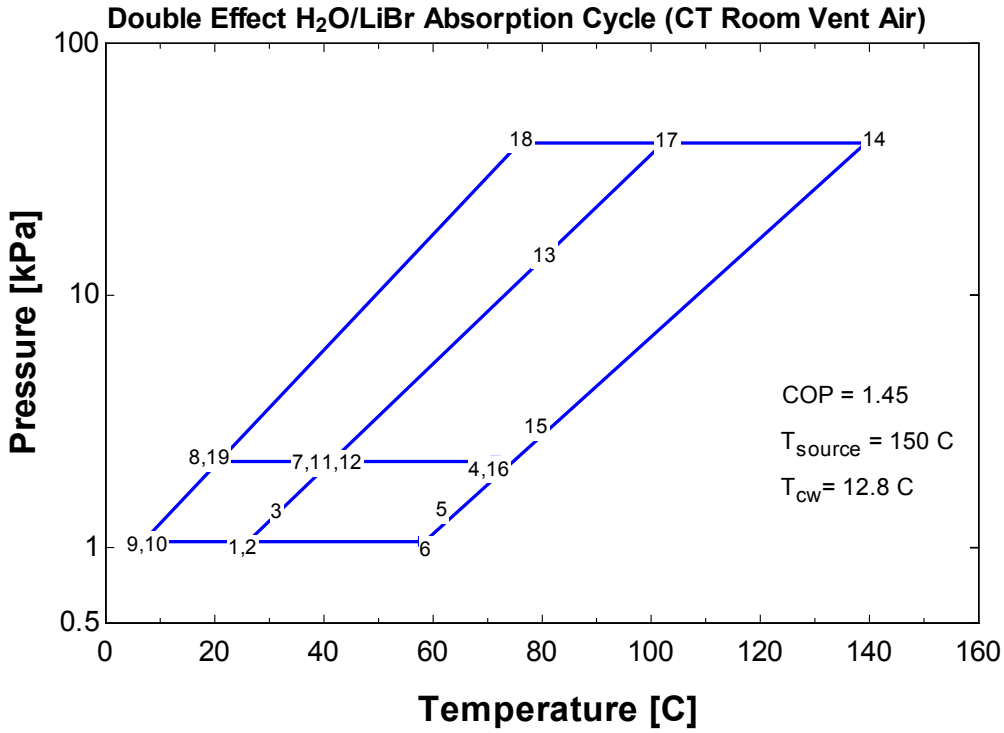

Figure 4.5. Double-effect H_2O/LiBr absorption cycle P-T diagram of CT room ventilation air heat source.

The CT room ventilation heat stream is used as the heat source of the cycle due to its high temperature profile. This heat source possibly allows the cycle to have a higher LiBr-concentration in the rich solution. However, due to crystallization, the cycle assumption was made to limit the LiBr-concentration of the rich solution to 0.65, in order to avoid crystallization in the absorber.

The top and bottom absorption circuits share the same circulation ratio. The weak solution has a LiBr-concentration of 48.8% and the rich concentration contains a LiBr-salt at 65% to prevent crystallization.

Table 4.7. State points of double-effect H_2O/LiBr absorption cycle P-T diagram of CT room ventilation air heat source, corresponding to Figure 4.5.

State Point	Enthalpy	Pressure	Quality	Temperature	LiBr concentration	Mass flow rate
	[kJ/kg]	[kPa]	[-]	[C]	[-]	[kg/s]
1	53.48	1.057	0	27	0.4879	145.5
2	53.48	2.203	-100	27	0.4879	145.5
3	68.41	2.203	-100	33.83	0.4879	145.5
4	208	2.203	0	71.46	0.65	109.2
5	188.1	2.203	-100	60.35	0.65	109.2
6	188.1	1.057	0.001221	58.19	0.65	109.2
7	2574	2.203	100	39.59	0	16.19
8	79.8	2.203	0	19.03	0	36.28
9	79.8	1.057	0.01898	7.778	0	36.28
10	2515	1.057	1	7.778	0	36.28
11	81.1	2.203	0	39.59	0.4879	80.57
12	81.14	40.98	-100	39.59	0.4879	80.57
13	165.4	40.98	-100	77.08	0.4879	80.57
14	332.7	40.98	0	140	0.65	60.48
15	220.5	40.98	-100	77.29	0.65	60.48
16	220.5	2.203	0.003998	71.46	0.65	60.48
17	2691	40.98	100	103.8	0	20.09
18	320.1	40.98	0	76.46	0	20.09
19	320.1	2.203	0.09785	19.03	0	20.09

The absorber has a temperature glide between 27°C to 58°C. It rejects 104,000-kW heat to the environment in order to absorb refrigerant steam. The bottom absorption-cycle operates at the low pressure-level and has similar operation as the single-effect cycle. The low-pressure generator operates at the intermediate pressure-level to desorb partial amount of refrigerant from the bottom circuit, and forward it to the low side condenser that operates at the same pressure-level. The remaining solution is mixed with the rich solution from the top circuit in this low side generator. The temperature glide of

the low side generator spreads from 40°C to 71.5°C. Performance of the low side generator is governed by the amount of heat rejected from the high side condenser which is equal to 45,600 kW, and the temperature of the high side condenser outlet must cover the range of low side generator temperature glide. The top absorption circuit also works similarly to a single-effect cycle. The CT room ventilation air stream is the heat input supplied to the high side generator which has the temperature glide from 103°C to 140°C. A heat input of 60,858-kW is provided from the waste heat source to boil refrigerant water out. The second part of refrigerant is condensed at the high side condenser and mixed with the first part at the low side condenser. The total refrigerant is expanded to the evaporator and provides a cooling capacity of 88,344 kW to the chilled water. All the state points shown in Table 4.7 seem to be consistent with a typical double-effect H_2O/LiBr absorption cycle.

The double-effect cycle is expected to have higher performance compared to the single-effect cycles, and conformably the COP of this cycle rises up to 1.45. Although the cycle gives such high COP but the exergy efficiency turns out to be approximately 50%, which is less than those of lube-oil-driven single-effect cycles. This means, in terms of exergy, the high COP does not reflect better exergy utilization.

The half-effect absorption cycle can be realized with both working-fluid pairs. The half-effect cycle is suitable for low-grade heat sources with temperatures lower than those of the single-effect absorption cycles. Hence, lubrication oil heat stream is used as a heat input to the half-effect cycles.

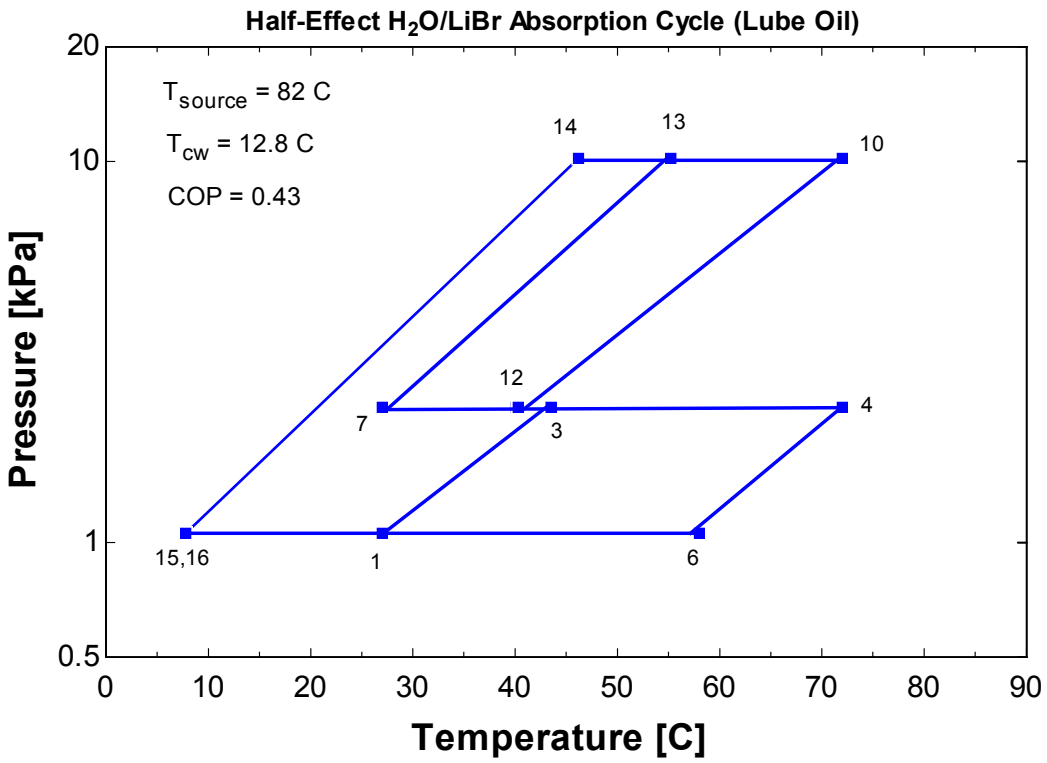

Figure 4.6. Half-effect H_2O/LiBr absorption cycle P-T diagram of lubrication oil heat source.

Figure 4.6 shows the half-effect H2O/LiBr absorption cycle plotted in a P-T diagram, and the corresponding state points are presenting in Table 4.8. Once again in order to avoid crystallization, H_2O/LiBr cycle is also given a cycle assumption to limit the highest LiBr-concentration. LiBr-concentrations at state point 1 and 7 can be defined by the operating temperatures and pressures. However, the rich concentration for the high-pressure circuit is selected from a parametric study in order to yield the best cycle performance.

Table 4.8. State points of half-effect H_2O/LiBr absorption cycle P-T diagram of lubrication oil heat source, corresponding to Figure 4.6.

State Point	Enthalpy [kJ/kg]	Pressure [kPa]	Quality [-]	Temperature [C]	LiBr-concentration [-]	Mass flow rate [kg/s]
1	53.48	1.057	0	27	0.4879	1.745
2	53.48	2.265	0	27	0.4879	1.745
3	89.76	2.265	0	43.5	0.4879	1.745
4	208.9	2.265	0	72	0.65	1.31
5	160.6	2.265	-100	45	0.65	1.31
6	160.6	1.057	-100	44.45	0.65	1.31
7	57.75	2.265	0	27	0.3546	1.497
8	57.76	10.19	0	27	0.3546	1.497
9	114.1	10.19	0	48.35	0.3546	1.497
10	153.8	10.19	0	72	0.5	1.061
11	74.39	10.19	0	36	0.5	1.061
12	74.39	2.265	-100	41.99	0.5	1.061
13	2584	10.19	1	55.23	0	0.4353
14	193.4	10.19	0	46.19	0	0.4353
15	193.4	1.057	0.06474	7.778	0	0.4353
16	2515	1.057	1	7.778	0	0.4353
17	2575	2.265	100	40.09	0	0.4353

The half-effect H_2O/LiBr absorption cycle is equipped with two absorbers which operate at the low and intermediate pressure-levels, and two generators which operate at the intermediate and high pressure-levels. The total heat rejected from the lubrication oil, which is equal to 2,355 kW, is split into two heat streams to supply each of the generators in the absorption circuits. Because the refrigerant that leaves the bottom cycle is completely forwarded to the high-absorber of the top cycle, it causes the top and bottom cycles to have different circulation ratios, hence different amounts of heat required for the two generators and different amounts of heat rejected from the two absorbers.

The low-absorber rejects heat of 1,212 kW to absorb the refrigerant steam. It has a temperature glide from 27°C to 44.5°C. The low-side generator has a temperature glide from 40°C to 72°C and receives a heat input of 1,238 kW from the lube oil stream. The bottom cycle has a circulation ratio of 4. For the top cycle, a heat of 1,113 kW is rejected from the high side absorber to the environment. The high-side absorber temperature glide ranges from 27°C to 42°C. The high-side generator operates between temperatures of 55.2°C to 72°C and requires 1,117-kW heat from the source. The top cycle has a circulation ratio of 3.4. The same amount of refrigerant that once left the bottom cycle leaves the high side generator at state point 13 and is then condensed. The saturated refrigerant water flows through the expansion process and enters the evaporator. Hence a cooling load of 1,010 kW is received in the evaporator. The half-effect cycle gives a COP of 0.43 with a 41% exergy efficiency.

The state points of the half-effect NH_3/H_2O absorption cycle are plotted in the T-x diagram as shown in Figure 4.7, while Table 4.9 presents the properties of all state points.

Similar to the half-effect cycle with the working fluid H_2O/LiBr, the input heat from the lubrication oil is divided to serve both generators. At the bottom cycle, the low side absorber rejects heat of 1,257 kW to the environment and has a temperature glide between 300K to 318.3K (27°C to 45°C). The low side generator acquires the input heat of 1,312 kW and operates between the temperatures of 317.9K to 345.1K (45°C to 72°C). Highly-concentrated refrigerant solution with NH_3-concentration of 99.7% is desorbed from this low side generator. The top cycle obtains strong refrigerant solution from the bottom cycle at the high side absorber, which has a temperature glide from 300K to

309.5K (27°C to 37°C). Then, it releases the purified refrigerant solution with NH_3-concentration of 99.9% at the high side generator. Heat input of 1,043 kW is required for the desorption process. The released solution is condensed and expanded to the evaporator. This cycle has the ability of provide a cooling capacity of 897.3 kW, which is relatively low due to contamination of water in the refrigerant flow. Accordingly, the cycle gives a COP of 0.38 along with an exergy efficiency of 35.8%.

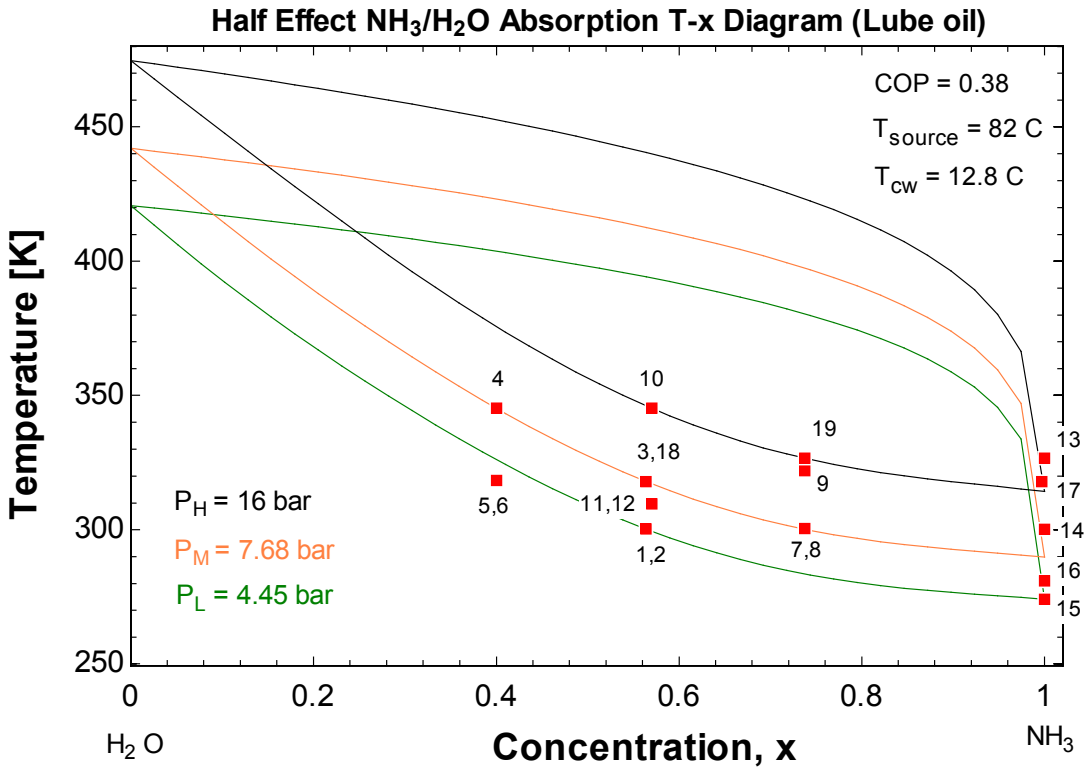

Figure 4.7. Half-effect NH_3/H_2O absorption cycle T-x diagram of lubrication oil heat source.

Table 4.9. State points of half-effect NH_3/H_2O absorption cycle T-x diagram of lubrication oil heat source, corresponding to Figure 4.7.

State Point	Enthalpy	Mass flow rate	Pressure	Quality	Temperature	NH3 Concentration
	[kJ/kg]	[kg/s]	[bar]	[-]	[K]	[-]
1	-113.3	2.814	4.445	0	300.1	0.5639
2	-112.6	2.814	7.678	-0.001	300.2	0.5639
3	-25.76	2.814	7.678	0.004215	318.1	0.5639
4	91.74	2.041	7.678	0	345.1	0.4
5	-28	2.041	7.678	-0.001	318.2	0.4
6	-28	2.041	4.445	-0.001	318.3	0.4
7	-50.78	1.985	7.678	0	300.1	0.7373
8	-48.87	1.985	16	-0.001	300.4	0.7373
9	52.13	1.985	16	-0.001	321.9	0.7373
10	95.97	1.213	16	0	345.1	0.57
11	-69.39	1.213	16	-0.001	309.4	0.57
12	-69.39	1.213	7.678	-0.001	309.5	0.57
13	1334	0.7726	16	1.001	326.6	0.9999
14	127.3	0.7726	16	-0.001	300.1	0.9999
15	127.3	0.7726	4.445	0.09732	274.1	0.9999
16	1289	0.7726	4.445	1	280.9	0.9999
17	1362	0.7726	7.678	1	317.9	0.997

Listed in Table 4.10 are the summaries of energy flows in each absorption cycle. The input energy flows are indicated by a plus sign and any energy flows leaving the cycles are presented with a minus sign. Internal energy transferred in the double-effect H_2O/LiBr absorption cycle from the high-side condenser to the low-side generator is not listed in the table. The internal energy transferred in the single-effect NH_3/H_2O absorption cycles, such as the rectifier heat transfer to the pumped rich solution, and the precooler heat transfer to vaporize the two-phase refrigerant vapor, are also not listed. These internal energy flows are rejected from one component and obtained by another.

The results show that every cycle is energy balanced as their summations of energy flows are equal to zero.

Table 4.10. Energy flows and balances of absorption cycles.

Component	Water-Lithium Bromide				Ammonia-Water		
	Single-Effect Cycle		Double-Effect Cycle	Half-Effect Cycle	Single-Effect Cycle		Half-Effect Cycle
	Lube Oil	CT Room Ventilation Air	CT Room Ventilation Air	Lube Oil	Lube Oil	CT Room Ventilation Air	Lube Oil
Absorber	- 2,294	- 57,508	- 104,000	- 2325	- 2,344	- 60,534	- 2,326
Pump	+ 0.01	+ 3	+ 4	+ 1	+ 6	+ 67	+ 6
Generator	+ 2,355	+ 60,858	+ 60,858	+ 2,355	+ 2,355	+ 60,858	+ 2,355
Condenser	- 2,008.01	- 45,192	- 45,206	- 1,041	- 1,703	- 39,676	- 932
Evaporator	+ 1,947	+ 41,839	+ 88,344	+ 1,010	+ 1,686	+ 39,285	+ 897
Summation	0	0	0	0	0	0	0

Table 4.11 summarizes the parameters chosen for evaluating the absorption cycles. These parameters are the second law effectiveness or exergy efficiency, and the cooling capacity. These parameters are chosen because the second law effectiveness indicates the cycle's ability to effectively utilize the energy in the heat source stream, whereas the cooling capacity serves as an indication of the theoretical output of the cycle which could directly benefit the end users.

Among the seven theoretical models studied in this work, the double-effect H_2O/LiBr absorption cycle is shown to have the ability to provide the largest cooling capacity due to the high heat source temperature of 150°C and the CT room ventilation air flow rate of 1200 kg/s. Furthermore, its ability to utilize the availability of the heat source is much improved from the other cycles. In addition to this, it is also shown that

the single-effect cycles can efficiently utilize the energy available in the 82°C-lubrication oil stream by giving higher exergy efficiencies. However, the cycles can only provide small amounts of cooling capacity to the chilled water, due to the small amount of heat available in the lube oil.

Table 4.11. Summary for evaluation of absorption chiller models.

Model	Working Fluid	Lubrication Oil		CT Room Ventilation Air	
		2nd Law Effectiveness	Cooling capacity (kW)	2nd Law Effectiveness	Cooling capacity (kW)
Single-effect	H_2O/LiBr	0.7914	1,947	0.2375	41,839
	NH_3/H_2O	0.6736	1,686	0.2224	39,285
Double-effect	H_2O/LiBr	-	-	0.5015	88,344
Half-effect	H_2O/LiBr	0.4107	1,010	-	-
	NH_3/H_2O	0.3582	897.0	-	-

4.3 Organic Rankine Cycle Modeling Results

The theoretical analyses of the various ORCs in this work have been carried out for both waste heat streams; the CT room ventilation air and heat rejected from the lubrication oil. The two working fluids selected for this study are R134a and R245fa. The state points of each ORC are plotted using the temperature-entropy diagrams of the working fluid. Results are presented in the order provided in Table 4.12.

The best performances of each ORC are presented in terms of the maximum second law effectiveness or exergy efficiency and the maximum net work output. All results presented in this subchapter are from the optimum performance models, which have been found by parametric studies of the evaporating pressures. The condensing

pressures are fixed by the sink fluid inlet temperature and the pinch point as given in the cycle assumptions from Chapter 3.3.2.

Table 4.12. Presentation of results for ORCs.

Model	Heat Source	Working Fluid
Baseline ORC	Lubrication oil	R134a
		R245fa
	CT room ventilation air	R134a
		R245fa
ORC with internal regenerator	Lubrication oil	R134a
		R245fa
	CT room ventilation air	R134a
		R245fa
Two-phase flash expansion ORC	Lubrication oil	R134a
		R245fa
	CT room ventilation air	R134a
		R245fa
ORC with multiple heat sources		R134a
		R245fa

Figure 4.8 compares the state points of the baseline ORCs driven by heat rejected from the lubrication oil for the two working fluids in their respective T-s diagrams. The two models happen to operate at the same optimal evaporation temperature which is 57.5°C. However the optimal evaporation pressures are different; the working fluid R134a evaporates at 1,585 kPa and the R245fa evaporates at 430 kPa. Although their thermal efficiencies are similar, the exergy efficiency and work output of the R134a-ORC are slightly higher than those of the R245fa-ORC; hence a larger mass flow rate of the R134a working fluid is used. The R134a-ORC yielded a 27.5% exergy efficiency and the R245fa-ORC yielded a 27.4% exergy efficiency.

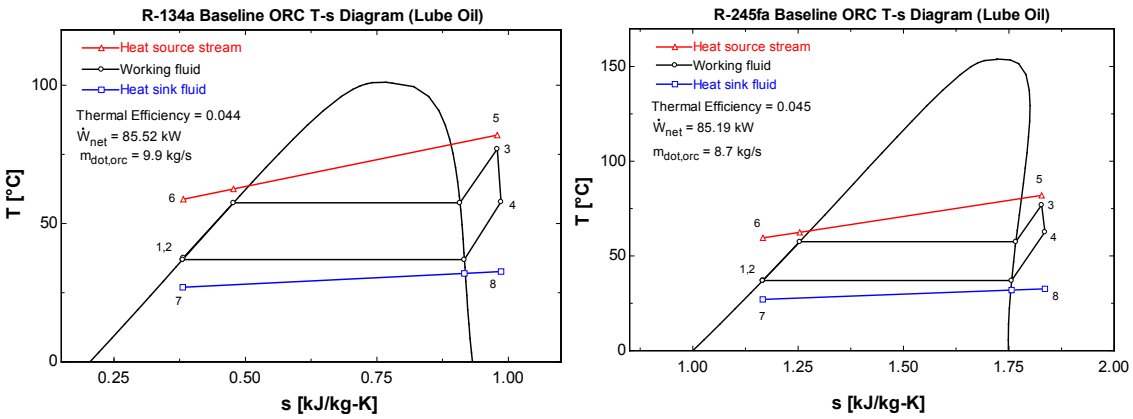

Figure 4.8. State points of the baseline ORCs in T-s diagrams for lubrication oil heat source.

The state points indicated in T-s diagrams of the baseline ORCs driven by hot CT room ventilation air are provided in Figure 4.9. Due to the heat source temperature of 150°C, a limitation occurs in the R134a-ORC. Since the R134a working fluid has a critical temperature of 101°C, which is below the heat stream's inlet temperature, the evaporation pressure of this model is limited to 100°C, in order to keep the cycle subcritical. The working fluid R245fa has a higher critical temperature of 154°C, which gives no restriction to the model on selecting the optimal evaporation pressure. The R245fa-ORC analysis resulted in an evaporating pressure of 1,200 kPa at an evaporation temperature of 97.5°C. The R134a-ORC analysis yielded significantly higher net work output with a 51% exergy efficiency, whereas the R245fa-ORC yielded only a 40% exergy efficiency. Evidently from the results shown in Figure 4.9, the R134a-ORC better utilizes the available energy in the heat stream by cooling it down to 60.1°C which is lower than that of the R245fa-ORC, which is at 79.3°C. Nevertheless, a larger mass flow rate of the R134a fluid is required to circulate in the cycle.

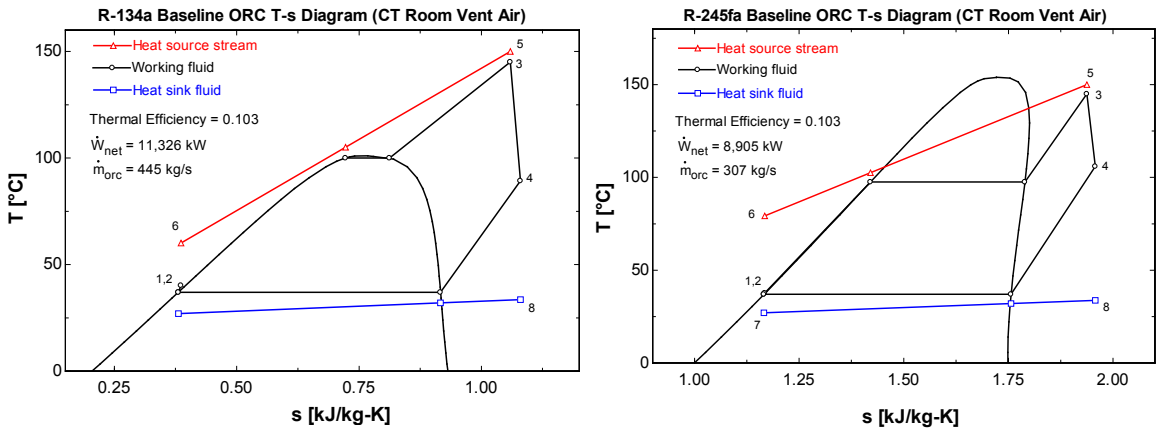

Figure 4.9. State points of the baseline ORCs in T-s diagrams for CT room ventilation air heat source.

Based on the results from the four baseline-ORC models discussed above, the R134a-ORC driven by CT room ventilation air heat stream has the best performance in terms of the second law effectiveness and the net work output generated.

Each of the next four ORC models presented is equipped with an internal regenerator. The superheated vapor discharged from the expander contains some energy that can be utilized internally using the regenerator. This internal regenerator allows the turbine-discharge stream to transfer its remaining energy to preheat the subcooled liquid working fluid before it enters the evaporator. The process from state points 5 to 6 indicates the turbine-discharge stream and the process from state points 2 to 3 indicates the preheated working fluid.

Figure 4.10 shows the state points of the regenerator-equipped ORCs driven by lube oil heat source for R134a and R245fa in T-s diagrams. The R134a-ORC has an optimal evaporation pressure of 1,585 kPa (evaporation temperature of 57.5°C), which results in an exergy efficiency of 27.4%. The R245fa-ORC has an optimum performance

of 27.3% exergy efficiency at an evaporation pressure of 432.2 kPa (evaporation temperature of 57.7°C). The net work output of the R134a-ORC is slightly higher.

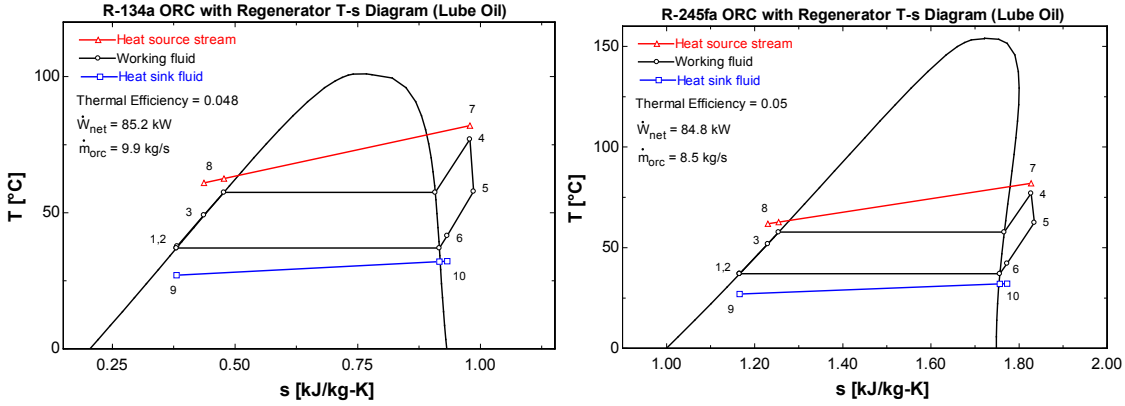

Figure 4.10. State points of the ORCs with internal regenerator in T-s diagrams for lubrication oil heat source.

Figure 4.11 shows the state points of the regenerator-equipped ORCs driven by the CT room ventilation air heat stream for R134a and R245fa in T-s diagrams. The optimized R134a-ORC has an evaporation pressure of 3,975 kPa (evaporation temperature of 100°C) and utilizes the heat source steam at an exergy efficiency of 49.6%. It generates a net work output of 11,054 kW. The R245fa-ORC operates at an optimal evaporation pressure of 1,263 kPa (evaporation temperature of 99.8°C) and has a net work output of 8,655 kW. This ORC has a lower exergy efficiency of 38.9% compared to the R134a-ORC.

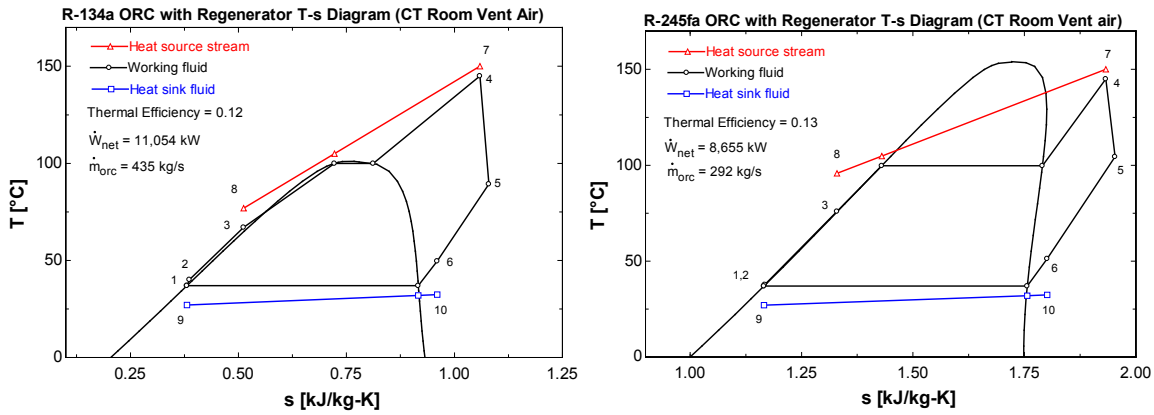

Figure 4.11. State points of the ORCs with internal regenerator in T-s diagrams for CT room ventilation air heat source.

It is reasonable to assume that the thermal efficiencies of the cycles increase when placing a regenerator in each cycle to preheat the working fluid before entering the evaporator. This is because the regenerator allows the cycle to effectively utilize the obtained energy ($\dot{Q}_{evap}$) internally, reducing the required energy consumed in the cycle, and resulting in an improved thermal efficiency. Nevertheless, the regenerator leaves a smaller gap for the heat streams to perform; and accordingly less energy is transferred from the heat source, which results in a higher exiting temperature of the heat source stream and a lower exergy efficiency. In other words, less energy is acquired out of the source stream when the ORC is equipped with a regenerator. The ORC with regenerator is beneficial when the heat input is obtained from a direct fuel-fired process, which is costly. However, in this case where the heat source is free as it is waste heat, the ORC with regenerator seems less suitable for serving as a potential waste heat recovery cycle.

The state points of the two-phase flash expansion ORCs driven by the lube oil heat source are presented in T-s diagrams in Figure 4.12. In the R134a-ORC, the pumped working fluid is heated to become saturated liquid at a pressure of 2,471 kPa (saturation

temperature of 77°C), and then expands into the two-phase region. The net work output of 78.1 kW is generated with a 25.1% exergy efficiency. Similarly, the R245fa-ORC reaches saturated liquid at the pressure of 732.7 kPa (saturation temperature of 77°C) and provides a net work output of 101 kW with a 32.5% exergy efficiency.

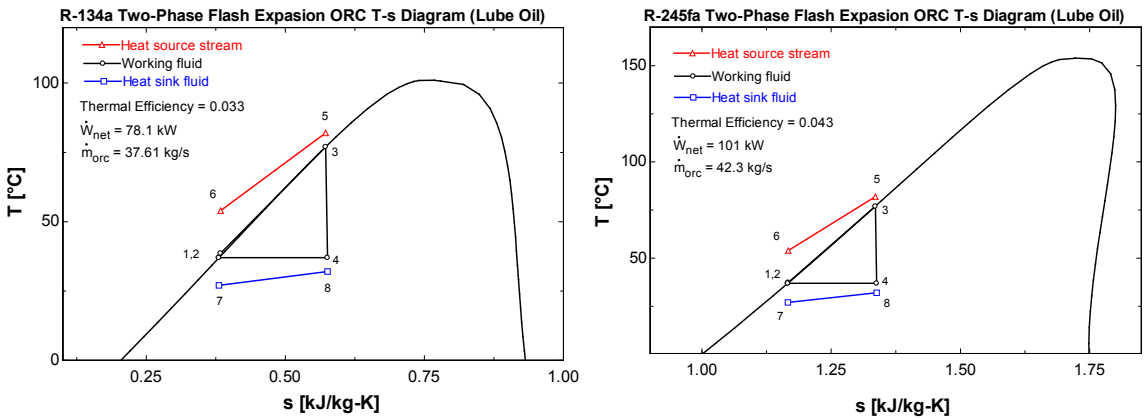

Figure 4.12. State points of the two-phase flash expansion ORCs in T-s diagrams for lubrication oil heat source.

Figure 4.13 presents the state points of the two-phase flash expansion ORCs driven by the CT room ventilation heat source in T-s diagrams. The R134a-ORC can only have a maximum saturated liquid pressure of 3,975 kPa (saturation temperature of 100°C), due to its critical temperature of 101°C. Its performance results in producing a net work output of 8,487 kW and a 38.1% exergy efficiency. Whereas, the R245fa-ORC can reach a pressure of 3,084 kPa (saturation temperature of 145°C) and generates a net work output of 14,851 kW. It should be noted that this ORC yielded the maximum exergy efficiency, among all ORC models in this study, of 65.5%.

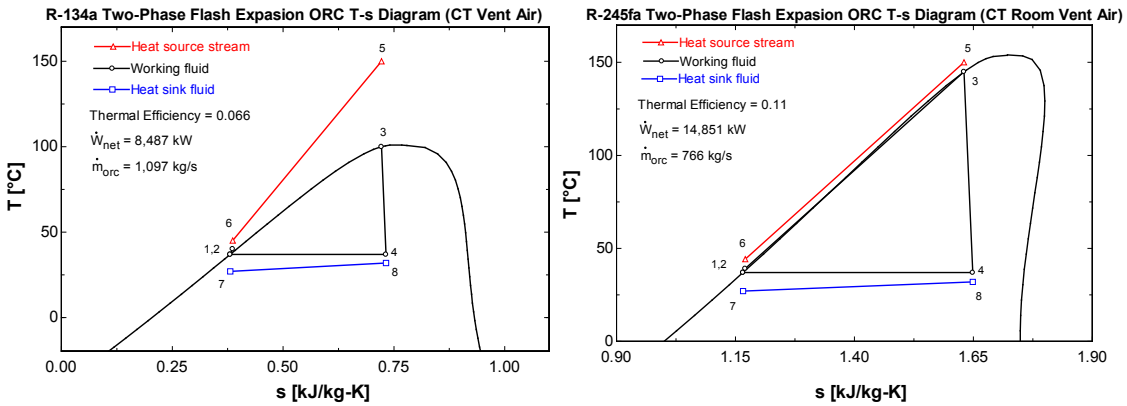

Figure 4.13. State points of the two-phase flash expansion ORCs in T-s diagrams of CT room ventilation air heat source.

It is evident that the two-phase flash expansion ORC using R245fa can best utilize the energy available in both waste heat streams. Since the working fluid R245fa does not have a critical temperature issue when applying the two heat sources, the cycles allows the use of the heat source streams down to the lowest possible temperatures of 44.2°C.

Moreover, the two heat streams also have the potential to drive one ORC using a cascaded heat input. To simulate this case, a model of the ORC with multiple heat sources has been developed in the study. The pump-discharged working fluid is preheated by the lube oil stream, and then obtains the heat from CT room ventilation air at the evaporator in the later stage. Figure 4.14 presents the state points of the ORCs with multiple heat sources for the working fluids R134a and R245fa in T-s diagrams. The R134a-ORC has an optimal evaporation pressure of 3,975 kPa (evaporation temperature of 100°C), which provides a net work output of 1,035 kW at a 4.6% exergy efficiency. The R245fa-ORC has an optimum evaporation pressure of 2,568 kPa (evaporation temperature of 135°C), which results in a net work output of 1,544 kW and an exergy efficiency of 6.8%.

According to the plots shown in Figure 4.14, the multiple heat source ORCs can effectively utilize the available energy in the lubrication oil in the preheating process, and let the working fluids leave the heaters at 77°C. Similar to the ORC with regenerator models, the preheaters reduce the amount of heat required for the evaporators. However, the thermal efficiencies are relatively low when the heat inputs from the two sources are combined. The exergy efficiencies of these models are extremely low compared to other models in this study because a significant amount of heat in the CT room ventilation air is not utilized when combining the two heat sources. Therefore, the ORCs with multiple heat sources are not preferable.

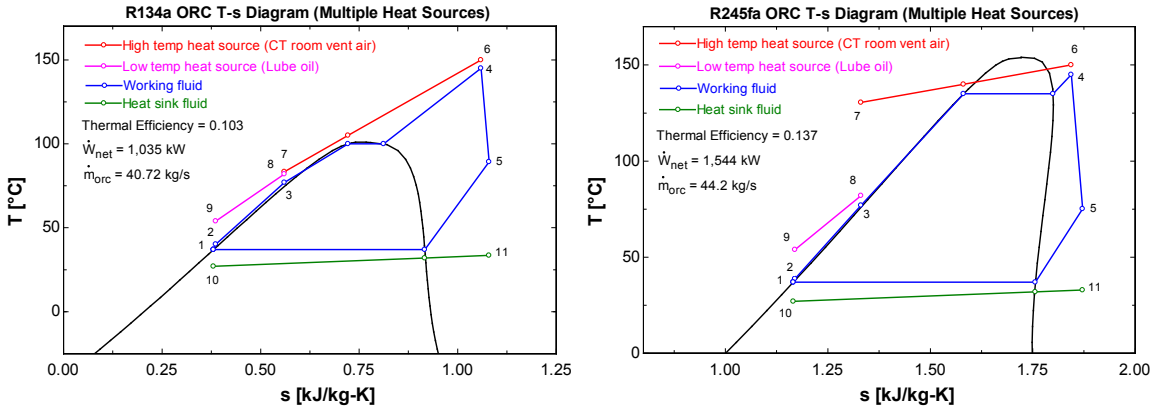

Figure 4.14. State points of the ORCs with multiple heat sources in T-s diagrams.

Energy balances of the single heat source ORCs with R134a and R245fa as the working fluid are presented in Table 4.13 and Table 4.14, respectively. The list of energy flows in the multiple heat sources ORCs are presented in Table 4.15. The input energy flows are indicated by a plus sign and any energy flows leaving the cycles are presented with a minus sign. In the case of ORCs with regenerator, the internal energy flows between two sides of working fluid at the regenerators are not listed in these tables as the

energy is transferred between the components of the cycles. All cycles give evident balances of energy as the net cycle energy flows are equal to zero.

Table 4.13. Energy flows and balances of ORCs with single heat source of R134a working fluid.

Component	R134a					
	Baseline ORC		ORC with Internal Regenerator		Two-Phase Flash Expansion ORC	
	Lube Oil	CT Room Ventilation Air	Lube Oil	CT Room Ventilation Air	Lube Oil	CT Room Ventilation Air
Evaporator	+ 1,952.5	+ 109,730	+ 1,774	+ 89,261	+ 2,355	+ 128,009
Expander	- 94.7	- 13,260	- 94	- 12,940	- 160.7	- 13,249
Condenser	- 1867	- 98,404	- 1,689	- 78,207	- 2,276.9	- 119,523
Pump	+ 9.2	+ 1,934	+ 9	+ 1,886	+ 82.6	+ 4,763
Summation	0	0	0	0	0	0

Table 4.14. Energy flows and balances of ORCs with single heat source of R245fa working fluid.

Component	R245fa					
	Baseline ORC		ORC with Internal Regenerator		Two-Phase Flash Expansion ORC	
	Lube Oil	CT Room Ventilation Air	Lube Oil	CT Room Ventilation Air	Lube Oil	CT Room Ventilation Air
Evaporator	+ 1,890	+ 86,347	+ 1,694	+ 66,192	+ 2,355	+ 129,219
Expander	- 87.4	- 9,286	- 87.1	- 9,041	- 128.4	- 17,368
Condenser	- 1,805	- 77,442	- 1,609.1	- 57,537	- 2,254	- 114,638
Pump	+ 2.4	+ 381	+ 2.2	+ 386	+ 27.4	+ 2,787
Summation	0	0	0	0	0	0

Table 4.15. Energy flows and balances of ORCs with multiple heat sources.

Component	ORC with Multiple Heat Sources	
	R134a	R245fa
Evaporator	+ 7,675	+ 8,960
Expander	- 1,212	- 1,676
Condenser	- 8,995	- 9,771
Pump	+ 177	+ 132
Heater	+ 2,355	+ 2,355
Summation	0	0

The results of all ORC models are summarized in Table 4.16 and Table 4.17, for single heat source and multiple heat sources, respectively. The results show the second law effectiveness or exergy efficiencies and the cycles' net work outputs.

Table 4.16. Summary of evaluations for ORC models with single heat source.

Model	Working Fluid	Lubrication Oil		CT Room Ventilation Air	
		2^{nd} Law Effectiveness	Work output (kW)	2^{nd} Law Effectiveness	Work output (kW)
Baseline ORC	R134a	0.2749	85.52	0.5086	11,326
	R245fa	0.2739	85.19	0.4000	8,905
ORC with Internal Regenerator	R134a	0.2738	85.16	0.4964	11,054
	R245fa	0.2727	84.83	0.3887	8,655
Two-Phase Flash Expansion ORC	R134a	0.2511	78.09	0.3811	8,487
	R245fa	0.3247	101.0	0.6548	14,851

Table 4.17. Summary of evaluations for ORC models with multiple heat sources.

Model	Working Fluid	2^{nd} Law Effectiveness	Work output (kW)
ORC with Multiple Heat Sources	R134a	0.0459	1,035
	R245fa	0.0684	1,544

Based on the results presented here, the ORCs driven by the CT room ventilation can generate larger net work outputs compared to the lube-oil-driven models. Likewise, these models can better utilize the available energy in the heat source steams. In the cases of baseline ORC and ORCs with regenerator, R134a is the working fluid that results in a better performance than R245fa. These results agree with a comparison of these working fluids and their second law effectiveness shown in Figure 2.12 provided in the literature review. Differently, the two-phase flash expansion ORC can achieve higher performance with R245fa as the working fluid. This is because the simulation models were limited to subcritical operation and the evaporating temperature of R134-model is limited at its critical temperature. According to this limitation, it allows R245fa, which has a higher critical temperature, to more effectively utilize the entire heat source stream of CT room ventilation air. Although the two-phase flash expansion ORC with R245fa can achieve the highest work output and exergy efficiency amongst all other cycles, the technology is novel and yet expensive due to the material needed to implement a two-phase expander. As this component is still underdeveloped, the affordable and commercial options are not yet available in the market. Therefore, the baseline ORC of R134a seems to be the most attractive candidate.

4.4 Economic Payback Periods

The input parameters of the simple economic analysis are the price of natural gas sold to the gas turbine combined power plant, the prices of the WHR systems available in the market, and the price of distributed electricity for state-enterprise companies. The costs of natural gas and electricity are based on Thailand's economic situation in 2014.

The prices of the WHR systems are obtained from commercial prices available in the current market and then scaled to the capacity of the studied systems. Investment cost of each system takes only the system price into account without installation, operation and maintenance cost. The top-performance model from each WHR technology is selected to be analyzed in this simple economic analysis. Table 4.18 summarizes prices related to the simple payback period analysis of the waste heat recovery systems. The results of payback periods are presented in Table 4.19.

Table 4.18. Prices of waste heat recovery systems and energy.

Double-effect H_2O/LiBr absorption chiller	
General market price	350 $/ton
Studied model (88,000 kW or 25,000 ton)	8,750,000 $
Baseline ORC	
General market price	2,250,000 $/MW
Studied model (11.3 MW)	25,425,000 $
Natural gas for power plant	0.068 $/kWh
Distributed electricity for office buildings	0.128 $/kWh

Market price reference: http://www.alibaba.com

Table 4.19. Payback periods of the selected waste heat recovery systems.

Model of Waste Heat Recovery Technology	Payback Period (year)
Double-effect H_2O/LiBr absorption chiller	0.72
Baseline ORC (R134a)	4.57

Normally, the gas-fired double-effect H_2O/LiBr absorption chillers have the estimated payback periods of 2 years (Thies and Bahnfleth, 1998). Payback periods of the ORCs used as combined-cycle power plants' bottoming cycles are suggested to be less than 7 years (Rowshanzadeh, 2006). It should be noted that the payback periods are dependent on the prices of fuel and electricity, which can be varied by regions and over

time. Based on the results in Table 4.19, the calculated payback periods are reasonable and acceptable as they comply with the ranges of practical payback periods of each technology.

CHAPTER 5. CONCLUSION AND RECOMMENDATIONS

This study presents options for waste heat recovery in a 700 MW gas-turbine combined cycle power plant in Thailand. Two approaches are considered: absorption chillers for space cooling and power production using the Organic Rankine cycle. These waste heat recovery alternatives aim to effectively utilize the two feasible waste heat streams at two different temperatures, which are the hot ventilation air from the combustion turbine rooms and the return lubrication oil from the power plant. The purpose of this work is to identify the best option for the investigated power plant. Various models have been theoretically studied taking into consideration the practical operating conditions of the power plant.

The second law effectiveness of an ORC is the measure of its heat utilization ability, and its cooling capacity is a measure of the cycle output. Based on these two parameters, absorption chiller models give one outstanding candidate - the double-effect H_2O/LiBr absorption cycle driven by CT room ventilation air heat stream. If compared on the basis of output cooling capacity alone, single-effect absorption cycles driven by CT room ventilation air also perform well; however, the energy utilization efficiency is much lower because the single-effect cycle cannot utilize the higher CT room ventilation air temperatures as much as the double-effect cycle. The high cooling capacities are the result of large mass flow rate of the hot ventilation air stream. In the energy utilization

aspect, the single-effect absorption chillers driven by lubrication oil heat source perform well since the model is suitable for low heat source stream. Nevertheless, small cooling capacity results from the low mass flow rate of lubrication oil, which is much smaller than that of the ventilation air.

ORC technology gives three top candidates by comparison of their second law effectiveness and power output. Two-phase flash expansion ORC with R245fa as the working fluid gives the best performance on both indicators among ORCs because the cycle can pull most of the energy in the heat stream to the cycle. Unfortunately, this technology requires high strength material for the expander in order to obtain two-phase working fluid expansion that drives up the cost of the machine. Research is intensively conducted in this area and the technology is being developed for commercial use in the future. The baseline ORC with R134a as the working fluid ranks second with slightly lower power produced compared to the two-phase flash expansion ORC, and the ORC with regenerator using R134a as the working fluid comes in third. Significantly, all three candidates can generate power output of more than 10-MW capacity by recovering heat from the hot CT room ventilation air stream. However, with less complexity in the configuration, it is reasonable to select the baseline ORC of R134a as the best ORC candidate.

Payback periods of the two WHR technologies are quite different as the absorption chiller takes shorter time to break even and recoup its investment cost. Considering a life span of the gas-turbine combined cycle power plant of 25 years, both technologies can have an amount of time to perform their duties. However, location of

the power plant must be taken into consideration. The plant should locate close to area where cooling load is needed, e.g. office buildings, in order to install absorption chiller and chilled water pipes.

The investigated power plant is in its early stage of operation and located in a suburban area of Thailand. It is surrounded by office buildings which makes the double-effect H_2O/LiBr absorption chiller feasible and reasonable to be installed. It can provide cooling capacity to the office buildings which are in reach of chilled water pipelines. On the other hand, a baseline ORC with R134a as working fluid can be a sophisticated option to enhance the power plant's efficiency and increase power supply to the electricity grid of the country. In conclusion, both alternatives can be worthily recommended as waste heat recovery options for this power plant.

LIST OF REFERENCES

LIST OF REFERENCES

ABB. (2011). Trends in global energy efficiency 2011 An analysis of of industry and utilities. Enerdata and the Economist Intelligence Unit, Switzerland.

Alefeld, G., & Radermacher, R. (1993). *Heat conversion systems*. CRC press.

Algieri, A., & Morrone, P. (2014). Energy analysis of Organic Rankine Cycles (ORCs) for biomass applications. *Thermal Science*, (00), 30-30.

Angelotti, A., & Caputo, P. (2007, September). Energy and Exergy Analysis of Heating and Cooling Systems in the Italian Context. In *Proceedings of the CLIMAMED Conference, Genova*.

Aphornratana, S. (1995). *Theoretical and experimental investigation of a combined ejector-absorption refrigerator* (Doctoral dissertation, University of Sheffield, Department of Mechanical and Process Engineering).

Arvay, P., Muller, M. R., & Ramdeen, V. Economic Implementation of the Organic Rankine Cycle in Industry.

Arzbaecher, C., Fouche, E., Parmenter, K. (2007). Industrial waste-heat recovery: benefits and recent advancements in technology and applications. ACEEE Summer Study on Energy Efficiency in Industry. Global energy partners.

Behrens, C. E. (2011). *US Energy: Overview and Key Statistics*. DIANE Publishing.

Bhattacharjee, S. (2012). VAPOUR & COMBINED POWER CYCLE, RANKINE CYCLE : THE IDEAL CYCLE FOR VAPOUR POWER CYCLES. Retrieved from http://sounak4u.weebly.com/index.html

Bombarda, P., Invernizzi, C. M., & Pietra, C. (2010). Heat recovery from Diesel engines: A thermodynamic comparison between Kalina and ORC cycles.*Applied Thermal Engineering*, *30*(2), 212-219.

Brasz, L. J., & Bilbow, W. M. (2004). Ranking of working fluids for organic Rankine cycle applications.

Chandra, S. (2013). *ORGANIC RANKINE CYCLE POWER GENERATION USING WASTE HEAT OF A TYPICAL POWER PLANT* (Doctoral dissertation, NATIONAL INSTITUTE OF TECHNOLOGY PATNA).

El-Wakil, M. M. (1984). *Powerplant technology*. Tata McGraw-Hill Education.

Electricity Generating Authority of Thailand (EGAT).

Energy Design Resources. (2009). Chilled water plant design guide.

Energy, Mines and Resources Canada. Waste heat recovery. Ontario, Canada.

Fujii, T., Nishiguchi, A., Uchida, S. (2010). Development activities of low temperature waste heat recovery appliances using absorption heat pumps. 2010 International Symposium on Next-generation Air Conditioning and Refrigeration Technology. Tokyo, Japan.

Gao, H., Liu, C., He, C., Xu, X., Wu, S., & Li, Y. (2012). Performance analysis and working fluid selection of a supercritical organic Rankine cycle for low grade waste heat recovery. *Energies*, *5*(9), 3233-3247.

Garimella, S., Brown, A. M., & Nagavarapu, A. K. (2011). Waste heat driven absorption/vapor-compression cascade refrigeration system for megawatt scale, high-flux, low-temperature cooling. *International Journal of Refrigeration*, *34*(8), 1776-1785.

Gomri, R. (2010). Solar Energy to Drive Half-Effect Absorption Cooling System. *Int. J. of Thermal & Environmental Engineering*, *1*(1), 1-8.

Groll, E. A. (1997). Current status of absorption/compression cycle technology.*ASHRAE Transactions*, *103*(1), 361-374.

Groll, E. A. (2012). Advanced thermodynamics. West Lafayette, IN. Purdue University

He, C., Liu, C., Gao, H., Xie, H., Li, Y., Wu, S., & Xu, J. (2012). The optimal evaporation temperature and working fluids for subcritical organic Rankine cycle. *Energy*, *38*(1), 136-143.

Herold, K., Radermacher, R., & Klein, S. A. (1996). *Absorption chillers and heat pumps*. CRC press.

Holman, J. (2011). Perspective waste heat to power – still waiting for a breakthrough. IDC Energy Insights: Renewable Energy Strategies: Perspective. Massachusetts.

Holmberg P, Berntsson T. Alternative working fluids in heat transformers. ASHRAE Trans 1990;96:1582–9.

Hugenroth, J. (2006). Liquid flooded Ericsson cycle cooler. West Lafayette, IN: Purdue University

Imran, K. M. (2013). Irreversibility Analysis of Double Effect LiBr-Water Vapor Absorption Chiller. *Journal of Engineering Science and Technology Review*,*6*(5), 115-122.

Incropera, F. P. (2011). *Fundamentals of heat and mass transfer*. John Wiley & Sons.

Jolley, Ainsley. 2006. *Technologies for Reducing Stationary Energy Use, Climate Change Working Paper No. 6*, Victoria University, Australia: Centre for Strategic Economic Studies.

Kapooria, R. K., Kumar, S. S., & Kasana, K. S. (2008). An analysis of a thermal power plant working on a Rankine cycle: A theoretical investigation. *J. Energy South. Africa*, *19*(1), 77-83.

Kaushik, S. C., & Chandra, S. (1985). Computer modeling and parametric study of a double effect generation absorption refrigeration cycle. *Energy conversion and management*, *25*(1), 9-14.

Keinath, C. M., Delahanty, J. C., Garimella, S., & Garrabrant, M. A. (2012). Diesel Engine Waste-Heat Driven Ammonia-Water Absorption System for Space-Conditioning Applications.

Kestin, J., DiPippo, R., Khalifa, H. E., & Ryley, D. J. (1980). *Sourcebook on the production of electricity from geothermal energy* (No. DOE/RA/28320-2; DOE/RA/4051-1). Brown Univ., Providence, RI (USA).

Khennich, M., & Galanis, N. (2012). Optimal design of ORC systems with a low-temperature heat source. *Entropy*, *14*(2), 370-389.

Kim, Y. J., Kim, S., Joshi, Y. K., Fedorov, A. G., & Kohl, P. A. (2012). Exergy Analysis of an Absorption Refrigeration System Using an Iconic Liquid as a Working Fluid in the Chemical Compressor.

Lawson, B. (2005). Steam Turbine Electricity Generation Plants. Retrieved from http://www.mpoweruk.com/steam_turbines.htm

Liu, C., He, C., Gao, H., Xu, X., & Xu, J. (2012). The optimal evaporation temperature of subcritical ORC based on second law efficiency for waste heat recovery. *Entropy*, *14*(3), 491-504.

Longo, G. A., Gasparella, A., & Zilio, C. (2002). Simulation of an absorption chiller driven by the heat recovery on an internal combustion engine.

Lukawski, M. (2010). Design and optimization of standardized organic Rankine cycle power plant for European conditions.

Ma, W. B., & Deng, S. M. (1996). Theoretical analysis of low-temperature hot source driven two-stage LiBr/H< sub> 2</sub> O absorption refrigeration system. *International Journal of refrigeration*, *19*(2), 141-146.

MAN Diesel & Turbo. (2012). Waste heat recovery system (WHRS) for reduction of fuel consumption, emissions and EEDI. Denmark.

Marcriss, R. A., Gutraj, J. M., & Zawacki, T. S. (1988). Absorption fluid data survey: final report on worldwide data, ORLN/sub/8447989/3, Inst. *Gas Tech*.

Murehwa, G., Zimwara, D., Tumbudzuku, W., Mhlanga, S. (2012). Energy Efficiency Improvement in Thermal Power Plants. International Journal of Innovative Technology and Exploring Engineering (IJITEE), 2, 20-25

Nouman, J. (2012). Comparative studies and analyses of working fluids for Organic Rankine Cycles-ORC. *Master of Science Thesis] KTH School of Industrial Engineering and Management, Stockholm, Sweden*.

Ohuchi, T., Aizawa, M., Nishiguchi, A., Hatada, T., Kunugi, Y., & Kawakami, R. (1994). A study on a hot-water driven air-cooled absorption refrigerating machine.

Padilla, M., Revellin, R., & Bonjour, J. (2010). Exergy analysis of R413A as replacement of R12 in a domestic refrigeration system. *Energy Conversion and Management*, *51*(11), 2195-2201.

PanahiZadeh, F., & Bozorgan, N. (2011). The energy and exergy analysis of single effect absorption chiller. *International Journal of Advanced Design and Manufacturing Technology*, *4*(4), 19-26.

Perez-Blanco, H. (1984). Absorption heat pump performance for different types of solutions. *International journal of refrigeration*, *7*(2), 115-122.

Poles, S., Venturin, M. Numerical simulation of an Organic Rankine Cycle. Open Source Engineering, A Scilab Professional Partner.

Prager, R. Chilled water HVAC systems. Brinco Mechanical Services, Incoperation.

Provincial Electricity Authorithy of Thailand (PEA).

Quoilin, S. (2008). An introduction to thermodynamics applied to Organic Rankine Cycles.

Rowshanzadeh, R. (2010). Performance and cost evaluation of Organic Rankine Cycle at different technologies.

Saleh, B., Koglbauer, G., Wendland, M., & Fischer, J. (2007). Working fluids for low-temperature organic Rankine cycles. *Energy*, *32*(7), 1210-1221.

Sami, S. M. (2008). Energy and exergy analysis of an efficient organic Rankine cycle for low temperature power generation. *International Journal of Ambient Energy*, *29*(1), 17-26.

Seraj, M., & Siddiqui, M. A. PERFORMANCE ANALYSIS OF PARALLEL FLOW SINGLE AND DOUBLE EFFECT ABSORPTION CYCLES.

Sinha, A. K., & NETRA. (2012). Cases of Acid Dew Point and Flow Accelerated Corrosion in HRSGs and their Remedial Measures. Greater Noida, India.

Smith, I. K., Stosic, N., & Kovacevic, A. (2001). Power recovery from low cost two-phase expanders. *TRANSACTIONS-GEOTHERMAL RESOURCES COUNCIL*, 601-606.

Srikhirin, P., Aphornratana, S., & Chungpaibulpatana, S. (2001). A review of absorption refrigeration technologies. *Renewable and sustainable energy reviews*, *5*(4), 343-372.

Stiedel, R. F., Brown, K. A., & Pankow, D. H. (1983, August). The empirical modeling of a Lysholm screw expander. In *Proc., Intersoc. Energy Convers. Eng. Conf.;(United States)* (Vol. 1, No. CONF-830812-). Mechanical Engineering Department, University of California, Berkeley, California.

Tchanche, B. F., Quoilin, S., Declaye, S., Papadakis, G., & Lemort, V. (2010, January). Economic feasibility study of a small scale Organic Rankine Cycle system in waste heat recovery application. In *ASME 2010 10th Biennial Conference on Engineering Systems Design and Analysis* (pp. 249-256). American Society of Mechanical Engineers.

Teng, H., Regner, G., & Cowland, C. (2007). *Waste heat recovery of heavy-duty diesel engines by organic Rankine cycle part I: hybrid energy system of diesel and Rankine engines* (No. 2007-01-0537). SAE Technical Paper.

Teng, H., & Regner, G. (2009). *Improving fuel economy for HD diesel engines with WHR rankine cycle driven by EGR cooler heat rejection* (No. 2009-01-2913). SAE Technical Paper.

Thies, R. M., & Bahnfleth, W. (1998). Gas-fired chiller-heaters as a central plant alternative for small office buildings. *Heating, piping and air conditioning*, *70*(1), 103-112.

Trane. (2000) Chilled water system design and operation: Cost reducing optimization strategies, American Standard Incoperation.

Trivedi, Kirtan K., Fouche, Ed and Parmenter, Kelly E. 2007. *Handbook of Energy Efficiency and Renewable Energy*, Edited by Kreith, Frank and D. Yogi Goswami, Boca Raton, FL: CRC Press.

U.S. Department of Energy. Industrial Technology Program. (2008). Waste heat recovery: technology and opportunities in U.S. industry. Washington, DC: BSC, Incorporation.

U.S. Environmental Protection Agency. (2012). Waste heat to power systems. Washington, DC: Combined heat and power partnership.

Vliet GC, Lawson MB, Lithgow RA. Water-lithium bromide double-effect absorption cooling cycle analysis. ASHRAE Trans 1982;88:811–22.

Wang, X., & Chua, H. T. (2009). Absorption cooling: a review of lithium bromide-water chiller technologies. *Recent Patents on Mechanical Engineering*, *2*(3), 193-213.

Woodland, B. (2013). Methods of Increasing Net Work Output of Organic Rankine Cycles for Low-Grade Waste-Heat Recovery. West Lafayette, IN: Purdue University.

Woodland, B., Braun, J., Groll E., Horton, T. (2014). Methods of Increasing Net Work Output of Organic Rankine Cycles for Low-Grade Waste-Heat Recovery. West Lafayette, IN: Purdue University.

Yu, G., Shu, G., Tian, H., Wei, H., & Liu, L. (2013). Simulation and thermodynamic analysis of a bottoming Organic Rankine Cycle (ORC) of diesel engine (DE). *Energy*, *51*, 281-290.

Ziegler, F., Kahn, R., Summerer, F., & Alefeld, G. (1993). Multi-effect absorption chillers. *International journal of refrigeration*, *16*(5), 301-311.

APPENDICES

Appendix A. Heat Loss Analysis EES Code

```
"Heat loss analysis - Combustion turbine (CT) room ventilation air"

"Energy Balance (100% GTLoad)"
"Combustion Analysis"

"Fuel - Natural Gas"
T_fuel = 150 [C]
"fuel temperature feeding to combustion chamber"
P_fuel = 30*convert(bar,kPa)                    "fuel pressure"
HHV = 35730 [kJ/kg]
"fuel higher specific heating value"

"Fuel consumption"
fuel_CT = 55*10^6 [ft^3]
"fuel volume consumption per day, unit MMscf - million standard cubic feet"
SG_fuel = 0.72                                  "fuel specific gravity"
rho_water = 1000 [kg/m^3]                       "water density at 4C"
rho_fuel = SG_fuel*rho_water                    "fuel density, kg/m^3"
V_fuel = fuel_CT*convert(ft^3,m^3)
"convert volume of fuel consumption, m^3"
m_fuel = rho_fuel*V_fuel
"fuel mass flow rate to combustion chamber"
"m_dot_fuel = m_fuel/(24*60*60)"                "fuel mass flow rate, kg/s"
m_dot_fuel = 17.84 [kg/s]

"Fuel composition enthalpy"
"Real properties"
h_CO2_f =Enthalpy(CarbonDioxide,T=T_fuel,P=P_fuel)
h_N2_f =Enthalpy(Nitrogen,T=T_fuel,P=P_fuel)
h_CH4_f =Enthalpy(Methane,T=T_fuel,P=P_fuel)
h_C2H6_f =Enthalpy(Ethane,T=T_fuel,P=P_fuel)
h_C3H8_f =Enthalpy(Propane,T=T_fuel,P=P_fuel)

"Ideal properties"
h_1=Enthalpy(CO2,T=T_fuel)
h_2=Enthalpy(N2,T=T_fuel)
h_3=Enthalpy(CH4,T=T_fuel)
h_4=Enthalpy(C2H6,T=T_fuel)
h_5=Enthalpy(C3H8,T=T_fuel)

M_CH4  =16                                      "CH4 molecular weight, g"
M_C2H6 = 30                                     "C2H6 molecular weight, g"
```

```
M_C3H8 = 44                                   "C3H8 molecular weight, g"

mm_CO2_f = 6.15*M_CO2                         "mass of CO2 in 100 mol fuel,g"
mm_N2_f = 16.02*M_N2                          "mass of N2 in 100 mol fuel,g"
mm_CH4_f = 72.51*M_CH4                        "mass of CH4 in 100 mol fuel,g"
mm_C2H6_f = 3.53*M_C2H6                       "mass of C2H6 in 100 mol fuel,g"
mm_C3H8_f = 1.07*M_C3H8                       "mass of C3H8 in 100 mol fuel,g"

mm_total_fuel = mm_CO2_f + mm_N2_f  + mm_CH4_f + mm_C2H6_f + mm_C3H8_f
"mass of 100 mol fuel, g"

mf_CO2_f = mm_CO2_f /mm_total_fuel            "CO2 mass fraction in fuel"
mf_N2_f = mm_N2_f /mm_total_fuel              "N2 mass fraction in fuel"
mf_CH4_f = mm_CH4_f /mm_total_fuel            "CH4 mass fraction in fuel"
mf_C2H6_f = mm_C2H6_f /mm_total_fuel          "C2H6 mass fraction in fuel"
mf_C3H8_f = mm_C3H8_f /mm_total_fuel          "C3H8 mass fraction in fuel"

m_dot_CO2_f = mf_CO2_f*m_dot_fuel             "mass flow rate of CO2 in fuel"
m_dot_N2_f = mf_N2_f*m_dot_fuel               "mass flow rate of N2 in fuel"
m_dot_CH4_f = mf_CH4_f*m_dot_fuel             "mass flow rate of CH4 in fuel"
m_dot_C2H6_f = mf_C2H6_f*m_dot_fuel           "mass flow rate of C2H6 in fuel"
m_dot_C3H8_f = mf_C3H8_f*m_dot_fuel           "mass flow rate of C3H8 in fuel"

{H_dot_1_sum = h_1*m_dot_CO2_f + h_2*m_dot_N2_f + h_3*m_dot_CH4_f +
h_4*m_dot_C2H6_f + h_5*m_dot_C3H8_f}
H_dot_fuel_sum = h_CO2_f*m_dot_CO2_f + h_N2_f*m_dot_N2_f +
h_CH4_f*m_dot_CH4_f + h_C2H6_f*m_dot_C2H6_f + h_C3H8_f*m_dot_C3H8_f

"Exhaust gas condition"
T_exhaust_gt = 621.2 [C]
"exhaust gas temperature at gas turbine outlet"
P_exhaust_gt = 1*convert(atm,kPa)
"exhaust gas pressure at gas turbine outlet"
T_exhaust_hrsg = 100 [C]
"exhaust gas temperature at HRSG outlet"
P_exhaust_hrsg = 1*convert(atm,kPa)
"exhaust gas pressure at HRSG outlet"

"Exhaust gas composition by mass fraction"
M_Ar = 40                                     "Argon molecular weight"
mm_Ar = 0.86*M_Ar
"mass of Ar in 100 mol exhaust, g"
M_N2 = 28                                     "N2 molecular weight"
mm_N2 = 72.55*M_N2
"mass of N2 in 100 mol exhaust, g"
```

```
M_O2 = 32                                   "O2 molecular weight"
mm_O2 = 11.97*M_O2
"mass of O2 in 100 mol exhaust, g"
M_CO2 = 44                                  "CO2 molecular weight"
mm_CO2 = 4.04*M_CO2
"mass of CO2 in 100 mol exhaust, g"


M_H2O = 18                                  "H2O molecular weight"
mm_H2O = 10.59*M_H2O
"mass of H2O in 100 mol exhaust, g"

mm_extotal = mm_Ar+mm_N2+mm_O2+mm_CO2+mm_H2O
"mass of 100 mol exhaust, g"

mf_Ar = mm_Ar/mm_extotal                    "Ar mass fraction"
mf_N2 = mm_N2/mm_extotal                    "N2 mass fraction"
mf_O2 = mm_O2/mm_extotal                    "O2 mass fraction"
mf_CO2 = mm_CO2/mm_extotal                  "CO2 mass fraction"
mf_H2O = mm_H2O/mm_extotal                  "H2O mass fraction"

"Exhaust gas composition mass flow rate"
m_dot_exhaust = 1645*1000/3600
"exhaust gass mass flow rate, from ton/h to kg/s" {!1973 t/h at 200 MW}
{!1645 t/h at data sheet interpulate}
m_dot_Ar = mf_Ar*m_dot_exhaust
"Ar mass flow rate in exhaust gas"
m_dot_N2 = mf_N2*m_dot_exhaust
"N2 mass flow rate in exhaust gas"
m_dot_O2 = mf_O2*m_dot_exhaust
"O2 mass flow rate in exhaust gas"
m_dot_CO2 = mf_CO2*m_dot_exhaust
"CO2 mass flow rate in exhaust gas"
m_dot_H2O = mf_H2O*m_dot_exhaust
"H2O mass flow rate in exhaust gas"

"Exhaust gas properties at GT outlet"
h_Ar_gt = Enthalpy(Argon,T=T_exhaust_gt,P=P_exhaust_gt)
h_N2_gt = Enthalpy(Nitrogen,T=T_exhaust_gt,P=P_exhaust_gt)
h_O2_gt = Enthalpy(Oxygen,T=T_exhaust_gt,P=P_exhaust_gt)
h_CO2_gt = Enthalpy(CarbonDioxide,T=T_exhaust_gt,P=P_exhaust_gt)
h_H2O_gt = Enthalpy(Water,T=T_exhaust_gt,P=P_exhaust_gt)

"Exhaust gas properties at HRSG outlet"
h_Ar_hrsg = Enthalpy(Argon,T=T_exhaust_hrsg,P=P_exhaust_hrsg)
```

```
h_N2_hrsg = Enthalpy(Nitrogen,T=T_exhaust_hrsg,P=P_exhaust_hrsg)
h_O2_hrsg = Enthalpy(Oxygen,T=T_exhaust_hrsg,P=P_exhaust_hrsg)
h_CO2_hrsg = Enthalpy(CarbonDioxide,T=T_exhaust_hrsg,P=P_exhaust_hrsg)
h_H2O_hrsg = Enthalpy(Water,T=T_exhaust_hrsg,P=P_exhaust_hrsg)

"Properties of exhaust gas cooled to ambient"
T_amb = 33 [C]                                  "ambient temperature at exhaust"
P_amb = 1*convert(atm,kPa)                      "ambient pressure at exhaust"
h_Ar_amb = Enthalpy(Argon,T=T_amb,P=P_amb)
h_N2_amb = Enthalpy(Nitrogen,T=T_amb,P=P_amb)
h_O2_amb = Enthalpy(Oxygen,T=T_amb,P=P_amb)
h_CO2_amb = Enthalpy(CarbonDioxide,T=T_amb,P=P_amb)
h_H2O_amb = Enthalpy(Water,T=T_amb,P=P_amb)

"Plant Operation"
GT_full = 2  "two gas turbines on operation - full block"
GT_half = 1 "one gas turbine on operation - half block"

"Gas turbine gross generationt"
W_GT =  4100000 [kWh]                           "daily energy from 1 gas turbine"
W_dot_GT = W_GT/24                              "kW"

"Heat rate, HR"
HR = 11950 [kJ/kWh]                             "gas turbine gross heat rate"
E_input_GT = HR*W_dot_GT/3600                   "kJ/s or kW"

"Turbine compartmemt heat loss - Combustion Energy Balance"
T_compartment = 150 [C] "turbine compartment temperature"
H_dot_air = (m_dot_air)*(h_air_in)
H_dot_exhaust_GT =
(m_dot_Ar)*(h_Ar_gt)+(m_dot_N2)*(h_N2_gt)+(m_dot_O2)*(h_O2_gt)+(m_dot_CO2)
*(h_CO2_gt)+(m_dot_H2O)*(h_H2O_gt)

H_dot_air + E_input_GT =  H_dot_exhaust_GT + W_dot_GT +Q_dot_GT_compartment
Q_dot_GT_compartment_total = GT_full*Q_dot_GT_compartment

{H_dot_air + m_dot_fuel*HHV =  H_dot_exhaust_GT + W_dot_GT +
Q_dot_GT_compartment}
{H_dot_air + H_dot_fuel_sum =  H_dot_exhaust_GT + W_dot_GT +
Q_dot_GT_compartment}

"Energy recovered in HRSG"
H_dot_exhaust_HRSG =
(m_dot_Ar)*(h_Ar_hrsg)+(m_dot_N2)*(h_N2_hrsg)+(m_dot_O2)*(h_O2_hrsg)+(m_dot
_CO2)*(h_CO2_hrsg)+(m_dot_H2O)*(h_H2O_hrsg)
```

```
Q_dot_HRSG_recover = H_dot_exhaust_GT - H_dot_exhaust_HRSG
Q_dot_HRSG_recover_total =  GT_full*Q_dot_HRSG_recover
"Exhaust gas heat loss to ambient"
H_dot_exhaust_amb =
(m_dot_Ar)*(h_Ar_amb)+(m_dot_N2)*(h_N2_amb)+(m_dot_O2)*(h_O2_amb)+(m_dot
_CO2)*(h_CO2_amb)+(m_dot_H2O)*(h_H2O_amb)
Q_dot_exhaust = H_dot_exhaust_HRSG - H_dot_exhaust_amb
Q_dot_exhaust_total = GT_full*Q_dot_exhaust

H_dot_exhaust_GT_total = GT_full*H_dot_exhaust_GT
H_dot_exhaust_HRSG_total = GT_full*H_dot_exhaust_HRSG

//Heat loss transfer as heat source

"Turbine compartment"
T_ventair_in = 32 [C]                          "ventilation air inlet temperature"
P_ventair = 1*convert(atm,kPa)                 "ventilation air pressure"
T_ventair_out = T_compartment
"ventilation air outlet temperature"
h_ventair_in =Enthalpy(Air_ha,T=T_ventair_in,P=P_ventair)
h_ventair_out =Enthalpy(Air_ha,T=T_ventair_out,P=P_ventair)
Q_dot_GT_compartment  = m_dot_ventair_halfblock*(h_ventair_out - h_ventair_in)
"neglect Q_loss"
Q_dot_GT_compartment_total = m_dot_ventair_fullblock*(h_ventair_out - h_ventair_in)

"HRSG exhaust gas"
m_dot_exhaust_halfblock = m_dot_exhaust
m_dot_exhaust_fullblock = GT_full*m_dot_exhaust_halfblock

{Exhaust gas composition by volume fraction
Ar = 0.86, N2 = 72.55, O2 = 11.97, CO2 = 4.04, H2O = 10.59}

{Cemical Balance
a*(20.95O2 + 78.08N2 + 0.934Ar) + d*(6.15CO2 + 16.02N2 + 72.51CH4 + 3.53C2H6 +
1.07C3H8) ---> e*(72.55N2 + 11.97O2 + 4.04CO2 + 10.59H2O + 0.86Ar)}

{volume fraction = mol fraction, PV=nRT}

"Ambient Air Condition - CT inlet"
{!use ideal gas properties instead of real gas}
T_air_in = 33 [C]                              "inlet air temperature"
P_air_in = 1*convert(atm,kPa)                  "inlet air pressure"
h_air_in = Enthalpy(Air_ha,T=T_air_in,P=P_air_in)
"inlet air specific enthalpy"
m_dot_air = 532.95 [kg/s]                      "!from EGAT"
```

```
"Heat Loss Analysis - Lube oil system"

"Base load Operation"

"Lubricant property (Oil - BP TH-HT 32)"
Cp_oil = 2.103                                  [kJ/kg-K]"lube oil specific heat"
rho_oil = 874                                   [kg/m^3]"lube oil density"

"Lubrication oil system"
T_H_lube = 82                                   [C]"lube oil high operating
temperature (return)"
T_L_lube = 54                                   [C]"lube oil low operating
temperature (feed in)"
V_dot_lube = 2551*convert(L/min, m^3/s)         "total lube oil volume flow rate"
m_dot_lube = V_dot_lube*rho_oil                 "total lube oil mass flow rate"

"Lubrication heat transfer"
Q_dot_lube = m_dot_lube * Cp_oil * (T_H_lube - T_L_lube)
"heat transfer rate to lube oil system"

"Generator seal oil system"
T_H_seal = 76                                   [C]
"seal oil high operating temperature (return)"
T_L_seal = 54                                   [C]
"seal oil low operating temperature (feed in)"
V_dot_seal = 246*convert(L/min,m^3/s)           "total seal oil volume flow rate"
m_dot_seal = V_dot_seal*rho_oil                 "total seal oil mass flow rate"

"Gen seal oil heat transfer"
Q_dot_seal = m_dot_seal * Cp_oil * (T_H_seal - T_L_seal)
"heat transfer rate to seal oil system"

"Total lubrication oil heat transfer rate"
Q_dot_lube_total = Q_dot_lube + Q_dot_seal
```

"Heat Loss Analysis - Cooling Water"

"Base Load Operation"

"Cooling water to cooling tower"
v_dot_w = 42000/3600 [m^3/s] "cooling water volume flow rate"
rho_w=Density(Water,T=average(T_w_in,T_w_out),P=P_w) "cooling water density"
m_dot_w = rho_w*v_dot_w "cooling water mass flow rate"
T_w_in = 27 [C] "cooling water inlet temperature"
T_w_out = 40 [C] "cooling water outlet temperature"
P_w = 101.3 [kPa]
Cp_w =Cp(Water,T=average(T_w_in,T_w_out),P=P_w)
"average specific heat of cooling water"

Q_dot_water = m_dot_w*Cp_w*(T_w_out-T_w_in)
"rejected heat of cooling water"

Appendix B. Modeling of Absorption Chillers EES Code

```
"H2O/LiBr Single-effect  Absorption Cycle (Lube oil)"

"Absorbant - LiBr"
"Refrigerant - H2O"
"Rich & weak mixtures according to the concentration of salt"
"LiBr property function, x = concentration of LiBr, Qu = quality"
"water property function, x = quality"

"Input variables"
T_L = T_cooling - DELTAT_L                  "evaporating temperature"
T_H = T_source-DELTAT_H                     "generator temperature"
DELTAT_L = 5 [C]                            "evaporator pinch point"
DELTAT_H = 10 [C]                           "generator pinch point"
T_cooling = converttemp(F,C,55)             "chilled water temperature"
T_sink = 27 [C]                             "sink fluid temperature"
T_amb = 32 [C]                              "ambient temperature, dead state"

eta_pump = 0.6                              "pump efficiency"
eta_hx = 0.45                               "heat exchanger effectiveness"

"Salt concentration in solution"
x_r = x[4]                                  "rich solution"
x_w = x[1]                                  "weak solution"
x_v = 0                                     "water vapor"

"Operating pressures"
P_L = P[10]
P_H = P[8]

"Solution properties"
Cp_w = Cp_LiBrH2O(T[2],X[2])
Cp_r = Cp_LiBrH2O(T[4],X[4])

"Generator mass balance"
CR = (x_r - x_v)/(x_r-x_w)
CR = m_dot_w/m_dot_v
m_dot_v = m_dot_w - m_dot_r

"Heat source properties (lube oil)"
T_source = 82 [C]                           "heat source temperature"
Cp_oil = 2.103 [kJ/kg-K]                    "lube oil specific heat"
m_dot_source = 40 [kg/s]                    "lube oil mass flow rate"
```

```
T_source_out = 54 [C]                                    "lube oil outlet temp"
Q_dot_source = m_dot_source*Cp_oil*(T_source - T_source_out)
Q_dot_source = Q_dot_gen


"State 10: saturated water vapor exiting evaporator"
T[10] = T_L
Q[10] = 1
P[10] = P_sat(Water,T=T[10])
h[10] =Enthalpy(Water,T=T[10],x=Q[10])
x[10] = 0
m_dot[10] = m_dot_v

"State 1: saturated liquid solution at the absorber outlet (weak solution)"
T[1] = T_sink
P[1] = P_L
x[1] = x_LiBrH2O(T[1],P[1])
h[1] = h_LiBrH2O(T[1],x[1])
CALL Q_LiBrH2O(h[1],P[1],x[1]: Q_1,T_1, x_1)
"very small number of quality from this call fuction, considered to be almost zero"
Q[1] = 0
rho_1 = rho_LiBrH2O(T[1],x[1])
m_dot[1] = m_dot_w

"State 2: pumping to internal heat exchanger (weak solution)"
P[2] = P_H
x[2] = x_w
h[2] = h[1] + ((P_H-P_L)/(rho_1*eta_pump))
h[2] = h_LiBrH2O(T[2],x[2])
CALL Q_LiBrH2O(h[2],P[2],x[1]: Q[2],T_2, x_2)
m_dot[2] = m_dot_w

"State 3: heat exchanger outlet (weak solution)"
P[3] = P_H
x[3] = x_w
Q_dot_shx = eta_hx*min(m_dot_w*Cp_w,m_dot_r*Cp_r)*(T[4]-T[2])
Q_dot_shx = m_dot_w*(h[3]-h[2])
CALL Q_LiBrH2O(h[3],P[3],x[2]: Q[3],T_3, x_3)
h[3] = h_LiBrH2O(T[3],x[3])
m_dot[3] = m_dot_w

"State 4: saurated vapor solution exiting generator (rich solution)"
T[4] = T_H
P[4] = P_H
Q[4] = 0
```

```
x[4] = x_LiBrH2O(T[4],P[4])
h[4] = h_LiBrH2O(T[4],x[4])
m_dot[4] = m_dot_r

"State 5: heat exchanger outlet (rich solution)"
P[5] = P_H
x[5] = x_r
Q_dot_shx = m_dot_r*(h[4]-h[5])
Q_dot_shx = m_dot_r*Cp_r*(T[4]-T[5])
CALL Q_LiBrH2O(h[5],P[5],x[4]: Q[5],T_5, x_5)
m_dot[5] = m_dot_r

"State 6: throttling (rich solution)"
h[6] = h[5]
P[6] = P_L
x[6] = x_r
CALL Q_LiBrH2O(h[6],P[6],x[5]: Q[6],T[6], x_6)
m_dot[6] = m_dot_r

"State 7: water vapor leaving generator"
P[7] = P_H
x[7] = 0
T[7] = T_LiBrH2O(P[7],x[3])
h[7] =Enthalpy(Water,T=T[7],P=P[7])
Q[7] =Quality(Water,T=T[7],h=h[7])
m_dot[7] = m_dot_v

"State 8: saturated liquid water leaving condenser"
T[8] =T_sink
x[8] = 0
Q[8] = 0
P[8] = Pressure(Water,T=T[8],x=Q[8])
h[8] =Enthalpy(Water,x=Q[8],P=P[8])
m_dot[8] = m_dot_v

"State 9: expansion of water refrigerant"
P[9] = P_L
x[9] = 0
h[9] = h[8]
Q[9] =Quality(Water,P=P[9],h=h[9])
T[9] =Temperature(Water,P=P[9],h=h[9])
m_dot[9] = m_dot_v

"Cycle Performance"
Q_dot_evap = m_dot_v*(h[10]-h[9])
```

```
Q_dot_gen = m_dot_r*h[4] + m_dot_v*h[7] - m_dot_w*h[3]
Q_dot_cond = m_dot_v*(h[7]-h[8])
Q_dot_abs = m_dot_v*h[10] + m_dot_r*h[6] - m_dot_w*h[1]
W_dot_pump = m_dot_w*(h[2]-h[1])
COP = Q_dot_evap/(Q_dot_gen+W_dot_pump)      "coefficient of performance"

//Exergy analysis
DELTAT_cw = 5 [C]
"chilled water temperature difference"
T_cw_o = T_cooling                           "chilled water outlet temperature"
T_cw_i = T_cooling + DELTAT_cw               "chilled water inlet temperature"
P_cw = 101.3 [kPa]                           "chilled water pressure"
Cp_cw =Cp(Water,T=T_cooling,P=P_cw)
"chilled water specific heat capacity"
Q_dot_evap = m_dot_cw*Cp_cw*(T_cw_i - T_cw_o)

PHI_cooling =
m_dot_cw*Cp_cw*(converttemp(C,K,T_amb)*ln(converttemp(C,K,T_amb)/converttem
p(C,K,T_cooling))-(T_amb - T_cooling))

PHI_source = m_dot_source*Cp_oil*((T_source - T_amb)-
converttemp(C,K,T_amb)*ln(converttemp(C,K,T_source)/converttemp(C,K,T_amb)))

eta_2nd = PHI_cooling/(PHI_source+W_dot_pump) "exergy efficiency"
```

```
"Ammonia-Water Single Effect Absorption Cycle (Lube oil)"

"Refrigerant - Ammonia"
"Absorbant - Water"

"Assumption paremeters"
T_L = T_cooling - DELTAT_L                          "evaporating temperature"
T_H = T_source-DELTAT_H                             "generator temperature"
DELTAT_L = 5 [C]                                    "evaporator pinch point"
DELTAT_H = 10 [C]                                   "generator pinch point"
T_cooling = converttemp(F,C,55)                     "chilled water temperature"
T_sink = 27 [C]                                     "sink fluid temperature"
T_amb = 32 [C]                                      "ambient temperature, dead state"
x_v = 0.9996
"NH3 refrigerant concentration, vapor concentration"
eta_pump = 0.6                                      "pump efficiency"
eta_hx = 0.45                                       "heat exchanger effectiveness"
DELTAT_HX = 5 [C]                                   "heat exchanger pinch point"
Qu_evap = 0.98
"refrigerant quality exiting evaporator"

"Operating Pressure"
P_H = P[11]
"high-side operating pressure, set through condenser"
P_L = P[14]
"low-side operating pressure, set through evaporator"

"Operating concentration"
x_r = x[1]                                          "rich solution, NH3 concentration"
x_w = x[5]

"Heat source properties (lube oil)"
T_source = 82 [C]                                   "heat source temperature"
Cp_oil = 2.103 [kJ/kg-K]                            "lube oil specific heat"
m_dot_source = 40 [kg/s]                            "lube oil mass flow rate"
T_source_out = 54 [C]                               "lube oil outlet temp"
Q_dot_source = m_dot_source*Cp_oil*(T_source - T_source_out)
Q_dot_source = Q_dot_gen

"State 1: absorber outlet (rich solution) (1)"
T_1 = converttemp(C,K,T_sink)
P_1 = P_L
Qu_1= 0                                             "saturated liquid rich solution"
Call NH3H2O(128, T_1, P_1, Qu_1: T[1], P[1], x[1], h[1], s[1], u[1], v[1], Qu[1])
m_dot[1] = m_dot_r
```

```
"State 2: pump outlet (rich solution) (2')"
P_2 = P_H
x_2 = x_r
h_2 = h[1]+(v[1]*((P_H-P_L)*convert(bar,kPa))/eta_pump)
Call NH3H2O(234, P_2, x_2, h_2: T[2], P[2], x[2], h[2], s[2], u[2], v[2], Qu[2])
m_dot[2] = m_dot_r

{State 3: regenerator heat exchange (2")}
P_3 = P_H
x_3 = x_r
m_dot_r*(h_3-h[2]) = Q_dot_rect
Call NH3H2O(234, P_3, x_3, h_3:T[3], P[3], x[3], h[3], s[3], u[3], v[3], Qu[3])
m_dot[3] = m_dot_r

"State 4: internal heat exchanger outlet (rich solution) (2)"
P_4 = P_H
x_4 = x_r
eta_hx = (T[5] - T_6)/(T[5]-T[2])
CR = (x_v - x_w)/(x_r - x_w)                    "circulation ratio"
m_dot_w = (CR - 1)*m_dot_v                      "weak solution mass flow rate"
m_dot_v = m_dot_r - m_dot_w                     "vapor refrigeranr mass flow rate"
m_dot_r*(h_4-h[3]) = m_dot_w*(h[5]-h[6])
Call NH3H2O(234, P_4, x_4, h_4: T[4], P[4], x[4], h[4], s[4], u[4], v[4], Qu[4])
m_dot[4] = m_dot_r

"State 5: exiting generator (weak solution) (3)"
T_5 = converttemp(C,K,T_H)
P_5 = P_H
Qu_5 = 0                                        "saturated liquid weak solution"
Call NH3H2O(128, T_5, P_5, Qu_5:  T[5], P[5], x[5], h[5], s[5], u[5], v[5], Qu[5])
m_dot[5] = m_dot_w

"State 6: exiting internal heat exchanger (weak solution) (3')"
P_6 = P_H
x_6 = x_w
Call NH3H2O(123, T_6, P_6, x_6: T[6], P[6], x[6], h[6], s[6], u[6], v[6], Qu[6])
m_dot[6] = m_dot_w

"State 7: throttling expansion (weak solution) (4)"
P_7 = P_L
x_7 = x_w
h_7 = h[6]
Call NH3H2O(234, P_7, x_7, h_7:T[7], P[7], x[7], h[7], s[7], u[7], v[7], Qu[7])
m_dot[7] = m_dot_w
```

```
{State 8: saturated rich solution exiting generator (5")}
P_8 = P_H
Qu_8 = 1
T_8 = T[9]
Call NH3H2O(128, T_8,P_8, Qu_8: T[8], P[8], x[8], h[8], s[8], u[8], v[8], Qu[8])
x[8]*m_dot[8] = x[10]*m_dot[10] + x[9]*m_dot[9] "rectifier mass balance on NH3"

"State 9: returning saturated liquid water back to generator (5')"
P_9 = P_H
x_9 = x_r
Qu_9 = 0
Call NH3H2O(238, P_9,x_9, Qu_9:T[9], P[9], x[9], h[9], s[9], u[9], v[9], Qu[9])
m_dot[8] = m_dot[9] +m_dot[10]

"State 10: refrigerant vapor exiting rectifier (refrigerant dominant) (5)"
P_10 = P_H
x_10 = x_v
Qu_10 = 1
Call NH3H2O(238, P_10, x_10, Qu_10:T[10], P[10], x[10], h[10], s[10], u[10], v[10],
Qu[10])
m_dot[10] = m_dot_v

"State 11: exiting condenser (refrigerant dominant) (6)"
Qu_11 = 0                                                    "saturated liquid refrigerant"
T_11 = converttemp(C,K,T_sink)
x_11 = x_v
Call NH3H2O(138, T_11, x_11, Qu_11:T[11], P[11], x[11], h[11], s[11], u[11], v[11],
Qu[11])
m_dot[11] = m_dot_v

"State 12: exiting precooler to throttling valve (6')"
P_12 = P_H
x_12 = x_v
Q_dot_precooler = m_dot_v*(h[11]-h_12)
Q_dot_precooler = m_dot_v*(h[15]-h[14])
Call NH3H2O(234, P_12,x_12, h_12: T[12], P[12], x[12], h[12], s[12], u[12], v[12],
Qu[12])
m_dot[12] = m_dot_v
```

```
"State 13: Throttling (refrigerant dominant) (7)"
P_13 = P_L
x_13 = x_v
h_13=h[12]
Call NH3H2O(234, P_13, x_13, h_13:T[13], P[13], x[13], h[13], s[13], u[13], v[13],
Qu[13])
m_dot[13] = m_dot_v

"State 14: exiting evaprator (refrigerant dominant) (8)"
T_14 = converttemp(C,K,T_L)
x_14 = x_v
Qu_14 = Qu_evap
Call NH3H2O(138, T_14, x_14, Qu_14: T[14], P[14], x[14], h[14], s[14], u[14], v[14],
Qu[14])
m_dot[14] = m_dot_v

"State 15: exiting precooler to absorber (refrigerant)"
Qu_15 = 1
P_15 = P_L
x_15 = x_v
Call NH3H2O(238, P_15, x_15, Qu_15: T[15], P[15], x[15], h[15], s[15], u[15], v[15],
Qu[15])
m_dot[15] = m_dot_v


"Cycle Performance"
Q_dot_evap = m_dot_v*(h[14]-h[13])
Q_dot_rect = m_dot[8]*h[8] - m_dot[9]*h[9] - m_dot_v*h[10]
Q_dot_gen = m_dot_w*h[5] + m_dot_v*h[10]- m_dot_r*h[4]+Q_dot_rect
Q_dot_abs = m_dot_w*h[7]+m_dot_v*h[15]-m_dot_r*h[1]
Q_dot_cond = m_dot_v*(h[10]-h[11])
W_dot_pump = m_dot_r*(h[2]-h[1])
COP = Q_dot_evap/(Q_dot_gen+W_dot_pump)      "coefficienct of performance"

//Exergy analysis
DELTAT_cw = 5 [C]
"chilled water temperature difference"
T_cw_o = T_cooling                           "chilled water outlet temperature"
T_cw_i = T_cooling + DELTAT_cw               "chilled water inlet temperature"
P_cw = 101.3 [kPa]                           "chilled water pressure"
Cp_cw =Cp(Water,T=T_cooling,P=P_cw)          "chilled water specific heat capacity"
Q_dot_evap = m_dot_cw*Cp_cw*(T_cw_i - T_cw_o)
```

```
PHI_cooling =
m_dot_cw*Cp_cw*(converttemp(C,K,T_amb)*ln(converttemp(C,K,T_amb)/converttem
p(C,K,T_cooling))-(T_amb - T_cooling))

PHI_source = m_dot_source*Cp_oil*((T_source - T_amb)-
converttemp(C,K,T_amb)*ln(converttemp(C,K,T_source)/converttemp(C,K,T_amb)))

eta_2nd = PHI_cooling/(PHI_source+W_dot_pump)
"exergy efficiency"

{"Plot variables"
//x_plot = 1
P_plot_H = P_H
P_plot_L = P_L
Qu_plot_v = 1
Qu_plot_f = 0
Call NH3H2O(238, P_plot_H, x_plot, Qu_plot_f: T[16], P[16], x[16], h[16], s[16], u[16],
v[16], Qu[16])
//Call NH3H2O(238, P_plot_H, x_plot, Qu_plot_v:  T[16], P[16], x[16], h[16], s[16],
u[16], v[16], Qu[16])
//Call NH3H2O(238, P_plot_L, x_plot, Qu_plot_f:  T[16], P[16], x[16], h[16], s[16],
u[16], v[16], Qu[16])
//Call NH3H2O(238, P_plot_L, x_plot, Qu_plot_v:  T[16], P[16], x[16], h[16], s[16],
u[16], v[16], Qu[16])}
```

“Double Effect LiBr-H2O Absorption Cycle (CT Ventilation air)"

"Absorbant - LiBr"
"Refrigerant - H2O"
"Rich & weak mixtures according to the concentration of salt"
"LiBr property function, x = concentration of LiBr, Qu = quality"
"water property function, x = quality"

"Input variables"
T_L = T_cooling - DELTAT_L "evaporating temperature"
T_H = T_source-DELTAT_H "generator temperature"
DELTAT_L = 5 [C] "evaporator pinch point"
DELTAT_H = 10 [C] "generator pinch point"
T_cooling = converttemp(F,C,55) "chilled water temperature"
T_sink = 27 [C] "sink fluid temperature"
T_amb = 32 [C] "ambient temperature, dead state"
pinch = 5 [C]
"pinch point temperature between HP condenser outlet and MP generator rich solution outlet"

"Operating pressures"
P_L = P[10]
"low pressure operating at evaporator"
P_M = P[4]
"medium pressure at MP generator"
P_H = P[14]
"high pressure operating at HP generator"

Cp_w_1 = Cp_LiBrH2O(T[2],X[2])
Cp_r_1 = Cp_LiBrH2O(T[4],X[4])
Cp_w_2 = Cp_LiBrH2O(T[12],X[12])
Cp_r_2 = Cp_LiBrH2O(T[14],X[14])

eta_pump = 0.6 "pump efficiency"
eta_hx_L = 0.25
eta_hx_H = 0.6

"Salt concentration in solution"
x_r = 0.65
"rich solution in the LP stage, salt concentration" "avoid crystallization"
x_w = x[1]
"weak solution in the LP stage, salt concentration"
x_v = 0
"salt concentration in vapor exiting HP generator to condenser, water only"
"Heat source conditions at generator"

```
T_source = 150 [C]                                  "heat source temperature"
m_dot_air = 1200 [kg/s]                             "vent air mass flow rate"
P_air = 101.3 [kPa]                                 "vent air pressure"
Cp_air=Cp(Air_ha,T=T_source,P=P_air)                "vent air specific heat capacity"
h_air_in = Enthalpy(Air_ha,T=T_source,P=P_air)
"vent air specific enthalpy at generator heat exchanger inlet"
Q_dot_source = m_dot_air*(h_air_in - h_air_out)     "energy transfer at generator"
T_source_out =Temperature(Air_ha,P=P_air,h=h_air_out)
"outlet vent air specific enthalpy at generator heat exchanger"
T_source_out = T_source-DELTAT_source
DELTAT_source = 50 [C]
"heat source temperature difference"
Q_dot_gen2 = Q_dot_source

"Cycle mass balance"
CR = (x_r - x_v)/(x_r - x_w)
m_dot_v = m_dot_v_1 + m_dot_v_2                     "evaporator"
m_dot_v = m_dot_w_1 - m_dot_r_1

"MP Generator mass balance"
m_dot_v = m_dot_w_1/CR
//m_dot_v_2*(h[17]-h[18]) + m_dot_w_1*h[3] + m_dot_r_2*h[16] = m_dot_w_2*h[11]
+ m_dot_v_1*h[7] + m_dot_r_1*h[4] "Q_dot_cond2=Q_dot_gen1"

"HP Generator mass balance"
m_dot_v_2 = m_dot_w_2/CR
m_dot_w_2 = m_dot_r_2 +m_dot_v_2

"State 1: saturated liquid solution exiting absorber (weak solution), not neccessary at sink
temperature"
T[1] = T_sink
P[1] = P_L
x[1] = x_LiBrH2O(T[1],P[1])
h[1] = h_LiBrH2O(T[1],x[1])
rho_1 = rho_LiBrH2O(T[1],x[1])
Q[1] = 0
m_dot[1] = m_dot_w_1

"State 2: pumping to medium pressure (weak solution)"
x[2] = x_w
P[2] = P_M
h[2] =h[1] + (P[2]-P[1])/(rho_1*eta_pump)
h[2] = h_LiBrH2O(T[2],x[2])
CALL Q_LiBrH2O(h[2],P[2],x[1]: Q[2],T_2, x_2)
m_dot[2] = m_dot_w_1
```

```
"State 3: MP heat exhanged (weak solution)"
x[3] = x_w
P[3] = P_M
Q_dot_shx1 = eta_hx_L*min(m_dot_w_1*Cp_w_1,m_dot_r_1*Cp_r_1)*(T[4]-T[2])
Q_dot_shx1 = m_dot_w_1*(h[3]-h[2])
h[3] = h_LiBrH2O(T[3],x[3])
CALL Q_LiBrH2O(h[3],P[3],x[2]: Q[3],T_3, x_3)
m_dot[3] = m_dot_w_1

"State 4: salt solution exiting MP generator (rich solution)"
x[4] = x_r
T[4] = T[18] - pinch
P[4] = P_LiBrH2O(T[4],x[4])
h[4] = h_LiBrH2O(T[4],x[4])
CALL Q_LiBrH2O(h[4],P[4],x[4]: Q[4],T_4, x_4)
"must be closest to 0, with given x_r and P_M"
m_dot[4] = m_dot_r_1

"State 5: exiting heat exchanger (rich solution)"
x[5] = x_r
P[5] = P_M
Q_dot_shx1 = m_dot_r_1*Cp_r_1*(T[4]-T[5])
Q_dot_shx1 = m_dot_r_1*(h[4]-h[5])
m_dot[5] = m_dot_r_1
CALL Q_LiBrH2O(h[5],P[5],x[4]: Q[5],T_5, x_5)

"State 6: throttling through expansion valve (rich solution)"
x[6] = x_r
P[6] = P_L
h[6] = h[5]
CALL Q_LiBrH2O(h[6],P[6],x[5]: Q[6],T[6], x_6)
m_dot[6] = m_dot_r_1

"State 7: superheated water vapor exiting MP generator"
x[7] = 0
P[7] = P_M
T[7] = T_LiBrH2O(P[7],x[3])
"thermal equilibrium with saturated weak solution in MP generator"
h[7] =Enthalpy(Water,T=T[7],P=P[7])
Q[7] =Quality(Water,T=T[7],h=h[7])
m_dot[7] = m_dot_v_1

"State 8: condensing at MP condenser"
x[8] = 0
P[8] = P_M
```

```
T[8]=T_sat(Water,P=P[8])
h[8] =Enthalpy(Water,T=T[8],x=0)
Q[8] = 0
m_dot[8] = m_dot_v

"State 9: water throttling from MP to LP"
x[9] = 0
P[9] = P_L
h[9] = h[8]
T[9] =Temperature(Water,P=P[9],h=h[9])
Q[9]=Quality(Water,P=P[9],h=h[9])
m_dot[9] = m_dot_v

"State 10: evaporating at evaporator"
T[10] = T_L
P[10] = P_sat(Water,T=T[10])
h[10] = Enthalpy(Water,x=1,T=T[10])
x[10] = 0
Q[10] = 1
m_dot[10] = m_dot_v

"State 11: saturated liquid solution exiting MP generator (weak solution)"
x[11] = x_w
P[11] = P_M
Q[11] = 0
T[11] = T_LiBrH2O(P[11],x[11])
h[11] = h_LiBrH2O(T[11],x[11])
rho_11 = rho_LiBrH2O(T[11],X[11])
m_dot[11] = m_dot_w_2
CALL Q_LiBrH2O(h[11],P[11],x[1]: Q_11,T_11, x_11)

"State 12: pumping to high pressure heat exchanger (weak solution)"
x[12] = x_w
P[12] = P_H
T[12] = T[11]
h[12] =h[11] + (P[12]-P[11])/(rho_11*eta_pump)
CALL Q_LiBrH2O(h[12],P[12],x[11]: Q[12],T_12, x_12)
m_dot[12] = m_dot_w_2

"State 13: HP heat exchanged (weak solution)"
x[13] = x_w
P[13] = P_H
Q_dot_shx2 = eta_hx_H*min(m_dot_w_2*Cp_w_2,m_dot_r_2*Cp_r_2)*(T[14]-T[12])
Q_dot_shx2 = m_dot_w_2*(h[13]-h[12])
h[13] = h_LiBrH2O(T[13],x[13])
```

```
CALL Q_LiBrH2O(h[13],P[13],x[12]: Q[13],T_13, x_13)
m_dot[13] = m_dot_w_2

"State 14: salt solution exiting HP generator (rich solution)"
T[14] = T_H
x[14] = x_r
P[14] = P_LiBrH2O(T[14],x[14])
h[14] = h_LiBrH2O(T[14],x[14])
CALL Q_LiBrH2O(h[14],P[14],x[14]: Q[14],T_14, x_14)
m_dot[14] = m_dot_r_2

"State 15: exiting HP heat exchanger (rich solution)"
x[15] = x_r
P[15] = P_H
Q_dot_shx2 = m_dot_r_2*Cp_r_1*(T[14]-T[15])
Q_dot_shx2 = m_dot_r_2*(h[14]-h[15])
CALL Q_LiBrH2O(h[15],P[15],x[14]: Q[15],T_15, x_15)
m_dot[15] = m_dot_r_2

"State 16:  throttling through expansion valve (rich solution)"
x[16] = x_r
P[16] = P_M
T[16] = T_LiBrH2O(P[16],x[16])
h[16] = h[15]
CALL Q_LiBrH2O(h[16],P[16],x[15]: Q[16],T_16, x_16)
m_dot[16] = m_dot_r_2

"State 17: superheated water vapor exiting HP generator"
x[17] = 0
P[17] = P_H
T[17] = T_LiBrH2O(P[17],x[13])
"thermal equilibrium with saturated weak solution in HP generator"
h[17] =Enthalpy(Water,T=T[17],P=P[17])
Q[17] =Quality(Water,T=T[17],h=h[17])
m_dot[17] = m_dot_v_2

"State 18: saturated water leaving HP condenser"
x[18] = 0
P[18] = P_H
Q[18] = 0
T[18] =T_sat(Water,P=P[18])
"!must be more than T[3]"
h[18] =Enthalpy(Water,T=T[18],x=0)
m_dot[18] = m_dot_v_2
```

```
"State 19: water throttling from HP to LP"
x[19] = 0
P[19] = P_M
h[19] = h[18]
T[19] =Temperature(Water,P=P[19],h=h[19])
Q[19] =Quality(Water,P=P[19],h=h[19])
m_dot[19] = m_dot_v_2
T_sat=T_sat(Water,P=P_H)

"Energy balance"
Q_dot_evap = m_dot_v*h[10] - m_dot_v*h[9]
Q_dot_abs = m_dot_v*h[10]+m_dot_r_1*h[6] - m_dot_w_1*h[1]
Q_dot_gen1= m_dot_w_2*h[11]+m_dot_r_1*h[4] +m_dot_v_1*h[7] - m_dot_w_1*h[3]
- m_dot_r_2*h[16]
Q_dot_cond2 = m_dot_v_2*h[17] - m_dot_v_2*h[18]
Q_dot_gen1 = Q_dot_cond2
Q_dot_gen2 = m_dot_r_2*h[14]+m_dot_v_2*h[17] - m_dot_w_2*h[13]
Q_dot_cond1 = m_dot_v_1*h[7]+m_dot_v_2*h[19] - m_dot_v*h[8]
Q_dot_hx1 = m_dot_r_1*(h[4]-h[5])
Q_dot_hx2 = m_dot_r_2*(h[14]-h[15])
W_dot_pump1 = m_dot_w_1*(h[2]-h[1])
W_dot_pump2 = m_dot_w_2*(h[12]-h[11])
W_dot_total = W_dot_pump1+W_dot_pump2

"Cycle performance"
COP = Q_dot_evap/(W_dot_total + Q_dot_gen2)

//Exergy analysis
DELTAT_cw = 5 [C]
"chilled water temperature difference"
T_cw_o = T_cooling                          "chilled water outlet temperature"
T_cw_i = T_cooling + DELTAT_cw              "chilled water inlet temperature"
P_cw = 101.3 [kPa]                          "chilled water pressure"
Cp_cw =Cp(Water,T=T_cooling,P=P_cw)
"chilled water specific heat capacity"
Q_dot_evap = m_dot_cw*Cp_cw*(T_cw_i - T_cw_o)

PHI_cooling =
m_dot_cw*Cp_cw*(converttemp(C,K,T_amb)*ln(converttemp(C,K,T_amb)/converttem
p(C,K,T_cooling))-(T_amb - T_cooling))

PHI_source = m_dot_air*Cp_air*((T_source - T_amb)-
converttemp(C,K,T_amb)*ln(converttemp(C,K,T_source)/converttemp(C,K,T_amb)))

eta_2nd = PHI_cooling/(PHI_source+W_dot_total)  "exergy efficiency"
```

```
"LiBr-Water Half Effect Absorption Cycle (Lube oil)"

"Absorbant - LiBr"
"Refrigerant - H2O"
"Rich & weak mixtures according to the concentration of salt"
"LiBr property function, x = concentration of LiBr, Qu = quality"
"water property function, x = quality"

"Input variables"
T_L = T_cooling - DELTAT_L                    "evaporating temperature"
T_H = T_source-DELTAT_H                       "generator temperature"
DELTAT_L = 5 [C]                              "evaporator pinch point"
DELTAT_H = 10 [C]                             "generator pinch point"
T_cooling = converttemp(F,C,55)               "chilled water temperature"
T_sink = 27 [C]                               "sink fluid temperature"
T_amb = 32 [C]                                "ambient temperature, dead state"

eta_pump = 0.6
"pump efficiency"
eta_hx_H = 0.8
"heat exchanger effectiveness, high side"
eta_hx_L = 0.6
"heat exchanger effectiveness, low side"

"Salt concentration in solution"
x_w_1 = x[1]
"weak solution in LP stage, salt concentration"
x_r_1 = 0.65
"rich solution in the LP stage, salt concentration"
x_w_2 = x[7]
"weak solution in HP stage, salt concentration"
x_r_2 = 0.5
"rich soliton in the HP stage, salt concentration"
//x_r_2 = x[10]
x_v_1 = 0
"salt concentration in vapor exiting HP generator to condenser, water only"
x_v_2 = 0

"Properties"
P_L = P[16]                                   "low-side operating pressure"
P_M = P[4]                                    "intermediate operating pressure"
P_H = P[10]                                   "high-side operating pressure"
//P_H = P[14]
```

```
Cp_w_1 = Cp_LiBrH2O(T[2],X[2])
Cp_r_1 = Cp_LiBrH2O(T[4],X[4])
Cp_w_2 = Cp_LiBrH2O(T[8],X[8])
Cp_r_2 = Cp_LiBrH2O(T[10],X[10])

"MP Generator mass balance"
CR_MP = (x_r_1 - x_v_1)/(x_r_1 - x_w_1)
CR_MP = m_dot_w_1/m_dot_v_2
m_dot_v_1 = m_dot_w_1 - m_dot_r_1

"HP Generator mass balance"
CR_HP = (x_r_2 - x_v_2)/(x_r_2-x_w_2)
CR_HP = m_dot_w_2/m_dot_v_2

m_dot_w_2 = m_dot_r_2 +m_dot_v_1
m_dot_v_2 = m_dot_w_2 - m_dot_r_2

"LP Absorber mass balance"
//m_dot_w_1 = m_dot_v_2 + m_dot_r_1

"Heat source properties (lube oil)"
T_source = 82 [C]                                   "heat source temperature"
Cp_oil = 2.103 [kJ/kg-K]                            "lube oil specific heat"
m_dot_source = 40 [kg/s]                            "lube oil mass flow rate"
T_source_out = 54 [C]                               "lube oil outlet temp"
Q_dot_source = m_dot_source*Cp_oil*(T_source - T_source_out)
Q_dot_source = Q_dot_gen_total

"State 1: exiting the LP absorber (LP weak solution), given T[1] = T_sink"
P[1] = P_L
T[1] = T_sink
x[1] = x_LiBrH2O(T[1],P[1])
h[1] = h_LiBrH2O(T[1],x[1])
rho_1 = rho_LiBrH2O(T[1],x[1])
Q[1] = 0
m_dot[1] = m_dot_w_1

"State 2: pumping to MP heat exchanger inlet (LP weak solution)"
h[2] = h[1] + ((P_M-P_L)/(rho_1*eta_pump))
P[2] = P_M
x[2] = x_w_1
h[2] = h_LiBrH2O(T[2],x[2])
m_dot[2] = m_dot_w_1
Q[2] = 0
```

```
"State 3: MP internal heat exchanger outlet (MP weak solution)"
x[3] = x_w_1
P[3] = P_M
Q_dot_shx1 = eta_hx_L*min(m_dot_w_1*Cp_w_1,m_dot_r_1*Cp_r_1)*(T[4]-T[2])
Q_dot_shx1 = m_dot_w_1*(h[3]-h[2])
h[3] = h_LiBrH2O(T[3],x[3])
m_dot[3] = m_dot_w_1
Q[3] = 0

//for plot
CALL Q_LiBrH2O(h[3],P[3],x[3]: Q_3,T_3, x_3)
T[19]=T_3
P[19] = P_M

"State 4: sat vapor exiting generator (MP rich solution)"
x[4] = x_r_1
T[4] = T_H
P[4] = P_LiBrH2O(T[4],x[4])
h[4] = h_LiBrH2O(T[4],x[4])
Q[4] = 0
m_dot[4] = m_dot_r_1

"State 5: MP internal heat exchanger outlet (MP rich solution)"
P[5] = P_M
Q_dot_shx1 = m_dot_r_1*Cp_r_1*(T[4]-T[5])
Q_dot_shx1 = m_dot_r_1*(h[4]-h[5])
x[5] = x_r_1
//Q[5] = 0
CALL Q_LiBrH2O(h[5],P[5],x[4]: Q[5],T_5, x_5)
m_dot[5] = m_dot_r_1

"State 6: throttling expansion from MP to LP (rich solution)"
P[6] = P_L
x[6] = x_r_1
h[6] = h[5]
CALL Q_LiBrH2O(h[6],P[6],x[5]: Q[6],T_6, x_6)
h[6] = h_LiBrH2O(T[6],x[6])
m_dot[6] = m_dot_r_1
//for plot
T[18]=T_6
P[18] = P_L

"State 17: vapor exiting MP generator  (pure refrigerant superheated vapor)"
P[17] = P_M
x[17] = x_v_1
```

```
T[17] =T_LiBrH2O(P[17],x[3])
"thermal equilibrium with saturated liquid weak solution at MP generator"
h[17] =Enthalpy(Water,P=P[17],T=T[17])
Q[17] =Quality(Water,P=P[17],h=h[17])
m_dot[17] = m_dot_v_1
P_17 =P_sat(Water,T=T[17])

"State 7: exiting MP absorber (HP weak solution), T[7] = T_sink"
P[7] = P_M
T[7] = T_sink
x[7] = x_LiBrH2O(T[7],P[7])
h[7] = h_LiBrH2O(T[7],x[7])
Q[7] = 0
rho_7 = rho_LiBrH2O(T[7],X[7])
m_dot[7] = m_dot_w_2

"State 8: pumping to HP internal heat exchanger inlet (weak solution)"
h[8] = h[7] + ((P_H-P_M)/(rho_7*eta_pump))
P[8] = P_H
x[8] = x_w_2
h[8] = h_LiBrH2O(T[8],x[8])
Q[8] =0
m_dot[8] = m_dot_w_2

"State 9: HP heat exchaner outlet rich solution to generator"
x[9] = x_w_2
P[9] = P_H
Q_dot_shx2 = eta_hx_H*min(m_dot_w_2*Cp_w_2,m_dot_r_2*Cp_r_2)*(T[10]-T[8])
Q_dot_shx2 = m_dot_w_2*(h[9]-h[8])
h[9] = h_LiBrH2O(T[9],x[9])
m_dot[9] = m_dot_w_2
Q[9] =0

"State 10: HP generator outlet (rich solution)"
x[10] = x_r_2
T[10] = T_H
P[10] = P_LiBrH2O(T[10],x[10])
h[10] = h_LiBrH2O(T[10],x[10])
Q[10] = 0
m_dot[10] = m_dot_r_2

"State 11: HP internal heat exchanger outlet (rich solution)"
P[11] = P_H
x[11] = x_r_2
Q_dot_shx2 = m_dot_r_2*(h[10]-h[11])
```

```
Q_dot_shx2 = m_dot_r_2*Cp_r_2*(T[10]-T[11])
m_dot[11] = m_dot_r_2
Q[11] =0

"State 12: throttling expasion from to absorber (rich solution)"
P[12] = P_M
x[12] = x_r_2
h[12] = h[11]
CALL Q_LiBrH2O(h[12],P[12],x[11]: Q[12],T_12, x_12)
T[12] = T_LiBrH2O(P[12],x[12])
m_dot[12] = m_dot_r_2

"State 13: vapor exiting HP generator (pure refrigerant vapor)"
P[13] = P_H
x[13] = x_v_2
Q[13] = 1
T[13] =T_LiBrH2O(P[13],x_w_2)
"thermal equilibrium with saturated liquid weak solution at MP generator"
h[13] =Enthalpy(Water,P=P[13],x=Q[13])
m_dot[13] = m_dot_v_2

"State 14: exiting the condenser (pure refrigerant sat liquid water)"
P[14] = P_H
T[14] =Temperature(Water,P=P[14],x=Q[14])
Q[14] =0
"sat liquid water at P_H set through HP condenser"
h[14] =Enthalpy(Water,x=Q[14],P=P[14])
x[14] = x_v_2
m_dot[14] = m_dot_v_2

"State 15: expansion from HP to LP (pure refrigerant)"
h[15] = h[14]
P[15] = P_L
T[15] =Temperature(Water,P=P[15],h=h[15])
Q[15] =Quality(Water,P=P[15],h=h[15])              "quality"
x[15] = x_v_2                                      "concentration"
m_dot[15] = m_dot_v_2

"State 16: exiting evaporator (pure refrigerant sat vapor)"
T[16] =T_L
P[16] = P_sat(Water,T=T[16])
h[16] =Enthalpy(Water,x=1,P=P[16])
x[16] = x_v_2                                      "concentration"
Q[16] = 1
m_dot[16] = m_dot_v_2
```

```
"Cycle Performance"
Q_dot_evap = m_dot_v_2*(h[16]-h[15])
Q_dot_gen_MP = m_dot_r_1*h[4] + m_dot_v_1*h[17] - m_dot_w_1*h[3]
Q_dot_gen_HP = m_dot_r_2*h[10] + m_dot_v_2*h[13] - m_dot_w_2*h[9]
Q_dot_gen_total = Q_dot_gen_HP + Q_dot_gen_MP
Q_dot_cond = m_dot_v_2*(h[13]-h[14])
Q_dot_abs_LP = m_dot_v_2*h[16] + m_dot_r_1*h[6] - m_dot_w_1*h[1]
Q_dot_abs_MP = m_dot_v_1*h[17] + m_dot_r_2*h[12] - m_dot_w_2*h[7]
W_dot_pump_1 = m_dot_w_1*(h[2]-h[1])
W_dot_pump_2 = m_dot_w_2*(h[8]-h[7])
W_dot_pump_total = W_dot_pump_1 + W_dot_pump_2

//Cycle performance
COP = Q_dot_evap/(Q_dot_gen_total+W_dot_pump_total)

//Exergy analysis
DELTAT_cw = 5 [C]
"chilled water temperature difference"
T_cw_o = T_cooling                          "chilled water outlet temperature"
T_cw_i = T_cooling + DELTAT_cw              "chilled water inlet temperature"
P_cw = 101.3 [kPa]                          "chilled water pressure"
Cp_cw =Cp(Water,T=T_cooling,P=P_cw)
"chilled water specific heat capacity"
Q_dot_evap = m_dot_cw*Cp_cw*(T_cw_i - T_cw_o)

PHI_cooling =
m_dot_cw*Cp_cw*(converttemp(C,K,T_amb)*ln(converttemp(C,K,T_amb)/converttem
p(C,K,T_cooling))-(T_amb - T_cooling))

PHI_source = m_dot_source*Cp_oil*((T_source - T_amb)-
converttemp(C,K,T_amb)*ln(converttemp(C,K,T_source)/converttemp(C,K,T_amb)))

eta_2nd = PHI_cooling/(PHI_source+W_dot_pump_total) "exergy efficiency"
```

```
"Ammonia-Water Half Effect Absorption Cyclem (Lube oil)"

"Refrigerant - Ammonia"
"Absorbant - Water"

"Assumption paremeters"
T_L = T_cooling - DELTAT_L                    "evaporating temperature"
T_H = T_source-DELTAT_H                       "generator temperature"
DELTAT_L = 5 [C]                              "evaporator pinch point"
DELTAT_H = 10 [C]                             "generator pinch point"
T_cooling = converttemp(F,C,55)               "chilled water temperature"
T_sink = 27 [C]                               "sink fluid temperature"
T_amb = 32 [C]                                "ambient temperature, dead state"

eta_pump = 0.6
"pump efficiency"
eta_hx_H = 0.8
"heat exchanger effectiveness, high side"
eta_hx_L = 0.6
"heat exchanger effectiveness, low side"

"Operating Pressure"
P_H = P[10]                                   "high-side operating pressure"
P_L = P[16]                                   "low-side operating pressure"
P_M = P[4]                                    "medium pressure"

"Operating concentration"
x_r_1 = x[1]
"rich solution in LP stage, NH3 concentration"
x_w_1 = 0.4
"weak solution in LP stage, NH3 concentration"
x_v_1 = x[17]
"concentration of vapor, MP"
x_r_2 = x[7]
"rich solution in MP stage, NH3 concentration"
x_w_2 = 0.55
"concentration difference of the two solutions, MP"
x_v_2 = 0.9999
"NH3 refrigerant concentration, vapor concentration, LP"

"Heat source properties (lube oil)"
T_source = 82 [C]                             "heat source temperature"
Cp_oil = 2.103 [kJ/kg-K]                      "lube oil specific heat"
m_dot_source = 40 [kg/s]                      "lube oil mass flow rate"
T_source_out = 54 [C]                         "lube oil outlet temp"
```

```
Q_dot_source = m_dot_source*Cp_oil*(T_source - T_source_out)
Q_dot_source = Q_dot_gen_total

"MP Generator mass balance"
CR_MP = (x_v_1 - x_w_1)/(x_r_1 - x_w_1)
m_dot_w_1 = (CR_MP - 1)*m_dot_v_1
m_dot_v_1 = m_dot_r_1 - m_dot_w_1

"HP Generator mass balance"
CR_HP = (x_v_2 - x_w_2)/(x_r_2-x_w_2)
m_dot_w_2 = (CR_HP-1)*m_dot_v_2
m_dot_r_2 = m_dot_v_1 + m_dot_w_2
m_dot_v_2 = m_dot_r_2 - m_dot_w_2

"LP Absorber mass balance"
//m_dot_r_1 = m_dot_v_2 + m_dot_w_1

"State 1: exiting LP absorber (LP rich solution)"
T_1 = converttemp(C,K,T_sink)
P_1 = P_L
Qu_1 = 0
Call NH3H2O(128, T_1, P_1, Qu_1: T[1], P[1], x[1], h[1], s[1], u[1], v[1], Qu[1])
m_dot[1] = m_dot_r_1

"State 2: pumping to MP heat exchanger inlet (LP rich solution)"
P_2 = P_M
x_2 = x_r_1
h_2 = h[1]+(v[1]*((P_M-P_L)*convert(bar,kPa))/eta_pump)
Call NH3H2O(234, P_2, x_2, h_2: T[2], P[2], x[2], h[2], s[2], u[2], v[2], Qu[2])
m_dot[2] = m_dot_r_1

"State 3: MP internal heat exchanger outlet (rich solution)"
P_3 = P_M
x_3 = x_r_1
m_dot_r_1*(h_3-h[2]) = m_dot_w_1*(h[4]-h[5])
Call NH3H2O(234, P_3, x_3, h_3: T[3], P[3], x[3], h[3], s[3], u[3], v[3], Qu[3])
m_dot[3] = m_dot_r_1

"State 4: exiting MP generator (weak solution)"
T_4 = converttemp(C,K,T_H)
Qu_4 = 0
x_4 = x_w_1
Call NH3H2O(138, T_4 ,x_4, Qu_4: T[4], P[4], x[4], h[4], s[4], u[4], v[4], Qu[4])
m_dot[4] = m_dot_w_1
```

```
"State 5: MP internal heat exchanger outlet (weak solution)"
P_5 = P_M
x_5 = x_w_1
eta_hx_L = (T[4]-T_5)/(T[4]-T[2])
Call NH3H2O(123, T_5, P_5, x_5: T[5], P[5], x[5], h[5], s[5], u[5], v[5], Qu[5])
m_dot[5] = m_dot_w_1

"State 6: throttling expansion from MP to LP (weak solution)"
P_6 = P_L
x_6 = x_w_1
h_6 = h[5]
Call NH3H2O(234, P_6, x_6, h_6: T[6], P[6], x[6], h[6], s[6], u[6], v[6], Qu[6])
m_dot[6] = m_dot_w_1

"[For properties] State 18: Saturated liquid rich solution at MP generator"
x_18 = x_r_1
P_18 = P_M
Qu_18 = 0
Call NH3H2O(238, P_18, x_18, Qu_18: T[18], P[18], x[18], h[18], s[18], u[18], v[18],
Qu[18])

"State 17: vapor exiting MP generator  (refrigerant dominant at x_v_1)"
T_17 = T[18]
"thermal equilibrium with saturated liquid rich solution at MP generator"
P_17 = P_M
Qu_17 = 1
Call NH3H2O(128, T_17, P_17, Qu_17: T[17], P[17], x[17], h[17], s[17], u[17], v[17],
Qu[17])
m_dot[17] = m_dot_v_1

"State 7: exiting MP absorber (HP rich solution)"
P_7 = P_M
T_7 = T[1]
Qu_7 = 0
Call NH3H2O(128, T_7, P_7, Qu_7: T[7], P[7], x[7], h[7], s[7], u[7], v[7], Qu[7])
m_dot[7] = m_dot_r_2

"State 8: pumping to HP internal heat exchanger inlet (rich solution)"
P_8 = P_H
x_8 = x_r_2
h_8 = h[7]+(v[7]*((P_H-P_M)*convert(bar,kPa))/eta_pump)
Call NH3H2O(234, P_8, x_8, h_8: T[8], P[8], x[8], h[8], s[8], u[8], v[8], Qu[8])
m_dot[8] = m_dot_r_2
```

```
"[For properties] State 19: Saturated liquid rich solution at HP generator"
x_19 = x_r_2
P_19 = P_H
Qu_19 = 0
Call NH3H2O(238, P_19, x_19, Qu_19: T[19], P[19], x[19], h[19], s[19], u[19], v[19],
Qu[19])

"State 9: HP heat exchaner outlet rich solution to generator"
P_9 = P_H
x_9 = x_r_2
m_dot_r_2*(h_9-h[8]) = m_dot_w_2*(h[10]-h[11])
Call NH3H2O(234, P_9, x_9, h_9: T[9], P[9], x[9], h[9], s[9], u[9], v[9], Qu[9])
m_dot[9] = m_dot_r_2

"State 10: HP generator outlet (weak solution)"
T_10 = converttemp(C,K,T_H)
x_10 = x_w_2
Qu_10 = 0
Call NH3H2O(138, T_10,x_10, Qu_10: T[10], P[10], x[10], h[10], s[10], u[10], v[10],
Qu[10])
m_dot[10] = m_dot_w_2

"State 11: HP internal heat exchanger outlet (weak solution)"
P_11 = P_H
x_11 = x_w_2
eta_hx_H = (T[10]-T_11)/(T[10]-T[8])
Call NH3H2O(123, T_11, P_11,x_11: T[11], P[11], x[11], h[11], s[11], u[11], v[11],
Qu[11])
m_dot[11] = m_dot_w_2

"State 12: throttling expasion from to absorber (weak solution)"
P_12 = P_M
x_12 = x_w_2
h_12 = h[11]
Call NH3H2O(234, P_12, x_12, h_12: T[12], P[12], x[12], h[12], s[12], u[12], v[12],
Qu[12])
m_dot[12] = m_dot_w_2
```

```
"State 13: vapor exiting HP generator (refrigerant dominant at x_v_2)"
T_13 = T[19]
"thermal equilibrium with saturated liquid rich solution at HP generator"
P_13 = P_H
x_13 = x_v_2
Call NH3H2O(123, T_13, P_13, x_13: T[13], P[13], x[13], h[13], s[13], u[13], v[13],
Qu[13])
m_dot[13] = m_dot_v_2

"State 14: exiting the condenser (refrigerant dominant)"
T_14 = T[1]
P_14 = P_H
x_14 = x_v_2
Call NH3H2O(123, T_14, P_14, x_14:T[14], P[14], x[14], h[14], s[14], u[14], v[14],
Qu[14])
m_dot[14] = m_dot_v_2

"State 15: expansion from HP to LP (refrigerant dominant)"
P_15 = P_L
h_15 = h[14]
x_15 = x_v_2
Call NH3H2O(234, P_15, x_15, h_15:  T[15], P[15], x[15], h[15], s[15], u[15], v[15],
Qu[15])
m_dot[15] = m_dot_v_2

"State 16: exiting evaporator (refrigerant dominant)"
T_16 = converttemp(C,K,T_L)
Qu_16 = 1
x_16 = x_v_2
Call NH3H2O(138, T_16, x_16, Qu_16: T[16], P[16], x[16], h[16], s[16], u[16], v[16],
Qu[16])
m_dot[16] = m_dot_v_2

"Cycle Performance"
Q_dot_evap = m_dot_v_2*(h[16]-h[15])
Q_dot_gen_MP = m_dot_r_1*h[4] + m_dot_v_1*h[17] - m_dot_w_1*h[3]
Q_dot_gen_HP = m_dot_r_2*h[10] + m_dot_v_2*h[13] - m_dot_w_2*h[9]
Q_dot_gen_total = Q_dot_gen_HP + Q_dot_gen_MP
Q_dot_cond = m_dot_v_2*(h[13]-h[14])
Q_dot_abs_LP = m_dot_v_2*h[16] + m_dot_r_1*h[6] - m_dot_w_1*h[1]
Q_dot_abs_MP = m_dot_v_1*h[17] + m_dot_r_2*h[12] - m_dot_w_2*h[7]
W_dot_pump_1 = m_dot_w_1*(h[2]-h[1])
W_dot_pump_2 = m_dot_w_2*(h[8]-h[7])
W_dot_pump_total = W_dot_pump_1 + W_dot_pump_2
```

```
//Cycle performance
COP = Q_dot_evap/(Q_dot_gen_total+W_dot_pump_total)

//Exergy analysis
DELTAT_cw = 5 [C]
"chilled water temperature difference"
T_cw_o = T_cooling                          "chilled water outlet temperature"
T_cw_i = T_cooling + DELTAT_cw              "chilled water inlet temperature"
P_cw = 101.3 [kPa]                          "chilled water pressure"
Cp_cw =Cp(Water,T=T_cooling,P=P_cw)
"chilled water specific heat capacity"
Q_dot_evap = m_dot_cw*Cp_cw*(T_cw_i - T_cw_o)

PHI_cooling =
m_dot_cw*Cp_cw*(converttemp(C,K,T_amb)*ln(converttemp(C,K,T_amb)/converttem
p(C,K,T_cooling))-(T_amb - T_cooling))

PHI_source = m_dot_source*Cp_oil*((T_source - T_amb)-
converttemp(C,K,T_amb)*ln(converttemp(C,K,T_source)/converttemp(C,K,T_amb)))

eta_2nd = PHI_cooling/(PHI_source+W_dot_pump_total) "exergy efficiency"


{"Plot variables"
//x_plot = 1
P_plot_H = P_H
P_plot_M = P_M
P_plot_L = P_L
Qu_plot_v = 1
Qu_plot_f = 0
//Call NH3H2O(238, P_plot_L, x_plot, Qu_plot_f: T[20], P[20], x[20], h[20], s[20],
u[20], v[20], Qu[20])
Call NH3H2O(238, P_plot_L, x_plot, Qu_plot_v: T[20], P[20], x[20], h[20], s[20],
u[20], v[20], Qu[20])
//Call NH3H2O(238, P_plot_M, x_plot, Qu_plot_f: T[20], P[20], x[20], h[20], s[20],
u[20], v[20], Qu[20])
//Call NH3H2O(238, P_plot_M, x_plot, Qu_plot_v: T[20], P[20], x[20], h[20], s[20],
u[20], v[20], Qu[20])
//Call NH3H2O(238, P_plot_H, x_plot, Qu_plot_f: T[20], P[20], x[20], h[20], s[20],
u[20], v[20], Qu[20])
//Call NH3H2O(238, P_plot_H, x_plot, Qu_plot_v: T[20], P[20], x[20], h[20], s[20],
u[20], v[20], Qu[20])}
```

Appendix C. Modeling of Organic Rankine Cycles EES Code

```
"ORC - Baseline Model (CT Ventilation air) "
R$ = 'R134a'                                    "ORC working fluid"
//R$ = 'R245fa'

"Input variables"
DELTAT_evap = 50 [C]
"temperature difference of heat source inlet and evaporating temp."
//optimum --> R134a = 50 [C], R245fa = 52.5 [C]
DELTAT_cond = 10 [C]
"temperature difference of sink fluid and condensing temp"
pinch =  5 [C]
"heat sink and source pinch point temperature"

T_amb = 32 [C]
"ambient temperature, dead state temp"
T_sink = 27 [C]                                 "sink fluid temperature"
T_cond = T_sink+DELTAT_cond                     "sink temperature at condenser"
T_evap = T_source - DELTAT_evap                 "evaporating temperature"
T_H = T_source - pinch                          "turbine inlet temperature"
T_L = T_cond                                    "condensing temperature"

eta_pump = 0.6                                  "pump efficiency"
eta_turbine = 0.8                               "turbine isentropic efficiency"

"Operating pressures"
P_H = P[4]
P_L = P[1]
PR = P_H/P_L                                    "pressure ratio"

"Heat source conditions"
T_source = 150 [C]                              "heat source temperature"
m_dot_source = 1200 [kg/s]                      "vent air mass flow rate"
P_air = 101.3 [kPa]                             "vent air pressure"
Cp_air =Cp(Air_ha,T=T_source,P=P_air)
"air specific heat, assume constant"
T_source_out_max =T[2]

"Boiler energy balance"
Q_dot_boiler = Q_dot_source_act
Q_dot_source_act = m_dot_source*Cp_air*(T_source - T_source_out)
Q_dot_source_max = m_dot_source*Cp_air*(T_source - T_source_out_max)
eta_boiler = Q_dot_source_act/Q_dot_source_max
```

```
T_source = m*s[5]+C                                    "m = heat source slope"
T_source_out = m*s[2]+C                                "C = constant"
T_source_pinch = m*s[3]+C
T_source_pinch = T_evap + pinch

"Heat sink properties (water)"
P_water = 101.3 [kPa]
Cp_water =Cp(Water,T=T_sink,P=P_water)
T_sink_out_max = T[6]
Q_dot_sink_act = Q_dot_cond
Q_dot_sink_max = m_dot_sink*Cp_water*(T_sink_out_max - T_sink)
eta_cond = Q_dot_sink_act/Q_dot_sink_max
Q_dot_sink_act = m_dot_sink*Cp_water*(T_sink_out - T_sink)

T_sink = n*s[1]+D                                      "n = heat sink slope"
T_sink_out = n*s[6]+D                                  "D = constant"
T_sink_pinch = n*s[7]+D
T_sink_pinch = T_cond - pinch

//Heat source and sink plots
"State 9: heat source inlet"
T[9] = T_source
s[9] = s[5]
"State 10: heat source pinch"
T[10] = T_source_pinch
s[10] = s[3]
"State 11: heat source outlet"
T[11] = T_source_out
s[11] = s[2]
"State 12: heat sink inlet"
T[12] = T_sink
s[12] = s[1]
"state 13: heat sink pinch"
T[13] = T_sink_pinch
s[13] = s[7]
"state 14: heat sink outlet"
T[14] = T_sink_out
s[14] = s[6]

"State 1: saturated liquid exiting condenser"
T[1] = T_cond
P[1] =P_sat(R$,T=T[1])
x[1] = 0
h[1] =Enthalpy(R$,T=T[1],x=x[1])
s[1] =Entropy(R$,T=T[1],x=x[1])
```

```
"State 2s: isentropic pumping"
P[2] = P_H
s_isen[2] = s[1]
h_isen[2] =Enthalpy(R$,P=P[2],s=s_isen[2])

"State 2: actual pumping"
eta_pump = (h_isen[2]-h[1])/(h[2]-h[1])
T[2] =Temperature(R$,P=P[2],h=h[2])
s[2] =Entropy(R$,P=P[2],h=h[2])
x[2] =Quality(R$,P=P[2],h=h[2])

"State 3: staturated liquid state point (for plot)"
P[3] = P_H
x[3] = 0
T[3] = T_evap
h[3] =Enthalpy(R$,T=T[3],x=x[3])
s[3] =Entropy(R$,P=P[3],x=x[3])

"State 4: saturated vapor state point (for plot)"
T[4] = T_evap
P[3] =P_sat(R$,T=T[4])
x[4] = 1
h[4] =Enthalpy(R$,T=T[4],x=x[4])
s[4] =Entropy(R$,P=P[4],x=x[4])

"State 5: vapor at turbine inlet"
T[5] = T_H
P[5] = P_H
h[5] =Enthalpy(R$,T=T[5],P=P[5])
s[5] =Entropy(R$,P=P[5],T=T[5])
x[5] =Quality(R$,P=P[5],T=T[5])

"State 6s: insentropic expansion"
P[6] = P_L
s_isen[6] = s[5]
h_isen[6] =Enthalpy(R$,P=P[6],s=s_isen[6])

"State 6: actual expansion at turbine outlet"
eta_turbine = (h[5]-h[6])/(h[5]-h_isen[6])
T[6] =Temperature(R$,P=P[6],h=h[6])
s[6] =Entropy(R$,P=P[6],h=h[6])
x[6] =Quality(R$,P=P[6],h=h[6])
```

```
"State 7: saturated vapor state point (for plot)"
P[7] = P_L
x[7] = 1
T[7] =Temperature(R$,P=P[7],x=x[7])
s[7] =Entropy(R$,P=P[7],x=x[7])

"State 8: close cycle"
P[8] = P[1]
T[8] = T[1]
h[8] = h[1]
s[8] = s[1]
x[8] = x[1]

"Cycle performance"
W_dot_pump = m_dot_orc*(h[2]-h[1])
W_dot_turbine = m_dot_orc*(h[5]-h[6])
W_dot_net = W_dot_turbine-W_dot_pump
Q_dot_cond = m_dot_orc*(h[6]-h[1])
Q_dot_boiler = m_dot_orc*(h[5] - h[2])
eta_ORC = W_dot_net/Q_dot_boiler                    "ORC efficiency"


//Exergy Analysis

PHI_source = m_dot_source*Cp_air*((T_source - T_amb)-
converttemp(C,K,T_amb)*ln(converttemp(C,K,T_source)/converttemp(C,K,T_amb)))

eta_2nd = W_dot_net/PHI_source                      "2nd law effectiveness"
```

```
"ORC with Internal Regenerator (Lube oil)"

R$ = 'R134a'                                    "ORC working fluid"
//R$ = 'R245fa'

"Input variables"
DELTAT_evap =24.5 [C]
"temperature difference of heat source inlet and evaporating temp."
//optimum --> R134a = 24.5 [C], R245fa = 24.3 [C]

DELTAT_cond = 10 [C]
"temperature difference of sink fluid and condensing temp"

pinch =  5 [C]
"heat sink and source pinch point temperature"

T_amb = 32 [C]
"ambient temperature, dead state inlet temp"
T_sink = 27 [C]                                 "sink fluid temperature"
T_cond = T_sink+DELTAT_cond                     "condensing temperature"
T_evap = T_source - DELTAT_evap                 "evaporating temperature"
T_H = T_source - pinch                          "turbine inlet temperature"
T_L = T_cond                                    "condensing temperature"

eta_pump = 0.6                                  "pump efficiency"
eta_turbine = 0.8                               "turbine isentropic efficiency"
eta_regen = 0.8
"regenerator heat exchanger effectivness"

"Operating pressures"
P_H = P[5]
P_L = P[1]
PR = P_H/P_L                                    "pressure ratio"

"Heat source properties (lube oil)"
T_source = 82 [C]                               "heat source temperature"
Cp_oil = 2.103 [kJ/kg-K]                        "lube oil specific heat"
m_dot_source = 40 [kg/s]                        "lube oil mass flow rate"
//T_source_out = 54 [C]                         "lube oul outlet temperature"

"Boiler energy balance"
Q_dot_boiler = Q_dot_source_act
Q_dot_source_act = m_dot_source*Cp_oil*(T_source - T_source_out)
Q_dot_source_max = m_dot_source*Cp_oil*(T_source - T[3])
eta_boiler = Q_dot_source_act/Q_dot_source_max
```

```
T_source = m*s[6]+C                                   "m = heat source slope"
T_source_out = m*s[3]+C                               "C = constant"
T_source_pinch = m*s[4]+C
T_source_pinch = T_evap + pinch

"Heat sink properties (water)"
P_water = 101.3 [kPa]
Cp_water =Cp(Water,T=T_sink,P=P_water)
T_sink_out_max = T[8]
Q_dot_sink_act = Q_dot_cond
Q_dot_sink_max = m_dot_sink*Cp_water*(T_sink_out_max - T_sink)
eta_cond = Q_dot_sink_act/Q_dot_sink_max
Q_dot_sink_act = m_dot_sink*Cp_water*(T_sink_out - T_sink)

T_sink = n*s[1]+D                                     "n = heat sink slope"
T_sink_out = n*s[8]+D                                 "D = constant"
T_sink_pinch = n*s[9]+D
T_sink_pinch = T_cond - pinch

//Heat source and sink plots
"State 11: heat source inlet"
T[11] = T_source
s[11] = s[6]
"State 12: heat source pinch"
T[12] = T_source_pinch
s[12] = s[4]
"State 13: heat source outlet"
T[13] = T_source_out
s[13] = s[3]
"State 14: heat sink inlet"
T[14] = T_sink
s[14] = s[1]
"state 15: heat sink pinch"
T[15] = T_sink_pinch
s[15] = s[9]
"state 16: heat sink outlet"
T[16] = T_sink_out
s[16] = s[8]

"State 1: saturated liquid exiting condenser"
T[1] = T_L
P[1] =P_sat(R$,T=T[1])
x[1] = 0
h[1] =Enthalpy(R$,T=T[1],x=x[1])
s[1] =Entropy(R$,T=T[1],x=x[1])
```

```
"State 2s: isentropic pumping"
P[2] = P_H
s_isen[2] = s[1]
h_isen[2] =Enthalpy(R$,P=P[2],s=s_isen[2])

"State 2: actual pumping"
eta_pump = (h_isen[2]-h[1])/(h[2]-h[1])
T[2] =Temperature(R$,P=P[2],h=h[2])
s[2] =Entropy(R$,P=P[2],h=h[2])
x[2] =Quality(R$,P=P[2],h=h[2])

"State 3: regenerator outlet"
P[3] = P_H
T[3] =Temperature(R$,P=P[3],h=h[3])
s[3] =Entropy(R$,P=P[3],h=h[3])
x[3] =Quality(R$,P=P[3],h=h[3])

"State 4: staturated liquid state point (for plot)"
P[4] = P_H
x[4] = 0
T[4] =Temperature(R$,P=P[4],x=x[4])
s[4] =Entropy(R$,P=P[4],x=x[4])
h[4] =Enthalpy(R$,P=P[4],x=x[4])

"State 5: saturated vapor state point (for plot)"
T[5] = T_evap
P[5] = P_sat(R$,T=T[5])
x[5] = 1
s[5] =Entropy(R$,P=P[5],x=x[5])
h[5] =Enthalpy(R$,P=P[5],x=x[5])

"State 6: vapor at turbine inlet"
Q_dot_boiler = m_dot_orc*(h[6] - h[3])
T[6] = T_H
P[6] = P_H
h[6] =Enthalpy(R$,T=T[6],P=P[6])
s[6] =Entropy(R$,T=T[6],P=P[6])
x[6] =Quality(R$,T=T[6],P=P[6])

"State 7s: insentropic expansion"
P[7] = P_L
s_isen[7] = s[6]
h_isen[7] =Enthalpy(R$,P=P[7],s=s_isen[7])
```

```
"State 7: actual expansion at turbine outlet"
eta_turbine = (h[6]-h[7])/(h[6]-h_isen[7])
T[7] =Temperature(R$,P=P[7],h=h[7])
s[7] =Entropy(R$,P=P[7],h=h[7])
x[7] =Quality(R$,P=P[7],h=h[7])

"State 8: saturated vapor exiting regenerator heat exchanged"
P[8] = P_L
T[8] =Temperature(R$,P=P[8],h=h[8])
x[8] =Quality(R$,P=P[8],h=h[8])
s[8] =Entropy(R$,P=P[8],h=h[8])

"Regenrator energy balance (internal heat exchanged)"
h_c_1 =Enthalpy(R$,T=T[7],P=P[2])
h_c_2 =Enthalpy(R$,T=T[2],P=P[2])
h_h_1 =Enthalpy(R$,T=T[7],P=P[7])
h_h_2 =Enthalpy(R$,T=T[2],P=P[7])
Q_dot_regen_max = m_dot_orc*min((h_c_1-h_c_2),(h_h_1-h_h_2))
eta_regen = Q_dot_regen/Q_dot_regen_max
Q_dot_regen = m_dot_orc*(h[3]-h[2])
Q_dot_regen = m_dot_orc*(h[7]-h[8])

"State 9: saturated vapor state point (for plot)"
P[9] = P[8]
x[9] = 1
T[9] =Temperature(R$,P=P[9],x=x[9])
s[9] =Entropy(R$,P=P[9],x=x[9])
h[9] =Enthalpy(R$,P=P[9],x=x[9])

"State 10: close cycle"
P[10] = P[1]
T[10] = T[1]
h[10] = h[1]
s[10] = s[1]
x[10] = x[1]


"Cycle performance"
W_dot_pump = m_dot_orc*(h[2]-h[1])
W_dot_turbine = m_dot_orc*(h[6]-h[7])
W_dot_net = W_dot_turbine-W_dot_pump
Q_dot_cond = m_dot_orc*(h[8]-h[1])
eta_ORC = W_dot_net/Q_dot_boiler                    "ORC thermal efficiency"
```

```
//Exergy Analysis

PHI_source = m_dot_source*Cp_oil*((T_source - T_amb)-
converttemp(C,K,T_amb)*ln(converttemp(C,K,T_source)/converttemp(C,K,T_amb)))

eta_2nd = W_dot_net/PHI_source                    "2nd law effectiveness"
```

```
"Two-phase flash expansion ORC (CT Room Ventilation Air)"

//R$ = 'R134a'                                    "ORC working fluid"
R$ = 'R245fa'

"Input variables"
DELTAT_cond = 10 [C]
"temperature difference of sink fluid and condensing temp."
pinch =  5 [C]
"heat sink and source pinch point temperature"
pinch_a = 50 [C]                                  "R134a pinch point"

T_amb = 32 [C]                                    "ambient temperature, dead state"
T_sink = 27 [C]                                   "sink fluid inlet temperature"
T_cond = T_sink+DELTAT_cond                       "sink temperature at condenser"
T_L = T_cond
"condenser outlet temperature, saturated liquid"
T_H = T_source - pinch
"!R245fa turbine inlet temperature"
//T_H = T_source - pinch_a                        "R134a turbine inlet temperature"

eta_pump = 0.6                                    "pump efficiency"
eta_turbine = 0.8                                 "turbine isentropic efficiency"

"Operating pressures"
P_H = P[3]
P_L = P[1]
PR = P_H/P_L                                      "pressure ratio"

"Heat source properties (lube oil)"
T_source = 150 [C]                                "heat source temperature"
m_dot_source = 1200 [kg/s]                        "vent air mass flow rate"
P_air = 101.3 [kPa]                               "vent air pressure"
Cp_air = Cp(Air_ha,T=T_source,P=P_air)
T_source_out = T[2] + pinch

"Boiler energy balance"
Q_dot_heater= Q_dot_source_act
Q_dot_source_act = m_dot_source*Cp_air*(T_source - T_source_out)
Q_dot_source_max = m_dot_source*Cp_air*(T_source - T[2])
eta_heater = Q_dot_source_act/Q_dot_source_max

"Heat sink properties (water)"
P_water = 101.3 [kPa]
Cp_water =Cp(Water,T=T_sink,P=P_water)
```

```
T_sink_out_max = T[4]
Q_dot_sink_act = Q_dot_cond
Q_dot_sink_max = m_dot_sink*Cp_water*(T_sink_out_max - T_sink)
Q_dot_cond = m_dot_sink*Cp_water*(T_sink_out - T_sink)
eta_cond = Q_dot_sink_act/Q_dot_sink_max
T_sink_out = T_cond - pinch

//Heat source and sink plots
"State 6: heat source inlet"
T[6] = T_source
s[6] = s[3]
"State 7: heat source outlet"
T[7] = T_source_out
s[7] = s[2]
"State 8: heat sink inlet"
T[8] = T_sink
s[8] = s[1]
"state 9: heat sink outlet"
T[9] = T_sink_out
s[9] = s[4]

"State 1: saturated liquid exiting condenser"
T[1] = T_L
P[1] =P_sat(R$,T=T[1])
x[1] = 0
h[1] =Enthalpy(R$,T=T[1],x=x[1])
s[1] =Entropy(R$,T=T[1],x=x[1])

"State 2s: isentropic pumping"
P[2] = P_H
s_isen[2] = s[1]
h_isen[2] =Enthalpy(R$,P=P[2],s=s_isen[2])

"State 2: actual pumping"
eta_pump = (h_isen[2]-h[1])/(h[2]-h[1])
T[2] =Temperature(R$,P=P[2],h=h[2])
s[2] =Entropy(R$,P=P[2],h=h[2])
x[2] =Quality(R$,P=P[2],h=h[2])

"State 3: staturated liquid exiting heater, to enter turbine"
T[3] = T_H
P[3] = P_sat(R$,T=T[3])
x[3] = 0
h[3] =Enthalpy(R$,x=x[3],P=P[3])
s[3] =Entropy(R$,P=P[3],x=x[3])
```

```
"State 4s: insentropic expansion"
P[4] = P_L
s_isen[4] = s[3]
h_isen[4] =Enthalpy(R$,P=P[4],s=s_isen[4])

"State 4a: actual expansion at turbine outlet"
eta_turbine = (h[3]-h[4])/(h[3]-h_isen[4])
T[4] =Temperature(R$,P=P[4],h=h[4])
s[4] =Entropy(R$,P=P[4],h=h[4])
x[4] =Quality(R$,P=P[4],h=h[4])

"State 5: close cycle"
P[5] = P[1]
T[5] = T[1]
h[5] = h[1]
s[5] = s[1]
x[5] = x[1]

"Cycle performance"
W_dot_pump = m_dot_orc*(h[2]-h[1])
W_dot_turbine = m_dot_orc*(h[3]-h[4])
W_dot_net = W_dot_turbine-W_dot_pump
Q_dot_cond = m_dot_orc*(h[4]-h[1])
Q_dot_heater = m_dot_orc*(h[3]-h[2])

//ORC efficiency
eta_ORC = W_dot_net/Q_dot_heater

//Exergy Analysis

PHI_source = m_dot_source*Cp_air*((T_source - T_amb)-
converttemp(C,K,T_amb)*ln(converttemp(C,K,T_source)/converttemp(C,K,T_amb)))

eta_2nd = W_dot_net/PHI_source                    "2nd law effectiveness"
```

```
"ORC with Multiple Heat Sources"

R$ = 'R134a'                                        "ORC working fluid"
TC=T_crit(R$)

"Input variables"
DELTAT_cond = 10 [C]
"condenser temperature pinch point"
DELTAT_evap = 50 [C]
"boiler temperature pinch point"
pinch =  5 [C]
"heat sink and source pinch point temperature"

T_amb = 32 [C]                                      "ambient temperature, dead state"
T_sink = 27 [C]                                     "sink fluid inlet temp"
T_cond = T_sink+DELTAT_cond                         "condensing temperature"
T_evap = T_air - DELTAT_evap                        "evaporating temperature"
T_H = T_air - pinch                                 "turbine inlet temperature"
T_L = T_cond
"condenser outlet temperature, saturated liquid"

eta_pump = 0.6                                      "pump efficiency"
eta_turbine = 0.8                                   "turbine isentropic efficiency"

"Operating pressures"
P_H = P[5]
P_L = P[1]
PR = P_H/P_L                                        "pressure ratio"

"Lube oil"
T_oil = 82 [C]                                      "lube oil inlet temperature"
Cp_oil = 2.103 [kJ/kg-K]                            "lube oil specific heat"
m_dot_oil = 40 [kg/s]                               "lube oil mass flow rate"
T_oil_out = 54 [C]                                  "lube oil outlet temperature"
Q_dot_oil = m_dot_oil*Cp_oil*(T_oil - T_oil_out)
Q_dot_oil_max = m_dot_oil*Cp_oil*(T_oil - T[2])
eta_hx_oil =Q_dot_oil/Q_dot_oil_max

"CT ventilation air"
T_air = 150 [C]
"heat source air inlet temperature"
m_dot_air = 1200 [kg/s]                             "vent air mass flow rate"
P_air = 101.3 [kPa]                                 "vent air pressure"
Cp_air =Cp(Air_ha,T=T_air,P=P_air)
//Q_dot_air = m_dot_air*Cp_air*(T_air - T_air_out) "energy transfer at generator"
```

```
Q_dot_air_max = m_dot_air*Cp_air*(T_air - T[4])
eta_boiler = Q_dot_air/Q_dot_air_max
Q_dot_air = Q_dot_boiler
T_air = m*s[6]+C                                    "m = heat source slope"
T_air_pinch = m*s[4]+C                              "C = constant"
T_air_pinch = T_evap + pinch
T_air_out = m*s[3]+C

"Heat sink properties (water)"
P_water = 101.3 [kPa]
Cp_water =Cp(Water,T=T_sink,P=P_water)
T_sink_out_max = T[7]
Q_dot_sink_act = Q_dot_cond
Q_dot_sink_act = m_dot_sink*Cp_water*(T_sink_out - T_sink)
Q_dot_sink_max = m_dot_sink*Cp_water*(T_sink_out_max - T_sink)
eta_cond = Q_dot_sink_act/Q_dot_sink_max

T_sink = n*s[1]+D                                   "n = heat sink slope"
T_sink_pinch = n*s[8]+D                             "D = constant"
T_sink_pinch = T_cond - pinch
T_sink_out = n*s[7]+D

//Heat source and sink plots
"State 11: heat source boiler inlet"
T[11] = T_air
s[11] = s[6]
"State 12: heat source boiler pinch"
T[12] = T_air_pinch
s[12] = s[4]
"State 13: heat source outlet"
T[13] = T_air_out
s[13] = s[3]
"State 14: lube oil inlet"
T[14] = T_oil
s[14] = s[3]
"State 15: lube oil out"
T[15] = T_oil_out
s[15] = s[2]
"State 16: heat sink inlet"
T[16] = T_sink
s[16] = s[1]
"State 17: heat sink pinch"
T[17] = T_sink_pinch
s[17] = s[8]
```

```
"State 18: heat sink outlet"
T[18] = T_sink_out
s[18] = s[7]

"State 1: saturated liquid exiting condenser"
T[1] = T_L
P[1] = P_sat(R$,T=T[1])
x[1] = 0
h[1] =Enthalpy(R$,P=P[1],x=x[1])
s[1] =Entropy(R$,P=P[1],x=x[1])

"State 2s: isentropic pumping"
P[2] = P_H
s_isen[2] = s[1]
h_isen[2] =Enthalpy(R$,P=P[2],s=s_isen[2])

"State 2a: actual pumping"
eta_pump = (h_isen[2]-h[1])/(h[2]-h[1])
T[2] =Temperature(R$,P=P[2],h=h[2])
s[2] =Entropy(R$,P=P[2],h=h[2])
x[2] =Quality(R$,P=P[2],h=h[2])

"State 3: HS1 heat exchange outlet (lube oil heat source)"
P[3] = P_H
T[3] = T_oil - pinch
h[3] =Enthalpy(R$,P=P[3],T=T[3])
s[3] =Entropy(R$,P=P[3],h=h[3])
x[3] =Quality(R$,P=P[3],h=h[3])
Q_dot_oil = m_dot_orc*(h[3]-h[2])

"State 4: saturated liquid state point (for plot)"
T[4] = T_evap
P[4] = P_H
x[4] = 0
s[4] =Entropy(R$,T=T[4],x=x[4])

"State 5: saturated vapor state point in boiler (for plot)"
T[5] = T_evap
P[5] = P_sat(R$,T=T[5])
x[5] = 1
s[5] =Entropy(R$,T=T[5],x=x[5])

"State 6: vapor at turbine inlet"
Q_dot_boiler = m_dot_orc*(h[6]-h[3])
T[6] = T_H
```

```
P[6] = P_H
h[6] =Enthalpy(R$,P=P[6],T=T[6])
s[6] =Entropy(R$,P=P[6],T=T[6])
x[6] =Quality(R$,P=P[6],T=T[6])

"State 7s: insentropic expansion"
P[7] = P_L
s_isen[7] = s[6]
h_isen[7] =Enthalpy(R$,P=P[7],s=s_isen[7])

"State 7a: actual expansion at turbine outlet"
eta_turbine = (h[6]-h[7])/(h[6]-h_isen[7])
T[7] =Temperature(R$,P=P[7],h=h[7])
s[7] =Entropy(R$,P=P[7],h=h[7])
x[7] =Quality(R$,P=P[7],h=h[7])

"State 8: saturated vapor state point (for plot)"
P[8] = P_L
x[8] = 1
T[8] =Temperature(R$,P=P[8],x=x[8])
s[8] =Entropy(R$,P=P[8],x=x[8])

"state 9: saturaed liquied state point (for plot)"
P[9] = P_L
x[9] = 0
T[9] =Temperature(R$,P=P[9],x=x[9])
s[9] =Entropy(R$,P=P[9],x=x[9])

"State 10: close cycle"
P[10] = P[1]
T[10] = T[1]
h[10] = h[1]
s[10] = s[1]
x[10] = x[1]

"Cycle performance"
W_dot_pump = m_dot_orc*(h[2]-h[1])
W_dot_turbine = m_dot_orc*(h[6]-h[7])
W_dot_net = W_dot_turbine-W_dot_pump
Q_dot_cond = m_dot_orc*(h[7]-h[1])
Q_dot_total = Q_dot_oil+Q_dot_air
eta_ORC = W_dot_net/Q_dot_total                    "ORC efficiency"
```

```
//Exergy Analysis

PHI_oil = m_dot_oil*Cp_oil*((T_oil - T_amb)-
converttemp(C,K,T_amb)*ln(converttemp(C,K,T_oil)/converttemp(C,K,T_amb)))

PHI_air = m_dot_air*Cp_air*((T_air - T_amb)-
converttemp(C,K,T_amb)*ln(converttemp(C,K,T_air)/converttemp(C,K,T_amb)))

PHI_total = PHI_oil+PHI_air

eta_2nd = W_dot_net/PHI_total                    "2nd law effectiveness"
```

```
"ORC with Multiple Heat Sources"

R$ = 'R245fa'                                   "ORC working fluid"
TC=T_crit(R$)

"Input variables"
DELTAT_cond = 10 [C]
"condenser temperature pinch point"
DELTAT_evap = 15 [C]
"boiler temperature pinch point"
pinch =  5 [C]
"heat sink and source pinch point temperature"

T_amb = 32 [C]                                  "ambient temperature, dead state"
T_sink = 27 [C]                                 "sink fluid inlet temperature"
T_cond = T_sink+DELTAT_cond                     "sink temperature at condenser"
T_evap = T_air - DELTAT_evap
"evaporating temperature at boiler"
T_H = T_air - pinch                             "turbine inlet temperature"
T_L = T_cond
"condenser outlet temperature, saturated liquid"

eta_pump = 0.6                                  "pump efficiency"
eta_turbine = 0.8                               "turbine isentropic efficiency"

"Operating pressures"
P_H = P[5]
P_L = P[1]
PR = P_H/P_L                                    "pressure ratio"

"Lube oil"
T_oil = 82 [C]                                  "lube oil inlet temperature"
Cp_oil = 2.103 [kJ/kg-K]                        "lube oil specific heat"
m_dot_oil = 40 [kg/s]                           "lube oil mass flow rate"
T_oil_out = 54 [C]                              "lube oil outlet temperature"
Q_dot_oil = m_dot_oil*Cp_oil*(T_oil - T_oil_out)
Q_dot_oil_max = m_dot_oil*Cp_oil*(T_oil - T[2])
eta_hx_oil =Q_dot_oil/Q_dot_oil_max

"CT ventilation air"
T_air = 150 [C]                                 "heat source temperature"
m_dot_air = 1200 [kg/s]                         "vent air mass flow rate"
P_air = 101.3 [kPa]                             "vent air pressure"
Cp_air =Cp(Air_ha,T=T_air,P=P_air)
//Q_dot_air = m_dot_air*Cp_air*(T_air - T_air_out) "energy transfer at generator"
```

```
Q_dot_air_max = m_dot_air*Cp_air*(T_air - T[4])
eta_boiler = Q_dot_air/Q_dot_air_max
Q_dot_air = Q_dot_boiler
T_air = m*s[6]+C                                    "m = heat source slope"
T_air_pinch = m*s[4]+C                              "C = constant"
T_air_pinch = T_evap + pinch
T_air_out = m*s[3]+C

"Heat sink properties (water)"
P_water = 101.3 [kPa]
Cp_water =Cp(Water,T=T_sink,P=P_water)
T_sink_out_max = T[7]
Q_dot_sink_act = Q_dot_cond
Q_dot_sink_act = m_dot_sink*Cp_water*(T_sink_out - T_sink)
Q_dot_sink_max = m_dot_sink*Cp_water*(T_sink_out_max - T_sink)
eta_cond = Q_dot_sink_act/Q_dot_sink_max

T_sink = n*s[1]+D                                   "n = heat sink slope"
T_sink_pinch = n*s[8]+D                             "D = constant"
T_sink_pinch = T_cond - pinch
T_sink_out = n*s[7]+D

//Heat source and sink plots
"State 11: heat source boiler inlet"
T[11] = T_air
s[11] = s[6]
"State 12: heat source boiler pinch"
T[12] = T_air_pinch
s[12] = s[4]
"State 13: heat source outlet"
T[13] = T_air_out
s[13] = s[3]
"State 14: lube oil inlet"
T[14] = T_oil
s[14] = s[3]
"State 15: lube oil out"
T[15] = T_oil_out
s[15] = s[2]
"State 16: heat sink inlet"
T[16] = T_sink
s[16] = s[1]
"State 17: heat sink pinch"
T[17] = T_sink_pinch
s[17] = s[8]
```

```
"State 18: heat sink outlet"
T[18] = T_sink_out
s[18] = s[7]

"State 1: saturated liquid exiting condenser"
T[1] = T_L
P[1] = P_sat(R$,T=T[1])
x[1] = 0
h[1] =Enthalpy(R$,P=P[1],x=x[1])
s[1] =Entropy(R$,P=P[1],x=x[1])

"State 2s: isentropic pumping"
P[2] = P_H
s_isen[2] = s[1]
h_isen[2] =Enthalpy(R$,P=P[2],s=s_isen[2])

"State 2a: actual pumping"
eta_pump = (h_isen[2]-h[1])/(h[2]-h[1])
T[2] =Temperature(R$,P=P[2],h=h[2])
s[2] =Entropy(R$,P=P[2],h=h[2])
x[2] =Quality(R$,P=P[2],h=h[2])

"State 3: HS1 heat exchange outlet (lube oil heat source)"
P[3] = P_H
T[3] = T_oil - pinch
h[3] =Enthalpy(R$,P=P[3],T=T[3])
s[3] =Entropy(R$,P=P[3],h=h[3])
x[3] =Quality(R$,P=P[3],h=h[3])
Q_dot_oil = m_dot_orc*(h[3]-h[2])

"State 4: saturated liquid state point (for plot)"
T[4] = T_evap
P[4] = P_H
x[4] = 0
s[4] =Entropy(R$,T=T[4],x=x[4])

"State 5: saturated vapor state point in boiler (for plot)"
T[5] = T_evap
P[5] = P_sat(R$,T=T[5])
x[5] = 1
s[5] =Entropy(R$,T=T[5],x=x[5])

"State 6: vapor at turbine inlet"
Q_dot_boiler = m_dot_orc*(h[6]-h[3])
T[6] = T_H
```

```
P[6] = P_H
h[6] =Enthalpy(R$,P=P[6],T=T[6])
s[6] =Entropy(R$,P=P[6],T=T[6])
x[6] =Quality(R$,P=P[6],T=T[6])

"State 7s: insentropic expansion"
P[7] = P_L
s_isen[7] = s[6]
h_isen[7] =Enthalpy(R$,P=P[7],s=s_isen[7])

"State 7a: actual expansion at turbine outlet"
eta_turbine = (h[6]-h[7])/(h[6]-h_isen[7])
T[7] =Temperature(R$,P=P[7],h=h[7])
s[7] =Entropy(R$,P=P[7],h=h[7])
x[7] =Quality(R$,P=P[7],h=h[7])

"State 8: saturated vapor state point (for plot)"
P[8] = P_L
x[8] = 1
T[8] =Temperature(R$,P=P[8],x=x[8])
s[8] =Entropy(R$,P=P[8],x=x[8])

"state 9: saturaed liquied state point (for plot)"
P[9] = P_L
x[9] = 0
T[9] =Temperature(R$,P=P[9],x=x[9])
s[9] =Entropy(R$,P=P[9],x=x[9])

"State 10: close cycle"
P[10] = P[1]
T[10] = T[1]
h[10] = h[1]
s[10] = s[1]
x[10] = x[1]

"Cycle performance"
W_dot_pump = m_dot_orc*(h[2]-h[1])
W_dot_turbine = m_dot_orc*(h[6]-h[7])
W_dot_net = W_dot_turbine-W_dot_pump
Q_dot_cond = m_dot_orc*(h[7]-h[1])
Q_dot_total = Q_dot_oil+Q_dot_air
eta_ORC = W_dot_net/Q_dot_total                    "ORC efficiency"
```

```
//Exergy Analysis

PHI_oil = m_dot_oil*Cp_oil*((T_oil - T_amb)-
converttemp(C,K,T_amb)*ln(converttemp(C,K,T_oil)/converttemp(C,K,T_amb)))

PHI_air = m_dot_air*Cp_air*((T_air - T_amb)-
converttemp(C,K,T_amb)*ln(converttemp(C,K,T_air)/converttemp(C,K,T_amb)))

PHI_total = PHI_oil+PHI_air

eta_2nd = W_dot_net/PHI_total                    "2nd law effectiveness"
```

Appendix D. Simple Economic Payback EES Code

```
"Simple economic analysis - payback period"

C_f= 0.0675 [$]
"power plant fuel cost per kWh of electricity in January 2014"
C_e = 0.128 [$]
"electricity cost per kWh in January 2014"

//ORC

//Market ORC
C_orc_m = 2250000 [$]
"market ORC total investment cost, 1 MWe, T_source>80 C"
P_m = 1 [MW]
"market power plant capacity"

//Power plant
P = 670 [MW]                                    "power generation capacity"
T= 20 [h/day]                                   "operating time per day"
D = 365 [day]                                   "days per year"
T_year = T*D                                    "operating time per year"
E_p_annual = P*T_year
"annual energy generation, MWh"

//Baseline ORC
P_orc = 11.3 [MW]                               "ORC power generation capacity"
E_orc_annual = P_orc*T_year
"annual ORC energy generation, MWh"
C_orc = (P_orc/P_m)*C_orc_m                     "ORC total investment cost"
savings_orc_annual = E_orc_annual*convert(MWh,kWh)*C_f
"annual fuel cost saving from ORC"
payback_orc = C_orc/savings_orc_annual


//Absorption chiller

//Market absorption chiller
C_abs_m = 350 [$/ton]
"market absorption chiller invesment cost"

//Double-effect H2O/LiBr absorption chiller
Q_abs = 88000 [kW]                              "cooling capacity, kW"
Q_abs_ton = 25000 [ton]                         "cooling capacity, ton"
```

C_abs = Q_abs_ton*C_abs_m
"absorption chiller investment cost"

Q_load = Q_abs_ton*T_year
"annual serving cooling output, ton/year"

E_aircond = 0.52 [kWh/ton]
"power comsumption for air conditioning per ton cooling capacity"
E_aircond_annual = E_aircond*Q_load
"annual power comsumption for air conditioning at absorption chiller cooling load"

savings_abs_annual = E_aircond_annual*C_e
"annual electricity cost saving from absorption chiller"
payback_abs = C_abs/savings_abs_annual